



Faculty of Resource Science and Technology

**MOLECULAR STUDY OF SELECTED DIFFERENTIALLY  
EXPRESSED GENES IN NASOPHARYNGEAL CARCINOMA**

**Chua Suk Ngo**

**Master of Science  
2011**



**Pusat Khidmat Maklumat Akademik  
UNIVERSITI MALAYSIA SARAWAK**

**MOLECULAR STUDY OF SELECTED DIFFERENTIALLY EXPRESSED  
GENES IN NASOPHARYNGEAL CARCINOMA**

**P.KHIDMAT MAKLUMAT AKADEMIK**

**UNIMAS**



**1000246092**

**CHUA SUK NGO**

**A thesis submitted  
in fulfillment of the requirements for the degree of Master of Science**

**Faculty of Resource Science and Technology  
UNIVERSITI MALAYSIA SARAWAK**

**2011**

## **ACKNOWLEDGEMENTS**

I would like to acknowledge the advice and guidance of my supervisor, Assoc. Prof. Dr Edmund Sim Ui Hang who has supported me throughout my thesis with his patience and knowledge whilst allowing me the room to work in my own way. I also thank the members of HMGL (Human Molecular Genetics Lab) for their guidance and suggestions, namely Ma Xiang Ru, Chia Sze Wooi, Johnson Chong, Nur Diana, Ang Chow Hiang and Tiong Wen ni for all their advice, encouragement, and help in retrieving journals articles.

I also thank the lab assistants especially Kak Lim, who has helped us a lot in lab purchasing. I acknowledge Unimas Postgraduate Scholarship for provision of fund to sustain my postgraduate pursuit. Thanks also to the Faculty for the equipment I have needed to produce and complete my thesis.

The major biopsy samples for this study were provided by Sarawak General Hospital and Hospital Serian Sarawak. Thanks also to Dr Selva, Dr Tiong Thung Sing, Mr Lai Wei Han and Mr Tan Sia Hong for sample collection and storage. Without these specimens, this study would have not been possible.

I would like to thank God for my family members and friends, who have always been supportive and encouraging.

## ABSTRACT

Nasopharyngeal Carcinoma (NPC) occurs as a consequence of multiple molecular events induced by environmental factors and Epstein–Barr virus (EBV) infections. The neoplastic processes may involve alterations of the tumor suppressor genes and oncogenes by genetic damage and interference with the normal cellular functions by the EBV latent gene products. Overexpression of TNF receptor-associated factor 6 (TRAF6) has been reported to suppress *oriP* activity and loss of EBV from Burkitt's lymphoma cell line. The role of vigilin in cytoplasmic mRNA metabolism has been suggested whereby alterations in mRNA regulation by RNA binding protein have been reported in diverse cancer types. BCL2/adenovirus E1B 19kD interacting protein like (*BNIP1*) has been reported to have tumor suppressor function. Human growth factor, augmenter of liver regeneration (*GFER*) is thought to be one of the factors responsible for the extraordinary regenerative capacity of the mammalian liver but its increased expression has also been reported in hepatocellular carcinoma (HCC) and cholangiocellular carcinoma (CCC). There have been several studies reporting the increased expression of macrophage migration inhibitory factor (MIF) in pre-cancerous, cancerous and metastatic tumours. Our earlier preliminary findings that revealed differential expression of these genes in NPC have led us to further investigate their expression. In this study, it aimed to examine the expression pattern (transcript and protein level) of these genes in local nasopharyngeal biopsy samples and cell lines and the existence of mutations (if any) in an effort to evaluate role(s) of these genes in NPC progression. The expression analysis study demonstrated that *TRAF6* mRNA was underexpressed in tumor in 3 out of 8 biopsy samples screened via conventional PCR approach. This trend of underexpression was further confirmed via quantitative PCR in 5 out of 9 samples. Mutational analysis found no mutation



in coding sequence of *TRAF6*. TRAF6 protein expression however failed to be detected via Western blot. The results suggested tumor suppressive role for *TRAF6* in NPC. Our results also revealed underexpression of vigilin in 1 out of 8 samples via conventional PCR and 1 out of 9 samples with real time PCR. Underexpression of vigilin protein was found not to be significant in NP cell lines (3 NPC cell lines and 1 normal NP cell line) via Western blot. Mutational analysis revealed no mutation in vigilin coding region. *BNIP2* was observed to be underexpressed in 3 out of 8 samples. However, further studies are needed to confirm the expression. No significant deregulation of *MIF* expression pattern was observed between tumor and normal samples via conventional PCR. Results also revealed underexpression of *GFER* mRNA in 1 out of 8 samples. Vigilin, *MIF* and *GFER* were suggested not directly associated with development of NPC.



**Kajian molekul gen-gen terpilih yang menunjukkan pengekspresan yang berbeza dalam  
Karsinoma Nasofaringeal.**

**ABSTRAK**

*Karsinoma Nasofaringeal (NPC) terjadi akibat penggabungan antara pengaruh infeksi dengan virus Epstein Barr (EBV), genetik dan faktor lingkungan lain. Proses neoplastik mungkin melibatkan perubahan gen supresor tumor dan onkogen melalui kerosakan genetik dan gangguan fungsi sel normal oleh produk gen laten EBV. Ekspresi dari TNF receptor-associated factor 6 (TRAF6) telah dilaporkan untuk menekan aktiviti oriP dan kehilangan EBV dari sel temurun limfoma Burkitt. Peranan vigilin dalam metabolisme mRNA sitoplasmik dicadangkan berdasarkan perubahan dalam regulasi mRNA yang disebabkan oleh protein pengikat RNA telah dilaporkan dalam pelbagai jenis kanser. BCL2/adenovirus E1B 19kD interacting protein like (BNIP2) telah dilaporkan mempunyai fungsi supresor tumor. Gen human growth factor, augmenter of liver regeneration (GFER) dianggap salah satu faktor yang bertanggung jawab ke atas keupayaan regenerasi hati mamalia yang luar biasa. Pengekspresan GFER yang meningkat juga telah dilaporkan pada karsinoma hepatoselular dan karsinoma cholangiocarcinomas (cholangiocellular carcinoma). Terdapat beberapa kajian yang melaporkan peningkatan ekspresi macrophage migration inhibitory factor (MIF) pada tumor pra-kanser, kanser dan metastasis. Penemuan awal yang menunjukkan perbezaan ekspresi gen-gen tersebut dalam NPC telah mendorong penyiasatan lebih lanjut pengekspresannya dari sampel biopsi nasofarinks dan sel temurun dan kehadiran mutasi (jika ada) dalam usaha untuk menilai peranan gen-gen tersebut dalam NPC.*



*Kajian analisa ekspresi kami menunjukkan bahawa mRNA TRAF6 mempunyai kadar pengekspresan yang rendah dalam tumor dalam 3 daripada 8 sampel melalui pendekatan PCR konvensional. Trend pengekspresan yang rendah ini disahkan selanjutnya melalui PCR kuantitatif dalam 5 daripada 9 sampel. Analisis mutasi ke atas TRAF6 tidak menemui sebarang mutasi dalam jujukan gen tersebut. Namun, ekspresi protein TRAF6 gagal dikesan melalui kaedah blot Western. Siasatan mencadangkan peranan penekan tumor bagi TRAF6 dalam NPC. Keputusan juga mendedahkan pengekspresan rendah transkrip vigilin dalam tumor melalui kaedah konvensional PCR (1 daripada 8 sampel) dan PCR kuantitatif (1 daripada 9 sampel). Pola pengekspresan rendah protein vigilin didapati tidak signifikan melalui kaedah blot Western yang menggunakan tiga jenis sel temurun kanser nasofarinks (HONE1, HK1 dan SUNE1) dan 1 sel temurun nasofarinks normal (NP69). Analisis mutasi mendedahkan tidak ada mutasi pada jujukan gen vigilin. BNIP2 juga didapati menunjukkan pengekspresan rendah dalam 3 daripada 8 sampel. Walaubagaimanapun, kajian lanjut diperlukan diperlukan untuk mengesahkan pola gen ekspresi ini. Tiada deregulasi ekspresan gen MIF yang signifikan diperhatikan antara sampel tumor dan normal melalui PCR konvensional. Keputusan juga mendedahkan pengekspresan rendah mRNA GFER dalam 1 daripada 8 sampel. Vigilin, MIF dan GFER dicadangkan tidak berperanan secara langsung dalam patogenesis NPC.*



TABLE OF CONTENTS

CHAPTERS		PAGE
	TITLE	i
	ACKNOWLEDGEMENTS	ii
	ABSTRACT	iii
	ABSTRAK	v
	TABLE OF CONTENTS	vii
	LIST OF TABLES	xiii
	LIST OF FIGURES	xvi
	ABBREVIATIONS	xvii
CHAPTER ONE	Introduction	1
CHAPTER TWO	Literature Review	5
	2.1 Definition	5
	2.2 Fossa of Rosenmuller	6
	2.3 Normal histology	8
	2.4 Histopathology	8
	2.5 Epidemiology and Incidence	9
	2.6 Etiologies	10
	2.6.1 Genetic susceptibility factors	10
	2.6.2 Environmental factors	11
	2.6.3 Epstein-Barr Virus (EBV)	12
	2.7 Molecular alteration and pathogenesis	12



2.7.1	Genetic and Epigenetic events	12
2.7.2	Alterations of subcellular mechanisms	13
2.7.3	Roles of EBV latent infection	17
2.7.4	Carcinogenesis of NPC	18
2.8	Genes of study	20
2.8.1	TNF RECEPTOR-ASSOCIATED FACTOR 6 ( <i>TRAF6</i> )	20
2.8.2	HIGH DENSITY LIPOPROTEIN-BINDING PROTEIN ( <i>HDLBP</i> ) /Vigilin	22
2.8.3	BCL2/ADENOVIRUS E1B-KD PROTEIN- INTERACTING PROTEIN 2-LIKE ( <i>BNIP1</i> )	24
2.8.4	MACROPHAGE MIGRATION INHIBITORY FACTOR ( <i>MIF</i> )	26
2.8.5	GROWTH FACTOR, ERV1-LIKE ( <i>GFER</i> )	28
2.9	Rationale	30
2.10	Research Objectives	31

## **CHAPTER THREE Materials and Methods 32**

3.1	Tissue Specimens	32
3.1.1	Sources of total RNA samples	32
3.1.2	Isolation of total RNA	34
3.1.3	Total RNA analysis and quantification	34
3.2	Oligonucleotides	35
3.3	Semi-quantitative RT-PCR	38



3.3.1	Preparation of first strand cDNA	38
3.3.2	PCR	38
3.3.3	PCR products verification	40
3.3.4	Statistical analysis	40
3.4	Quantitative PCR	40
3.4.1	Dnase treatment	40
3.4.2	Purification	41
3.4.3	Preparation of first strand cDNA	41
3.4.4	Quantitative PCR amplification	41
3.4.5	Efficiency test	42
3.4.6	Delta Delta C <sub>T</sub> Relative Quantitation	42
3.5	Cloning, screening and sequencing for mutational analysis	43
3.6	Protein analysis	43
3.6.1	Protein isolation using Nonidet P-40 lysis buffer	43
3.6.2	Protein quantification using Bradford assay	44
3.6.2.1	Reagents and standard curve preparation	44
3.6.2.2	Protein quantification	45
3.6.3	Western blot	45
3.6.3.1	Preparing SDS-PAGE	45
3.6.3.2	Preparing samples, gel-loading and running the gel	46



3.6.3.3	Electrophoretic blotting	47
3.6.3.4	Coomassie blue staining	48
3.6.3.5	Blocking and immunoprobng	48
3.6.3.6	Chemiluminescent detection	49
3.6.3.7	Membrane stripping by low pH	49

<b>CHAPTER FOUR</b>	<b>Expression Analysis <i>TRAF6</i>, vigilin, <i>BNIPL2</i>, <i>MIF</i> and <i>GFER</i> in Nasopharyngeal Carcinoma via conventional RT-PCR</b>	<b>50</b>
4.1	Introduction	50
4.2	General methodology	52
4.3	Results	53
4.3.1	Total RNA samples assessment	53
4.3.2	Internal control	55
4.3.3	<i>TRAF6</i>	57
4.3.4	Vigilin	61
4.3.5	<i>BNIPL2</i>	64
4.3.6	<i>MIF</i>	67
4.3.7	<i>GFER</i>	70
4.4	Discussion	73

<b>CHAPTER FIVE</b>	<b>Expression Analysis <i>TRAF6</i> and vigilin in Nasopharyngeal Carcinoma via Quantitative PCR</b>	<b>77</b>
5.1	Introduction	77
5.2	General methodology	79



5.3	Results	81
5.3.1	Total RNA samples assessment	81
5.3.2	Validation of Target and Control Genes for the Comparative CT Method	82
5.3.3	Dissociation (melting) curves	87
5.3.4	Negative RT control	89
5.3.5	Data analysis using the $\Delta\Delta C_T$ Method	92
5.3.5.1	<i>TRAF6</i>	94
5.3.5.2	vigilin	97
5.3.6	Comparison of <i>TRAF6</i> and vigilin mRNA expression via conventional PCR and quantitative PCR	100
5.4	Discussion	102

<b>CHAPTER SIX</b>	<b>PROTEIN EXPRESSION OF TRAF6 AND VIGILIN IN NASOPHARYNGEAL CELL LINES</b>	<b>105</b>
6.1	Introduction	107
6.2	General Methodology	107
6.3	Results	109
6.3.1	Protein sample concentration determination	109
6.3.2	Vigilin and TRAF6 protein expression	112
6.4	Discussion	115



<b>CHAPTER SEVEN</b>	<b>General Discussion</b>	<b>117</b>
7.1	<i>TRAF6</i> , vigilin, <i>BNIP1</i> , <i>MIF</i> and <i>GFER</i>	117
7.2	Limitations	119
7.3	Conclusions and future direction	119
	<b>REFERENCES</b>	<b>121</b>
	<b>APPENDICES</b>	



## LIST OF TABLES

TABLE NO.	TITLE	PAGE
Table 2.1	Major gene alterations in nasopharyngeal carcinoma	15
Table 2.2	Preliminary findings of down-regulated genes in nasopharyngeal carcinoma	16
Table 3.1	List of total RNA from biopsy tissues and their source information	33
Table 3.2	List of total RNA from NPC cell lines (HONE, HK1 and SUNE1) and normal NP 69 cell line	33
Table 3.3	List of synthetic oligonucleotide primers designed for amplification of vigilin, <i>TRAF6</i> , <i>BNIP1</i> , <i>MIF</i> , <i>GFER</i> , <i>GAPDH</i> , and <i>ACTB</i> in semi-quantitative reverse transcription polymerase chain reaction (RT- PCR)	36
Table 3.4	List of synthetic oligonucleotide primers designed for amplification of vigilin and <i>TRAF6</i> in mutational analysis	37
Table 3.5	List of synthetic oligonucleotide primers designed for amplification of vigilin, <i>TRAF6</i> , and <i>GAPDH</i> in real time PCR	37
Table 3.6	Conventional PCR reaction setup	39
Table 3.7	Conventional PCR cycling conditions	39
Table 3.8	Quantitative PCR Cycling conditions	42
Table 3.9	Recipe for resolving and stacking gels for SDS-PAGE	46
Table 3.10	Primary and secondary antibody dilutions.	49
Table 4.1	Expression (fold change) of <i>TRAF6</i> in biopsy samples screened	60
Table 4.2	Expression (fold change) of <i>TRAF6</i> in nasopharyngeal cell lines.	60



Table 4.3	Expression (fold change) of vigilin in biopsy samples screened	63
Table 4.4	Expression (fold change) of <i>BNIP1</i> in biopsy samples screened	66
Table 4.5	Expression (fold change) of <i>MIF</i> in biopsy samples screened	69
Table 4.6	Expression (fold change) of <i>GFER</i> in biopsy samples screened	72
Table 5.1	<i>GAPDH</i> standard curve involving five-fold dilutions: 50, 10, 2, 0.4, 0.08 (ng) with two replicates at each point.	84
Table 5.2	<i>TRAF6</i> standard curve involving five-fold dilutions: 50, 10, 2, 0.4, 0.08 (ng) with two replicates at each point.	84
Table 5.3	Vigilin standard curve involving five-fold dilutions: 50, 10, 2, 0.4, 0.08 (ng) with two replicates at each point	84
Table 5.4	Slope, amplification and reaction efficiency for <i>GAPDH</i> , <i>TRAF6</i> and vigilin	86
Table 5.5	Negative RT control amplification $C_T$ using <i>GAPDH</i>	91
Table 5.6	<i>TRAF6</i> and <i>GAPDH</i> amplification $C_T$ of replicate 1	93
Table 5.7	Expression (fold change) of <i>TRAF6</i> in 9 nasopharyngeal samples	96
Table 5.8	Expression (fold change) of vigilin in 9 nasopharyngeal samples	99
Table 5.9	Summary of expression analysis of target gene expression (after normalization) in paired tumor and normal nasopharyngeal biopsy samples via conventional and quantitative PCR approach.	101
Table 6.1	Standard curve preparation	109
Table 6.2	Quantification of protein extract from cell lines.	111
Table 6.3	Expression (fold change) of vigilin protein in 3 NPC cell lines relative to one normal cell line (NP69).	114



## LIST OF FIGURES

FIGURE NO.	TITLE	PAGE
Figure 2.1	Lateral relations of the fossa of Rosenmuller	7
Figure 2.2	Multistep carcinogenesis of nasopharyngeal carcinoma	19
Figure 4.1	Total RNA isolated from paired biopsy samples using Trizol method.	54
Figure 4.2	Total RNA isolated from nasopharyngeal cell lines using Trizol method.	54
Figure 4.3	Expression of <i>GAPDH</i> and <i>ACTB</i> in all nasopharyngeal biopsy samples screened.	55
Figure 4.4	Expression of <i>GAPDH</i> and <i>ACTB</i> in three NPC cell lines (HONE1, HK1, SUNE1) and 1 normal NP (NP69) cell line	56
Figure 4.5	Expressions of <i>TRAF6</i> in eight paired samples from local biopsies on 2.0% (w/v) agarose gel	59
Figure 4.6	Expressions of <i>TRAF6</i> in three NPC cell lines (HONE1, HK1, SUNE1) and one normal cell line (NP69) on 2.0% (w/v) agarose gel.	59
Figure 4.7	Expressions of vigilin in eight paired samples from local biopsies on 2.0% (w/v) agarose gel.	62
Figure 4.8	Expressions of <i>BNIP1</i> in eight paired samples from local biopsies on 2.0% (w/v) agarose gel.	65
Figure 4.9	Expressions of <i>MIF</i> in eight paired samples from local biopsies on 2.0% (w/v) agarose gel	68



Figure 4.10	Expressions of <i>GFER</i> in eight paired samples from local biopsies on 2.0% (w/v) agarose gel.	71
Figure 5.1	Total RNA isolated from paired biopsy sample 55 using Trizol method.	81
Figure 5.2	Standard curve plots: log of input cDNA (HONE1, NPC cell line) from a 5-fold serial dilution	83
Figure 5.3	Standard curve (a) <i>GAPDH</i> (b) <i>TRAF6</i> (c) vigilin	85
Figure 5.4	Melting curve for samples used in quantitative study for (a) <i>GAPDH</i> (b) <i>TRAF6</i> (c) vigilin	88
Figure 5.5	<i>GAPDH</i> (a) NAC amplification curve and (b) NAC melting curve for nine paired biopsy samples	90
Figure 5.6	A bar chart showing relative concentration of <i>TRAF6</i> .	95
Figure 5.7	A bar chart showing relative concentration of vigilin.	98
Figure 6.1	Protein quantification using Bradford assay.	110
Figure 6.2	Vigilin and <i>GAPDH</i> protein expression from 10µg total protein extracted from <i>nasopharyngeal cell lines</i> .	113

## ABBREVIATIONS

%	percent
°C	degree Celsius
μl	microlitre
A <sub>260</sub>	absorbance at wavelength 260
A <sub>280</sub>	absorbance at wavelength 280
<i>BNIP1</i>	BCL2/adenovirus E1B 19 kDa protein interacting protein-like-2
bp	base pairs
BSA	bovine serum albumin
cDNA	complementary DNA
DEPC	diethyl pyrocarbonate
dH <sub>2</sub> O	distilled water
DNA	deoxyribonucleic acid
dNTP	dinucleotide triphosphate
EBV	Epstein–Barr virus
EDTA	ethylenediamine tetra-acetic acid
EtBr	ethidium bromide
<i>GFER</i>	growth factor, augments liver regeneration
kb	kilobases
MgCl <sub>2</sub>	magnesium chloride
<i>MIF</i>	macrophage migration inhibitory factor
M-MLV	Moloney Murine Leukemia Virus



mRNA	messenger RNA
NaOH	Sodium Hydroxide
ng	nano gram
NP	nasopharyngeal
NPC	nasopharyngeal carcinoma
PBS	phosphate buffered saline
PCR	polymerase chain reaction
PMSF	phenylmethysulfonyl fluoride
PVDF	polyvinylidene difluoride
RNA	ribonucleic acid
rpm	revolutions per minute
RT	reverse transcription
RT-PCR	reverse transcription-polymerase chain reaction
SDS-PAGE	sodium dodecyl sulfate polyacrylamide gel electrophoresis
TAE	tris-acetate EDTA
<i>TRAF6</i>	TNF receptor associated factor 6

## **CHAPTER ONE**

### **INTRODUCTION**

Nasopharyngeal carcinoma (NPC) is a cancer originating in the nasopharynx, the uppermost region of the pharynx or "throat", where the nasal passages and auditory tubes join the remainder of the upper respiratory tract. It has a remarkably distinctive ethnic and geographical distribution (Kwok *et al.*, 2004). In 2005, 85 248 new cases were registered worldwide, and more than 68% of those were reported from China and Southeast Asia (Parkin *et al.*, 2005). Yu and Yuan in 2002 (cited in Kwok *et al.*, 2004) stated that regardless of race/ethnicity, men are 2-3 fold more frequently affected than women.

According to Kwok and Dolly (2002), there is strong evidence linking NPC to three well defined factors; a close association with the ubiquitous Epstein-Barr virus, certain traditional Southern Chinese diets containing chemical carcinogens, and an inherited genetic predisposition/susceptibility to the disease in certain patients. It is thought that these factors (in isolation or in combination) cause multiple genetic alterations that result in the disruption of various cellular mechanisms including cell cycle regulation, apoptosis, signal transduction, cell adhesion and other novel pathways (Kwok and Dolly, 2002).

By the comprehensive genome-wide studies, multiple genetic defects have been identified in NPC (Lo *et al.*, 2004). Consistently high frequencies of genetic losses are observed on chromosomes 3p, 9, 11q, 13q, 14q, and 16q, while recurrent chromosomal gains were identified on chromosome 12 (Hui *et al.*, 1999; Lo *et al.*, 2000). Genes located on



chromosomes 9p21 (*p14*, *p16*) and 3p21.3 (*RASSF1A*) were found to be defective due to deletion or promoter hypermethylation (Lo *et al.*, 1996, 2001; Kwong *et al.*, 2002). The tumor suppressor properties of *p16* and *RASSF1A* have also been demonstrated in NPC cells (Wang *et al.*, 1999; Chow *et al.*, 2004).

Previous preliminary data (Sim *et al.*, 2008) has detected differential expression of vigilin and *TRAF6* via the GeneFishing<sup>TM</sup> Differential Expressed Genes (DEG) analysis techniques. In accordance with previous unpublished microarray-based transcriptional profiling data by our research group, *BNIP1* showed down expression (0.176 fold change) in NPC tumor sample. Shen *et al.* (2003) reported interaction of *BNIP1* with MIF and GFER tested via yeast two-hybrid system. These observations suggested that many more genes may be involved in the multistep progression of NPC as the cause and mechanism of nasopharyngeal carcinoma (NPC) progression are multigenic in nature. Therefore, we aimed to study the existence of mutations (if any) and the expression pattern of these genes in local NPC biopsy samples using reverse transcription-polymerase chain reaction (RT-PCR) and Western blot approach, in an effort to evaluate the role(s) of these genes in NPC progression.

Vigilin, also known as high density lipoprotein-binding protein, is a 110-kD and 1268 amino acids long protein encoded by *HDLBP* gene located at chromosome 2q37.3 (UniProtKB, 2007). Vigilin is a ubiquitous and highly conserved protein containing 14 related, but non-identical, K-homology (KH) nucleic acid binding domains (Goolsby and Shapiro, 2003). Vigilin is identified as important in the regulation of mRNA stability (Dodson and Shapiro, 2002). Many clinically relevant mRNAs including several encoding cytokines, growth factors and oncoproteins are regulated by differential RNA stability (Wilkinson, 2007).

Dysregulation of mRNA stability has been associated with human diseases including cancer, inflammatory disease, and Alzheimer's disease (Hollams *et al.*, 2002).

TNF receptor-associated factor 6 is a member of the TNF receptor associated factor (TRAF) protein family encoded by *TRAF6* located at chromosome 11p12 (NCBI, 2007b). TRAF6 that mediates activation of nuclear factor kappa-B (NF- $\kappa$ B) and the subsequent production of cytokines, chemokines, growth factors, and antiapoptotic proteins have been found to be involved in cancer progression and chemoresistance (Inoue, 2007). Toll-like receptors are thought possibly the signal initiators for NF- $\kappa$ B activation and inflammation-induced carcinogenesis (Chen *et al.*, 2007).

BCL2/adenovirus E1B 19kD interacting protein like (*BNIP1*) is a gene located at chromosome 1q21.1. Overexpression of *BNIP1* has been reported to increase cell migration and invasion *in vitro* and promoted the metastasis of hepatocellular carcinoma (HCC) cells *in vivo*. Overexpression of *BNIP1* has also been shown to inhibit colony formation and cell proliferation in BEL-7402 cells. Their results indicated that *BNIP1* might inhibit cell growth and promote apoptosis (Shen *et al.*, 2003).

Paralkar and Wistow (1994) showed that the *MIF* gene is remarkably small; it has only 3 exons and covers less than 1 kb. The gene is localized to human chromosome 22q11.2. Intense MIF protein was observed in the metastatic prostatic adenocarcinoma and the human prostatic adenocarcinoma cell line, LNCaP. Higher expression of MIF in tumor tissues was detected to be significantly higher than that of normal lung tissue. (Tomiyasu *et al.*, 2002).



Growth factor, augmenter of liver regeneration (*GFER*) gene resides on chromosome 16, at 16p13.3-p13.12. Increased GFER serum levels were detected for various types of acute liver disease (Tanigawa *et al.*, 2000); in addition, increased expression of GFER in livers from patients with cirrhosis and hepatocellular and cholangiocellular carcinoma was reported (Thasler *et al.*, 2006).

There is increasing knowledge about the genetic basis of NPC. Tumor suppressor genes (e.g. *p16* and *ARF*) and oncogenes (e.g. *Bcl 2*) have been shown to be involved in the development of NPC (Kwok *et al.*, 2004). Despite the increasing knowledge about the genetic basis of NPC, proposed tumorigenesis model for NPC is not yet complete.

## **CHAPTER TWO**

### **LITERATURE REVIEW**

#### **2.1 Definition**

The nasopharynx is defined as that portion of the pharynx which lies behind the nasal fossae and extends inferiorly as far as the level of the soft palate (Prasad, 2000). Its role is solely respiratory, probably functioning as a collecting space where the inspired air is filtered of impurities by the lymphoid tissue (Hasselt and Gibb, 1999).

Nasopharynx comprises of two distinct components, an upper anterior segment which developmentally, morphologically and histologically has all the features of the nasal cavity and a lower portion which is developed from foregut and has similarities to the alimentary tract (Hasselt and Gibb, 1999).

The close proximity to the nose and pharynx, plus its connection with the middle ear via eustachian tube, identify the nasopharynx as the central hub around which the otorhinolaryngology revolves (Hasselt and Gibb, 1999).



## **2.2 Fossa of rosenmuller**

Immediately above and behind the tubal elevation lies the pharyngeal recess or fossa of Rosenmuller (Prasad, 2000). It extends laterally into the sinus of Morgagni immediately above the upper limit of the superior constrictor muscle of the pharynx (Prasad, 2000). The fossa is variable in size and depth and is conical or slit-like in shape (Prasad, 2000). Visualization of the fossa may be difficult. In children, the fossa is usually small and often obliterated with lymphoid tissue, while in adults fibrous trabeculae at the entrance may obscure the view, especially in cases where previous adenoidectomy has caused scarring of the area (Prasad, 2000). The fossa of Rosenmmuler is of great clinical importance since it represents by far the commonest site of origin of nasopharyngeal carcinoma (Prasad, 2000).

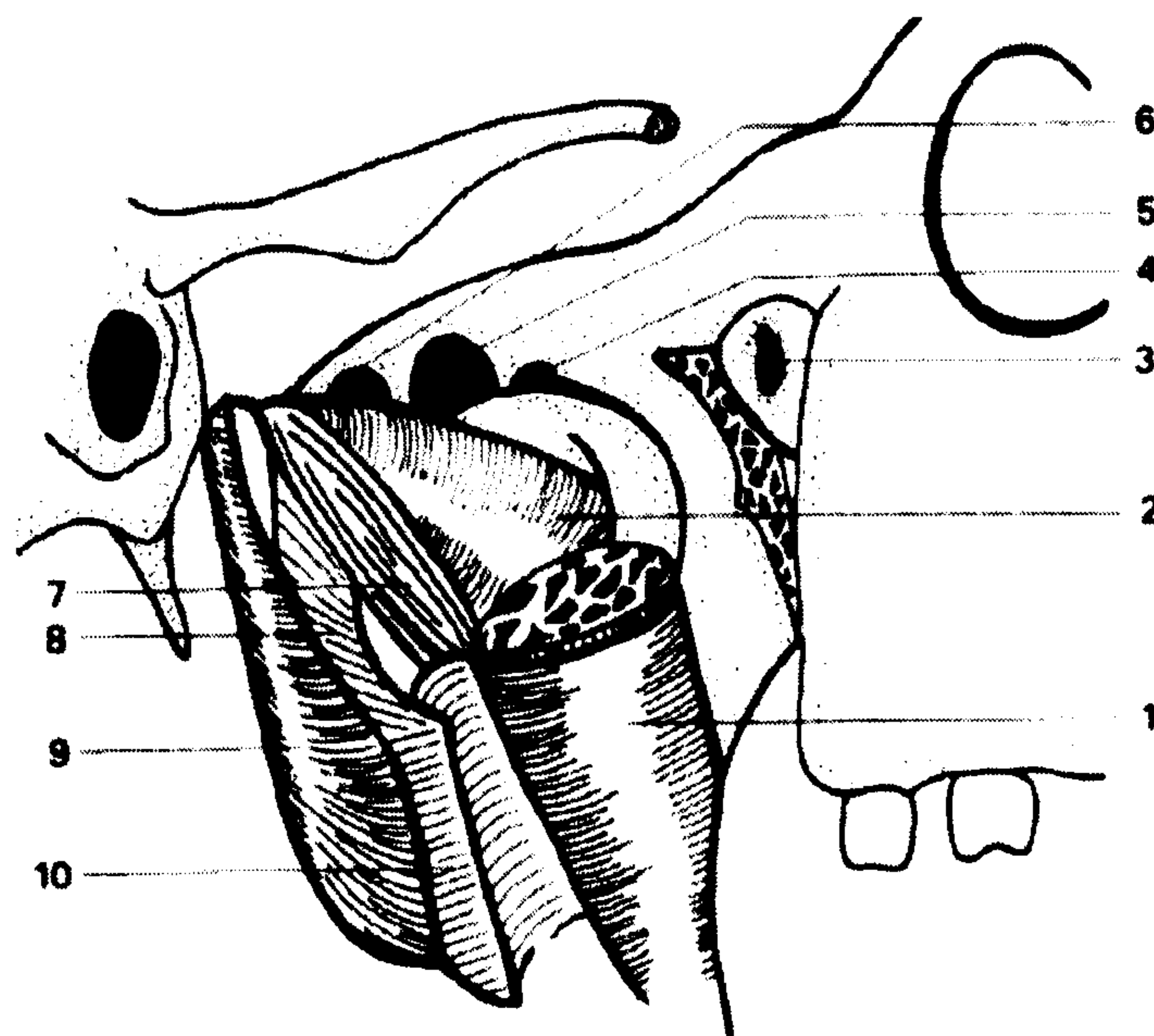


**Figure 2.1:** Lateral relations of the fossa of Rosenmuller (Taken from Hasselt and Gibb, 1999).

- 1 Tensor veli palatini ensheathed by pharyngeal fascia
- 2 Eustachian tube
- 3 Sphenopalatine foramen
- 4 Foramen rotundum
- 5 Foramen ovale
- 6 Foramen spinosum
- 7 Levator veli palatini muscle
- 8 Fascia covering external surface of fossa of rosenmuller
- 9 Superior constrictor muscle
- 10 External lamina of pharyngeal fascia  
(buccopharyngeal fascia)



## **2.3 Normal Histology**

Specimens obtained from the normal nasopharyngeal mucosa consists of columnar cells (ciliated or non-ciliated), goblet cells, squamous cells, reserve cells and lymphoid cells (Hasselt and Gibb, 1999).

Along the posterior wall, 80 to 90% of the surface area and about 60% of the anterior wall are lined by squamous epithelium (Prasad, 2000). The rest of the areas along these walls are lined by ciliated columnar epithelium. Along the lateral walls and the roof of the nasopharynx patches of pseudo-stratified ciliated columnar epithelium coordinates with the squamous epithelium (Prasad, 2000).

## **2.4 Histopathology**

Nasopharyngeal Carcinoma is a distinctive type of head and neck cancer. The World Health Organization (WHO) classification distinguishes three histopathological types of NPC based on the degree of differentiation (Lo *et al.*, 2004). Type I is keratinizing squamous cell carcinoma (SCC), similar to other head and neck cancer (Lo *et al.*, 2004). Type II is nonkeratinizing carcinoma, and Type III is undifferentiated carcinoma (Shanmugaratnam and Sobin, 1991). The undifferentiated carcinoma has a typical morphology with a prominent lymphoplasmacytic infiltrate, and is also referred as “lymphoepithelioma” (Lo *et al.*, 2004). Different prevalent histologic types of NPC are found in endemic and nonendemic regions (Lo *et al.*, 2004). In endemic areas such as Southern China, WHO Type III accounts for more than 97%, while keratinizing SCC is more common in the Western countries (~75%) (Marks *et al.*, 1998). Aside from differences in histological features, latent Epstein-Barr virus (EBV) infection is uniquely present in almost all NPC from endemic regions, but absent in WHO

Type I NPC from nonendemic regions (Raab-Traub, 2002). Alternative pathogenic processes of EBV- negative NPC, especially WHO Type I from Western populations, may be involved (Lo *et al.*, 2004).

## **2.5 Epidemiology and Incidence**

Nasopharyngeal carcinoma (NPC) is a disease that has remarkable racial and geographic distribution (Wei and Sham, 2005). This cancer is one of the most common cancers in Southeast Asia and southern China, while the disease is rare in most other parts of the world. In the year 2005, 85 248 new cases were registered worldwide, and more than 68% of those were reported from China and Southeast Asia (Parkin *et al.*, 2005). In China, NPC is prevalent in the southern part of China including Guangdong and other southern provinces (25 – 50/100 000) but less so among northern Chinese (3/100 000) (Lo *et al.*, 2004). Moreover, the incidence rate of NPC in southern China is nearly 100- fold higher than that in the Western world (McDermott *et al.*, 2001, Lo and Huang, 2002). In the context of Malaysia, NPC ranked second in terms of cancer prevalence among Malaysian Chinese males (Lim and Halimah, 2004). Malaysian Chinese are largely southern Chinese (Armstrong, 1979). High incidence of NPC has also been reported among the natives of Sarawak, East Malaysia (Devi *et al.*, 2004).

Early-age onset of NPC is observed in high-risk populations. Independent of race/ethnicity, men are 2- to 3-fold more frequently affected than women (Yu and Yuan, 2002). The dramatic difference in the incidence among populations and geographic areas suggests a strong association of NPC with genetic and environmental factors. An unusually early-age



onset in the high-risk populations implies that early events in life may be important (Lo *et al.*, 2004).

## **2.6 Etiologies**

The ethnic clustering of NPC in Southern Chinese strongly suggests the involvement of genetic susceptibility and environmental factors in its development (Lo *et al.*, 2004). Three major etiological factors, including genetic, environmental, and viral factors are as follows.

### **2.6.1 Genetic susceptibility factors**

Early linkage analysis on Chinese sib pair studies of NPC suggested the association of susceptibility human leukocyte antigen (HLA) haplotypes with NPC development (Lo *et al.*, 2004). The investigators hypothesized that some of the HLA antigens have reduced efficiency in activating host immune response to EBV infection, which plays a critical role in the pathogenesis of NPC (Lo *et al.*, 2004). Most studies conducted among Chinese showed that individuals with *HLA-A2* are at increased risk (Lo *et al.*, 2004). A recent high-resolution genotyping study has detected a consistent association between NPC and the prevalent Chinese A2 subtype (*HLA-A\*0207*), but not the prevalent Caucasian subtype (*HLA-A\*0201*) (Hildesheim *et al.*, 2002). Supported by affected sib pair haplotype sharing analysis and association study on HLA regions, a NPC susceptible gene/locus closely linked to the Major Histocompatibility Complex (MHC) region but distinct from the HLA genes was proposed (Lu *et al.*, 1990). However, recent linkage analysis of Chinese NPC pedigrees using highly polymorphic microsatellite markers further identified two susceptibility loci on chromosomes

4p15.1-q12 and 3p21, respectively, but not on MHC region (Feng *et al.*, 2002; Xiong *et al.*, 2004). Polymorphisms of genes for carcinogen metabolism (*CYP2E1*), detoxification (*GSTM1*), and DNA repair (*XRCC1* and *hOGG1*) were also reported to be associated with increased risk of NPC (Hildesheim *et al.*, 1997; Nazar-Stewart *et al.*, 1999; Cho *et al.*, 2003).

## **2.6.2 Environmental factors**

The traditional foods of Southern Chinese, such as Cantonese-style salted fish and other preserved foods containing volatile nitrosamines, are an important carcinogenic factor for NPC (Lo *et al.*, 2004). The childhood consumption of salted fish has been shown to be related to an increased risk of NPC in Southern Chinese (Yu and Yuan, 2002). In animal studies, rats nasal and nasopharyngeal tumors could be induced by a diet of Chinese salted fish (Huang *et al.*, 1978). These traditional diets may contain chemical carcinogens *eg.* nitrosamines that induce genetic damage in nasopharyngeal epithelial cells (Lo *et al.*, 2004). The decreasing trend in NPC incidences (~30%) in Hong Kong may be attributed to the change of traditional lifestyle, particularly the avoidance of feeding young children salted fish (Lo *et al.*, 2004). The use of Chinese medicinal herbs has been suggested to increase the risk for NPC by reactivating EBV infection in the host (Lo *et al.*, 2004). The association of NPC with other nondietary factors such as cigarette smoking or formaldehyde exposure is either weak or controversial (Lo *et al.*, 2004).



### **2.6.3 Epstein-Barr virus (EBV)**

In contrast to other head and neck cancer and epithelial malignancy in general, a unique feature of NPC is its strong association with EBV (Lo *et al.*, 2004). Higher EBV antibody titers, especially of IgA class, are observed in most NPC patients (Lo *et al.*, 2004). Latent EBV infection is identified in cancer cells of virtually all cases of NPC in endemic regions (Lo *et al.*, 2004). The clonal EBV genome is consistently detected in invasive carcinomas and high-grade dysplastic lesions (Raab-Traub and Flynn, 1986; Raab-Traub, 2002). Such observations imply that viral latent infection may have taken place before the expansion of the malignant cell clone (Lo *et al.*, 2004). A current hypothesis proposes that EBV plays a critical role in transforming nasopharyngeal epithelial cells into invasive cancers (Lo *et al.*, 2004).

## **2.7 Molecular alterations and pathogenesis**

### **2.7.1 Genetic and epigenetic events**

The genetic, environmental, and viral causative factors, either acting alone or in combination, would lead to multiple genetic and epigenetic alterations (Lo *et al.*, 2004). By comprehensive genome-wide studies, multiple genetic defects have been identified in this EBV-associated cancer. Consistently high frequencies of genetic losses are observed on chromosomes 3p, 9, 11q, 13q, 14q, and 16q, while recurrent chromosomal gains were identified on chromosome 12 (Hui *et al.*, 1999; Lo *et al.*, 2000). In particular, the inactivation of tumor suppressor genes on 3p, 9p, and 14q appears to be a critical event, since deletion of these chromosomal regions was detected in almost all microdissected NPC samples (Lo *et al.*, 2000). Genes located on

chromosomes 9p21 (*p14*, *p16*) and 3p21.3 (*RASSF1A*) were found to be defective due to deletion or promoter hypermethylation (Lo *et al.*, 1996; 2001; Kwong *et al.*, 2002).

Frequent promoter hypermethylation of cancer genes is an important feature of NPC (Lo *et al.*, 2004). Apart from the common tumor suppressors, such as *RASSF1A* and *p16*, genome-wide aberrant methylation disrupts multiple cellular functions through the inactivation of retinoid signaling pathway (e.g., *RARB2*), endothelin-1 pathway (e.g., *EDNRB*), cell adhesion (e.g., *E-cadherin*, *TSLC-1*), and other novel pathways (e.g., *HIN-1*) (Lo and Huang, 2002; Kwong *et al.*, 2002; Hui *et al.*, 2003). Such widespread hypermethylation in the NPC genome may imply a “methylator” phenotype of this EBV-associated cancer. Induction of epigenetic alterations of cellular genes was proposed as one of the mechanisms for enhancing the transformation of nasopharyngeal epithelial cells by EBV infection (Lo and Huang, 2002).

### **2.7.2 Alterations of subcellular mechanisms**

In NPC, multiple genetic abnormalities result in the disruption of various cellular mechanisms (Table 2.1). Alteration of cell cycle regulation by disrupting Rb and p53 pathways appears to be a critical event for NPC (Lo *et al.*, 2004). The *p16* gene, an important cell cycle regulator for Gap 1 (G1) restriction checkpoint, is inactivated in 62%–86% of primary tumors (Lo *et al.*, 2004). Loss of *p16* may result in constitutional Rb phosphorylation and uncontrolled proliferation of NPC cells (Lo *et al.*, 1996). On the other hand, in spite of the absence of *p53* mutation, functional disruption of p53 pathway through inactivation of *p14* and overexpression of truncated  $\Delta$ N-isoform of *p63* was common in this cancer (Crook *et al.*, 2000; Kwong *et al.*, 2002). Transcriptional silencing of the newly identified tumor



suppressor, *RASSF1A*, is found in a majority of NPCs, although it is rarely involved in other head and neck cancers (Lo *et al.*, 2004).

Aside from cell cycle regulation, multiple abnormalities associated with apoptosis and growth signals have been found. Consistent upregulation of B-cell lymphoma 2 (*Bcl2*) in precancerous lesions and invasive tumors suggests that alterations in apoptotic response are early events in the transformation pathway (Lu *et al.*, 1993). Overexpression of metallothionein (MT) and *Id1*, and loss of DAP-kinase may also contribute to the inhibition of apoptosis (Jayasurya *et al.*, 2000, Kwong *et al.*, 2002; Wang *et al.*, 2002). Specific activation of NF- $\kappa$ B p50 homodimer and overexpression of *Bcl3* may increase the proliferative capacity of NPC cells through transcriptional upregulation of target genes, such as epidermal growth factor receptor (*EGFR*) (Thornburg *et al.*, 2003). Furthermore, the c-Met tyrosine kinase, metalloproteinases (MMPs), and the hypoxia proteins such as HIF-1  $\alpha$  and CA IX were found to be overexpressed in the majority of NPCs and associated with the progression or metastasis of this cancer ( Hui *et al.*, 2002; Qian *et al.*, 2002; Lu *et al.*, 2003).

Of the ten preliminary down-regulated genes reported in nasopharyngeal carcinoma (Sim *et al.*, 2008, refer Table 2.2), two encode products that belong to the class of membrane receptors that are involved in cholesterol metabolism; two are ribosomal protein genes that code for the small ribosomal subunit proteins; one is a member of the Tumour Necrosis Factor receptor-associated factor (TRAF) gene family; two are enzyme-encoding (or enzyme domain-encoding) genes; and three are genes (section of genes) whose functions are yet to be properly characterised.

**Table 2.1: Major gene alterations in nasopharyngeal carcinoma**

Gene	Mechanisms	Frequencies	Chromosome regions	Refs
<b>Cell cycle regulation</b>				
<i>p16/CDNK2A</i>	Homozygous deletion and hypermethylation	62-86%	9p21	Lo <i>et al.</i> , 1996, 2001; Kwong <i>et al.</i> , 2002
<i>p14/ARF</i>	Homozygous deletion and hypermethylation	54%	9p21	same as above
<i>DN-p63</i>	Overexpression	100%	3q27-28	Kwong <i>et al.</i> , 2002; Crook <i>et al.</i> , 2000
<b>Apoptosis</b>				
<i>Bcl 2</i>	Overexpression	80%	18q21.3	Lu <i>et al.</i> , 1993
<i>DAP-kinase</i>	Hypermethylation	76%	9q34.1	Jayasurya <i>et al.</i> , 2000; Kwong <i>et al.</i> , 2002; Wang <i>et al.</i> , 2002
<b>Signal Transduction</b>				
<i>Bcl 3</i>	Overexpression	60%	19q13.1-13.2	Thornburg <i>et al.</i> , 2003
<i>EGFR</i>	Overexpression	85%	7p12	same as above
<b>Cell adhesion</b>				
<i>E-cadherin</i>	Hypermethylation	52%	16q22.1	Lo and Huang, 2002; Hui <i>et al.</i> , 2003
<i>TSLC 1</i>	Hypermethylation	34.20%	11q23.2	same as above
<b>Other novel pathways</b>				
<i>RASSF1A</i>	Hypermethylation and mutation	67-83%	3p21.3	Lo <i>et al.</i> , 2001; Kwong <i>et al.</i> , 2002
<i>RARB2</i>	Hypermethylation	80%	3p24	Lo and Huang, 2002; Kwong <i>et al.</i> , 2002; Hui <i>et al.</i> , 2003



**Table 2.2:** Preliminary findings of down-regulated genes in nasopharyngeal carcinoma (Sim *et al.*, 2008).

GenBank acc. no. (& chr. location)	Name of gene / gene product
NM_203346 (2q36-q37.2)	high density lipoprotein binding protein ( <i>HDLBP</i> ), vigilin
BC017905 (15q26.1)	abhydrolase domain containing 2 ( <i>ABHD2</i> )
NM_152789 (7q21.2)	family with sequence similarity 133, member B ( <i>FAM133B</i> )
BC022834 (3p25.3)	protein weakly similar to serine/threonine kinase Kp78
NM_001013693 (1p36.12)	low density lipoprotein receptor class A domain containing 2 ( <i>LDLRAD2</i> )
NM_004651 (Xp11.23)	ubiquitin specific peptidase 11 ( <i>USP11</i> )
NM_001029 (12q13)	ribosomal protein S26 ( <i>RPS26</i> )
AL354862 (9q22)	Human DNA sequence from clone RP11-83L6 14 on chromosome 9 Contains an olfactory receptor pseudogene, the SYK gene for spleen tyrosine kinase and a CpG island
NM_001030 (1q21)	ribosomal protein S27 (metallopanstimulin-1), mRNA Kp78
AY228337 (11p12)	TNF receptor-associated factor 6 ( <i>TRAF6</i> )

### 2.7.3 Roles of EBV latent infection

As a cancer-associated herpesvirus, EBV infects over 90% of the world's population (Lo *et al.*, 2004). After primary infection at early age, persistent EBV latent infection is found in some resting B cells, but not in the nasopharyngeal epithelia of healthy individuals (Lo *et al.*, 2004). The mechanisms for EBV entry into epithelial cells and maintenance of latency remain poorly understood. Recent evidence demonstrated the association of distinct lytic promoter sequence variation with NPC in Southern Chinese and suggested the participation of a lytic-latent switch of EBV in NPC carcinogenesis (Tong *et al.*, 2003). In NPC cells, the virus is in the form of episome and not integrated into the host genome. EBV adopts a specific form of latent infection, latency II, in NPC cells (Lo *et al.*, 2004). Only limited viral genes, including *EBERs*, *EBNA1*, *LMP1*, *LMP2*, *BARF1*, and several *BamH1A* transcripts are expressed (Raab-Traub, 2002). *LMP1* and *BARF1* have profound effects on cellular gene expression and may contribute to EBV-mediated tumorigenesis (Lo *et al.*, 2004). *LMP1* is considered to be a viral oncogene, since it shows transforming activity in various cell types *in vitro*. Expression of *LMP1* in immortalized nasopharyngeal epithelial cells induces an array of genes involved in growth stimulation, enhanced survival, and increased invasive potentials (Lo *et al.*, 2004). *BARF1* is able to immortalize primate epithelial cells and enhance growth rate of the transfected cells (Wei *et al.*, 1997). Nevertheless, *in vitro* EBV infection of nasopharyngeal epithelial cells did not result in apparent growth stimulation or changes in cell cycle and apoptosis (Lo *et al.*, 2004). In contrast, enhancement in invasiveness and migration of the infected cells was observed (Lo *et al.*, 2004). It appears that EBV infection may promote tumorigenicity of NPC cells by enhancing its invading activity (Lo *et al.*, 2004). Moreover, EBV-infected normal nasopharyngeal epithelial cells were not able to form tumors



in nude mice. Thus, in addition to EBV, other somatic genetic changes or epigenetic events appear to be necessary for the malignant transformation of nasopharyngeal epithelial cells (Lo *et al.*, 2004).

#### **2.7.4 Carcinogenesis of NPC**

Preinvasive lesions in the nasopharynx are rarely encountered in clinical settings; however, such preinvasive dysplastic lesions are considered to precede the development of invasive NPC (Lo *et al.*, 2004). High frequencies of chromosome 3p and 9p deletions were found in both low-grade and high-grade dysplastic lesions (Chan *et al.*, 2000; 2002a). However, EBV infection is consistently observed in NPC and high-grade but not low-grade dysplastic lesions (Lo *et al.*, 2004). These findings suggest that the involvement of those specific genetic changes precedes EBV infection during the initiation of NPC development (Lo *et al.*, 2004). Furthermore, chromosome 3p and 9p deletions were also commonly observed in histologically normal nasopharynx epithelia from Southern Chinese, the high-risk population (Lo *et al.*, 2004). Disruption of the NPC-associated tumor suppressor genes on these critical regions, such as *p16* and *p14* on 9p21 and *RASSF1A* on 3p21.3, may lead to immortalization and clonal proliferation of multiple genetic lesions in the nasopharyngeal mucosa during the initiation stage (Lo *et al.*, 2004). On the other hand, early genetic changes may predispose the epithelial cells to EBV infection or persistent maintenance of latent cycle (Lo *et al.*, 2004). Expression of latent genes in the EBV-infected cells may enhance its transformation capacities and, subsequently, clonal expansion may result in the rapid progression to invasive carcinoma (Figure 2.9) (Lo *et al.*, 2004).



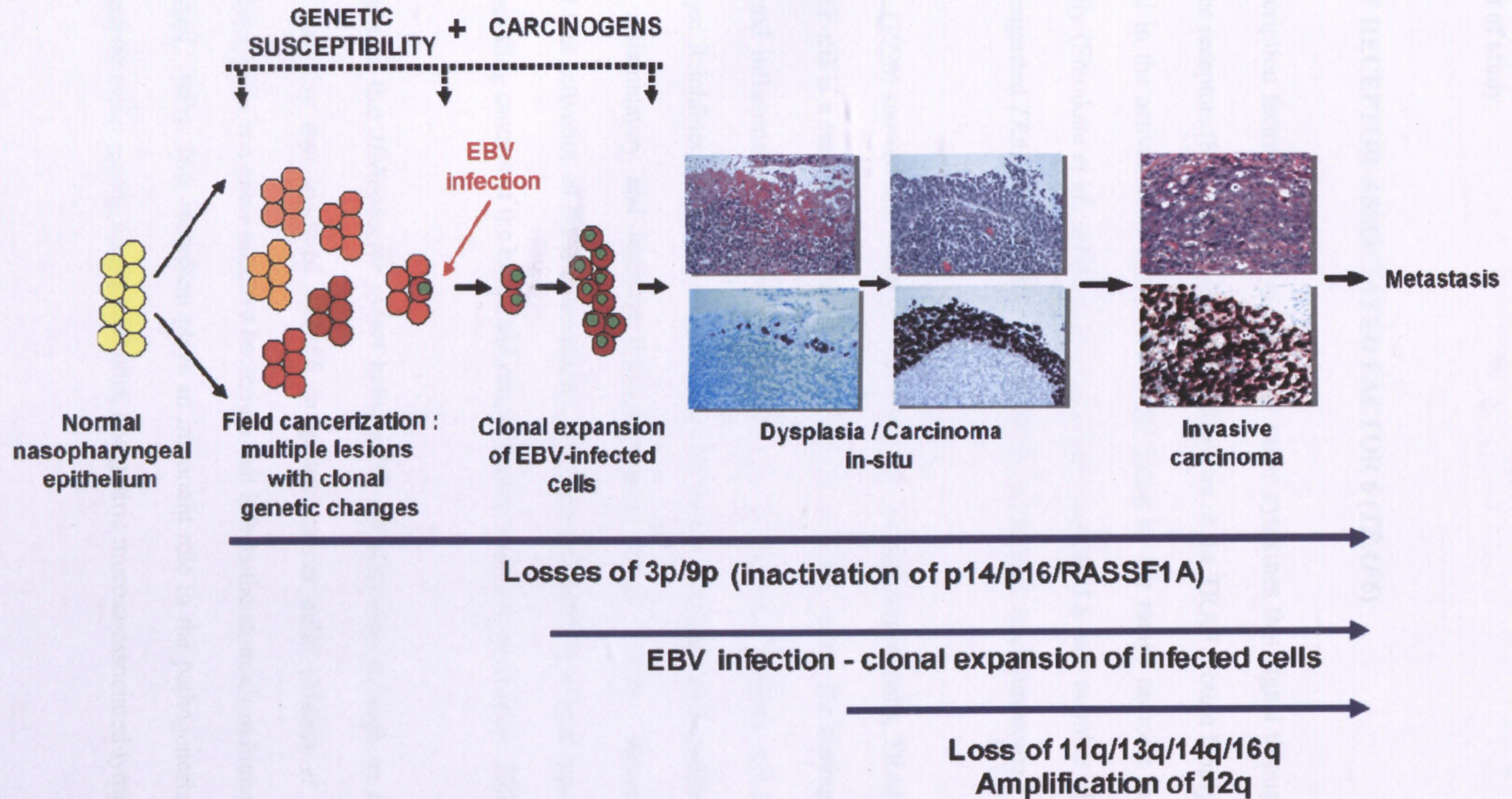


**Figure 2.2:** Multistep carcinogenesis of nasopharyngeal carcinoma (Source: Lo *et al.*, 2004)



## **2.8 Genes of study**

### **2.8.1 TNF RECEPTOR-ASSOCIATED FACTOR 6 (*TRAF6*)**

The transcription factor NF- $\kappa$ B is activated by many cytokines that signal through different cell surface receptors (Shirakata *et al.*, 2001). Members of the TRAF protein family have been implicated in the activation of this transcription factor by the tumor necrosis factor (TNF) superfamily (Shirakata *et al.*, 2001). Cao *et al.* (1996) identified a new member of the TRAF family, designated *TRAF6*. Gene *TRAF6* is 26.56 kb and located on chromosome 11 at 11p12.

Cao *et al.* (1996) showed that when overexpressed in cultured human cells, TRAF6 activates NF- $\kappa$ B. NF- $\kappa$ B is a transcription factor that serves as a master switch for turning on certain immune and inflammatory responses (Dolcet *et al.*, 2005). NF- $\kappa$ B alters cell behavior in many ways; it inhibits apoptosis (programmed cell death), increases cell proliferation, and increases inflammatory and immune response (Dolcet *et al.*, 2005). Recent evidence suggested that activation of NF- $\kappa$ B contributes to the development of several types of human cancer, including cancers of the blood and certain breast cancers (Dolcet *et al.*, 2005).

It was reported that *Helicobacter pylori* induces NF- $\kappa$ B activation through an intracellular signaling pathway that involved TRAF6 in gastric cancer cells (Maeda *et al.*, 2000). *Helicobacter pylori* is a gram-negative bacterium that infects the stomach in humans (Warren and Marshall, 1983). This bacterium plays an important role in the pathogenesis of chronic gastritis, peptic ulcer, gastric adenocarcinoma, and gastric mucosa-associated lymphoid tissue



lymphoma (Graham *et al.*, 1992; Parsonnet *et al.*, 1991; Nomura *et al.*, 1991; Forman *et al.*, 1991).

Overexpression of TRAF5 and/or TRAF6 has been found to suppress *oriP* activity that maintains Latent Epstein-Barr virus (EBV) (Shirakata *et al.*, 2001). EBV, discovered more than 40 years ago from a Burkitt's lymphoma biopsy, was the first virus to be directly associated with human cancer (Pattle and Farrell, 2006). The virus has been reported in different types of human cancer, particularly Burkitt's lymphoma, Hodgkin's lymphoma, lymphomas and lymphoproliferative diseases in the immunocompromised, and nasopharyngeal and gastric carcinoma (Pattle and Farrell, 2006). Activation of TRAF6 signal cascade has been reported resulting in loss of EBV from Burkitt's lymphoma cell line Akata (Shirakata *et al.*, 2001).

TRAF6 was identified to regulate Akt activation (Yang *et al.*, 2009). Akt is a signaling protein that plays a central role in numerous biological functions, including cell growth and programmed cell death, or apoptosis (Yang *et al.*, 2009). Deregulated Akt expression has been reported to contribute to cancer development (Yang *et al.*, 2009). A mutant form of Akt implicated in human breast cancer was analysed and it was demonstrated that increased Akt ubiquitination (activation) contributed to the hyperactivation of Akt in the mutant cells (Yang *et al.*, 2009). *TRAF6* depletion in prostate cancer cells was shown to reduce Akt activation and mice with *TRAF6* knocked down developed smaller prostate cancer tumors than those with active *TRAF6* (Yang *et al.*, 2009).

### **2.8.2 HIGH DENSITY LIPOPROTEIN-BINDING PROTEIN (HDLBP) /Vigilin**

The entire vigilin gene spans a region of about 50 kb and has been assigned to chromosome 2q36-q37.2 (Plenz *et al.*, 1994). The vigilin gene is localized in a chromosomal region comprising a cluster of collagen genes (COL1A3, COL1A3) and the locus of the Waardenburg syndrome I. Only one mRNA species of 4.4 kb is transcribed from the human vigilin gene (Plenz *et al.*, 1994).

Vigilin was shown to bind to a region of the vitellogenin mRNA 3'-untranslated region (3'-UTR) implicated in estrogen-mediated stabilization (Cunningham *et al.*, 2000). The vigilin-binding site in the vitellogenin B1 mRNA 3'-UTR contains two consensus mRNA endonuclease PMR-1 cleavage sites (Cunningham *et al.*, 2000). Their results provide direct evidence for differential susceptibility to endonuclease-mediated mRNA decay resulting from the differential affinity of a RNA-binding protein for *cis*-acting stability determinants.

RNA binding proteins may act either directly to alter translational efficiency or indirectly by bridging proteins together on the mRNA (Audic and Hartley, 2004). They may also serve to tag a mRNA for rapid deadenylation or degradation or to protect it from nucleases (Audic and Hartley, 2004). Competition between protection or degradation factors or translation activators/inhibitors will ultimately determine the overall amount of protein produced by one mRNA (Audic and Hartley, 2004). It is probable that different RNA-protein complexes are formed on different mRNAs (Audic and Hartley, 2004). In the human genome there are about 500 proteins containing known RNA binding domains (Anantharaman *et al.*, 2002). Mutations in *cis*-regulatory elements or aberrant expression of RNA binding protein can modify the regulation of a given mRNA as can modulation of signalling pathways that post-translationally modify RNA-BPs or other associated proteins (Audic and Hartley, 2004).



These alterations occur in diverse cancer types and are often correlated with advanced stage and grade of tumors, resulting in misregulation of genes involved in cancer progression (Audic and Hartley, 2004).

Woo *et al.* (2010) identified the 69nt *c-fms* mRNA 3'UTR sequence as a cellular vigilin target through which vigilin inhibits the expression of *c-fms* mRNA and protein. *C-fms* is expressed by the tumor epithelium in several human epithelial cancers (Kacinski *et al.*, 1991; Chamber *et al.*, 1997; Chambers, 2009). Activation and overexpression of *c-fms* in breast cancer confers invasive and metastatic properties (Lin *et al.*, 2001; Toy *et al.*, 2005). Studies by Woo *et al.* (2010) showed that vigilin decreased *c-fms* mRNA stability. Furthermore, vigilin inhibited *c-fms* translation. Vigilin suppresses cellular motility and invasion of breast cancer cells. Based on these observations, they suggested a role for vigilin in suppression of breast cancer progression.

### 2.8.3 BCL2/ADENOVIRUS E1B 19-KD PROTEIN-INTERACTING PROTEIN 2-LIKE (*BNIPL*)

Using a high-throughput transfection screen for suppressors of cell growth from a human placental cDNA library, followed by 5-prime RACE, Qin *et al.* (2003) independently cloned *BNIPL*. They identified 2 alternatively spliced isoforms that used different start codons: a deduced 275-amino acid isoform, *BNIPL1* and a longer 357-amino acid isoform, *BNIPL2*, containing 82 additional N-terminal amino acids, followed by the 275-amino acid sequence identical to *BNIPL1*. By radiation hybrid analysis, Qin *et al.* (2003) mapped the *BNIPL* gene to chromosome 1q21.1.

*BNIPL-2* was demonstrated to interact with *Bcl-2* and *Cdc42GAP* through a BCH domain (Qin *et al.*, 2003). *BNIPL-2* protein was proposed to play an important role in regulation of both pathways for DNA fragmentation and for formation of membrane blebs in apoptotic cells (Qin *et al.*, 2003).

It was found that *BNIPL* interacted with MIF and GFER through a yeast two-hybrid system (Shen *et al.*, 2003). The interactions were confirmed by glutathione *S*-transferase pull-down assay *in vitro* and co-immunoprecipitation assay *in vivo*.

Overexpression of *BNIPL-2* has been reported to increase cell migration and invasion *in vitro* and promoted the metastasis of hepatocellular carcinoma (HCC) cells *in vivo* (Xie *et al.*, 2007). Nude mice implanted with tumor graft transfected stably with *BNIPL-2* showed increased rates of intrahepatic and pulmonary metastasis (Xie *et al.*, 2007). It was found that the hepatocellular carcinoma MHCC97-L cells transiently transfected with *BNIPL-2* were more irregular in shape (Xie *et al.*, 2007). *BNIPL-2* induced filopodia formation in almost



50% of the transfected cells (Xie *et al.*, 2007). The data revealed that *BNIP-2* caused the increase in Cdc42 activity and the formation of filopodia, which led to cell migration and cancer metastasis.

*BNIP-2* overexpression in Hep3B human hepatoma cells has been reported to alter the expression level of 15 genes, of which 8 genes involving in growth inhibition (*IGFBP-1*, *TGF- $\beta$* ) or cell apoptosis (*p21*, *E2A*) were up-regulated (Xie *et al.*, 2004). Overexpression of *BNIP-2* has also been shown to inhibit colony formation and cell proliferation in hepatocellular carcinoma BEL-7402 cells (Shen *et al.*, 2003). Their results indicated that *BNIP-2* might inhibit cell growth and promote apoptosis (Shen *et al.*, 2003).

#### **2.8.4 MACROPHAGE MIGRATION INHIBITORY FACTOR (*MIF*)**

Migration inhibitory factor for guinea pig macrophages was the first lymphokine to be discovered (Bloom and Bennett, 1966; David, 1966). Weiser *et al.* (1989) isolated a cDNA encoding human macrophage migration inhibitory factor. By Northern blot analysis, Paralkar and Wistow (1994) demonstrated a single size of *MIF* mRNA (about 800 nucleotides) in all human tissues examined. Paralkar and Wistow (1994) showed that the *MIF* gene is remarkably small; it has 3 exons separated by introns of only 189 and 95 bp, and covers less than 1 kb. Budarf *et al.* (1997) performed somatic cell hybrid panel PCR with human-specific primers to localize the gene to human chromosome 22q11.2.

An immunohistochemistry study showed that intense MIF protein was observed in the metastatic prostatic adenocarcinoma and the human prostatic adenocarcinoma cell line LNCaP (Meyer *et al.*, 1998). Using quantitative ELISA, MIF expression was found to be at least three times higher in metastatic adenocarcinoma than in normal, benign prostatic hyperplasia (BPH), or focal carcinoma in the adult prostate (Meyer *et al.*, 1998).

Cell growth rate of human melanoma G361 cells transfected with an antisense human *MIF* plasmid was shown to be markedly suppressed (Shimizu *et al.*, 1999). In a migration assay, MIF was found to enhance the migration of G361 cells in a dose-dependent manner (Shimizu *et al.*, 1999). Tumor -bearing mice administered with anti-MIF antibody showed suppressed tumor-induced angiogenesis (Shimizu *et al.*, 1999).

Mean copy number of *MIF* mRNA in tumor tissues was detected to be significantly higher than that of normal lung tissue (Tomiyasu *et al.*, 2002). Higher expression of *MIF* was also found in male lung cancer patients and heavy smokers (Tomiyasu *et al.*, 2002). It was



revealed that higher expression of *MIF* mRNA in patients with squamous cell carcinomas was significantly associated with unfavorable prognosis (Tomiyasu *et al.*, 2002). NPC cell lines, CNE-1 and CNE-2 treated with *MIF* showed increased invasion ability as compared with that of non-*MIF* treated NPC cells (Li *et al.*, 2004).

Expression of MIF was observed to correlate with both tumor differentiation and lymph node status in patients with Esophageal Squamous Cell Carcinoma (ESCC) (Ren *et al.*, 2005). It was suggested that through its effects on VEGF and IL-8, MIF serves as an autocrine factor in angiogenesis and plays an important role in the pathogenesis of Esophageal Squamous Cell Carcinoma (ESCC) (Ren *et al.*, 2005).

*MIF* was identified to be upregulated in pathologically-confirmed cases of poorly-differentiated NPC tissues (Fang *et al.*, 2008). *MIF* upregulation was suggested to be involved in the promotion of the malignant conversion of nasopharyngeal epithelium (Fang *et al.*, 2008).

Transgenic (Tg) mice overexpressing MIF showed an early onset of carcinogenesis and a higher tumor incidence after chronic UVB irradiation compared to wild-type (WT) mice (Honda *et al.*, 2009). UVB-induced apoptosis of epidermal keratinocytes was observed to be inhibited in the *MIF* Tg mice (Honda *et al.*, 2009). A decrease in the expression of apoptosis-regulatory genes (*i.e.*, p53 and bax), in the *MIF* Tg mice after UVB irradiation was also observed. A previous study by Kitaichi *et al.* (2008) has confirmed that similar protective effects were observed in the corneas of *MIF* Tg mice in response to acute UVB light. Similarly, other studies reported that *MIF*-deficient mice showed a significant increase in p53 activity and reduced tumor incidence compared to WT mice after acute and chronic exposure

to UVB radiation, respectively (Martin *et al.*, 2009). MIF has also been shown to have an inhibitory effect on UVB-induced photo-damage by blocking the expression of apoptosis-regulatory genes (Honda *et al.*, 2009). Roles of MIF with regard to UV-induced skin cancer has also been suggested.

### **2.8.5 GROWTH FACTOR, AUGMENTER OF LIVER REGENERATION (*GFER*)**

*GFER* is thought to be one of the factors responsible for the extraordinary regenerative capacity of mammalian liver. It has also been called hepatic regenerative stimulation substance (HSS). The gene resides on chromosome 16, at 16p13.3-p13.12 in the interval containing the locus for polycystic kidney disease (PKD1). The putative gene product is 42% similar to the scERV1 protein of yeast. The yeast scERV1 gene had been found to be essential for oxidative phosphorylation, the maintenance of mitochondrial genomes, and the cell division cycle. The human gene is both the structural and functional homolog of the yeast *scERV1* gene.

Treatment of primary human hepatocytes with *GFER* resulted in reduced P450 enzyme protein and mRNA expression (Thasler *et al.*, 2006). Reduction of *P450* gene expression in association with liver disease and liver regeneration were widely studied (Morgan, 2001; Villeneuve and Pichette, 2004). Increased *GFER* serum levels were detected for various types of acute liver disease (Tanigawa *et al.*, 2000). In addition, increased expression of *GFER* in livers from patients with cirrhosis and hepatocellular and cholangiocellular carcinoma was reported (Thasler *et al.*, 2006).

Effects of *GFER* depletion in hepatocytes by antisense oligonucleotide transfection revealed apoptosis as the predominant cause of cell death (Thirunavukkarasu *et al.*, 2008). It was



suggested that *GFER* is critically important for the survival of hepatocytes (Thirunavukkarasu *et al.*, 2008).

*GFER* expression was found to be up-regulated in both hepatocellular carcinoma (HCC) tissues and multiple hepatoma cell lines and correlated significantly with increased radiation clonogenic survival after radiation treatment (Cao *et al.*, 2009). Exogenous expression of *GFER* increased radiation resistance in human hepatoma cells SMMC-7721, and the increased survival was accompanied by a decrease in apoptosis and a prolonged G(2)-M arrest after irradiation (Cao *et al.*, 2009).

Knockdown of *GFER* by small interfering RNA (siRNA) resulted in inhibition of viability in the absence of exogenously added oxidative stress and radiation sensitization in human liver carcinoma cell line HepG2 cells (Cao *et al.*, 2009). *GFER* expression was detected at very low levels in normal hepatocyte L02 cells, and *GFER* silencing had a minimal effect on L02 viability and radiation sensitivity. Their results indicated that human *GFER* is important for hepatoma cell viability and is involved in the protection of hepatoma cells against irradiation-induced damage. It has been suggested that targeting *GFER* may be a promising novel approach to enhance the radiosensitivity of hepatoma cancers (Cao *et al.*, 2009).

*GFER* has been reported among other genes as potential new candidate oncogenes for epithelial ovarian cancer (Zheng *et al.*, 2004). *GFER* was found to be overexpressed in the study of cDNA microarray (Zheng *et al.*, 2004) to seek differentially expressed genes among 3 subtypes of ovarian tumors (serous borderline ovarian tumors, serous ovarian cancers, and endometrioid ovarian carcinomas).

## 2.9 Rationale

Like some of the solid tumors, NPC is believed to arise as a consequence of multiple molecular events induced by environmental factors and EBV infection. The neoplastic process may involve alterations of the tumor suppressor genes and oncogenes by genetic damage and interference with the normal cellular functions. The accumulation of somatic changes in the NPC cells have been investigated by way of cytogenetics and molecular genetic approaches (Hasselt and Gibb, 1999). Although the studies have led to the identification of many consistent changes affecting chromosomal regions and individual genes, the genetic basis for the tumorigenesis of this cancer is poorly understood.

Preliminary findings by Sim *et al.* (2008) identified vigilin and *TRAF6* mRNA to be differentially expressed via the GeneFishing<sup>TM</sup> Differential Expressed Genes (DEG) Analysis techniques. Microarray-based transcriptional profiling carried out by other members in our group showed down expression of *BNIP2* (0.176 fold change) (unpublished data) whereas MIF and GFER were reported to interact with BNIP1 via yeast two-hybrid system (Shen *et al.*, 2003). Deregulation of these genes may be implicated in the multistep progression of NPC. Therefore, this project aimed to study the expression (transcript and protein level) and cDNA mutational analysis of the selected differentially expressed genes which were identified in our previous study.



## **2.10 Research objectives**

The objectives of the study were:

- a. To determine the transcript (mRNA) level of *TRAF6*, *vigilin*, *BNIP1L2*, *MIF* and *GFER* in normal and tumor nasopharyngeal samples via PCR approach
- b. To perform protein expression study of TRAF6 and *vigilin* via Western blot
- c. To perform mutation analysis of cDNA coding region of genes that show differential expression at transcriptional level
- d. To delineate the role(s) of these genes as tumour enhancing or tumour suppressive genes in NPC tumourigenesis.

## **CHAPTER THREE**

### **MATERIALS AND METHODS**

#### **3.1 Tissue specimens**

##### **3.1.1 Sources of total RNA samples**

Total RNAs for normal and tumour samples in this study comprised of local biopsies (provided by Sarawak General Hospital and Hospital Serian Sarawak) and NPC cell lines (HONE, HK1 and SUNE1) and normal NP 69 cell line. The biopsy samples were generally designated as T for tumor and N for normal. Details of the total RNAs are listed in Table 3.1 and 3.2.



**Table 3.1** List of total RNA from biopsy tissues and their source information

No	Sample name	Sex	Ethnic	Type
1	T20, N20	M	Iban	Undifferentiated
2	T22, N22	M	Chinese	Undifferentiated
3	T24, N24	M	Iban	Undifferentiated
4	T27, N27	M	Malay	Non keratinising
5	T41, N41	M	Bidayuh	Undifferentiated
6	T48, N48	M	Malay	Non keratinising
7	T55, N55	F	Ulu	Non-keratinising
8	T67, N67	M	Bidayuh	Non keratinising
9	T96, N96	M	Bidayuh	Undifferentiated

**Table 3.2** List of total RNA from NPC cell lines (HONE, HK1 and SUNE1) and normal NP 69 cell line

No	Sample name	Type
1	HONE1	poorly differentiated
2	HK1	undifferentiated
3	SUNE1	poorly differentiated
4	NP69	normal nasopharyngeal

### **3.1.2 Isolation of total RNA**

The total RNAs were isolated using Trizol method. According to the method, 50-100 mg of frozen tissue was transferred into a 1.5 ml tube with 1 ml TRIzol (GIBCO BRL) and homogenized for 60 sec in the polytron. Two hundred microlitres of chloroform was then added and mixed by inverting the tube for 15 sec. The mixture was incubated for 3 min at room temperature followed by centrifugation at 12,000 g for 15 min. The aqueous phase was transferred into a fresh Eppi tube. Five hundred microlitres of isopropanol was added and centrifuged at max. 12,000 g for 10 min in the cold room. The pellet was washed with 500  $\mu$ l 70 % ethanol followed by centrifugation at 7500 g for 5 min in the cold room. The pellet was air-dried for 10 min and then dissolved in 30-100  $\mu$ l DEPC-H<sub>2</sub>O.

### **3.1.3 Total RNA analysis and quantification**

The quality of the total RNAs was assessed using agarose gel electrophoresis system. The gel was prepared using Ultra Pure DNA Grade Agarose (Bio-Rad, USA) powder and 1X TAE buffer. Ethidium bromide staining solution (0.5 $\mu$ g/ml) was added into the gel prior casting of the gel. Electrophoresis was performed with 1.0% (w/v) agarose gels for an hour at 100 V in 1X TAE buffer. All buffer used for RNA work was treated with 0.1% (v/v) diethyl pyrocarbonate (DEPC). The stained gels were visualized under ultraviolet light and documented using Red<sup>TM</sup> Imaging System (Alpha Innotech, USA). The isolated RNAs were quantified using Amersham Pharma Ultrospec® 1100 *pro* UV/Visible Spectrophotometer (Biochrom, England) at wavelengths of 230, 260 and 280 nm. Spectrophotometric assay was performed in a 25-times dilution factor by adding 2  $\mu$ l of RNA sample and 48  $\mu$ l of nuclease free water into a quartz cuvette.



### **3.2 Oligonucleotides**

All the cDNA oligonucleotide primers used in conventional PCR and mutational analysis were designed using Primer3.0 program developed by Whitehead Institute for Biomedical Research (Rozen and Skaletsky, 2000) and is freely available online ([http://frodo.wi.mit.edu/cgi-bin/primer3/primer3\\_www.cgi](http://frodo.wi.mit.edu/cgi-bin/primer3/primer3_www.cgi)) while oligonucleotide primers used in quantitative PCR were designed using qPrimerDepot developed by National Cancer Institute, National Institutes of Health, USA (<http://primerdepot.nci.nih.gov>). The oligonucleotides were synthesized by Research Biolabs (Singapore). Details of the primers are shown in Table 3.3, 3.4 and 3.5.

**Table 3.3.** List of synthetic oligonucleotide primers designed for amplification of vigilin, *TRAF6*, *BNIP1L2*, *MIF*, *GFER*, *GAPDH*, and *ACTB* in semi-quantitative reverse transcription polymerase chain reaction (RT- PCR)

Primer name	Sequence (5' to 3')	Ta (°C)	Expected Product size (bp)
Vig F Vig R	CATTGAGGACCTGGAAGCTC TCTCCTGGACAACCTGGCTCT	55	336
TRAF6 F TRAF6 R	AGGGATGCAGGTCACAAATG TGCCAAAGGACAGTTCTGGT	50	262
BNIP1L2 F BNIP1L2 R	CTAGGAGCAGCCCTGAGACA CAGGAGAGGAAGGTGCAGAC	52	277
MIF F MIF R	CTCCTGGTCCTTCTGCCATC GCTTGCTGTAGGAGCGGTTC	52	255
GFER F GFER R	CGACCTCCGATTCTCCTGTC GGCACAGCCACTGTGTGAAG	52	351
GAP F GAP R	AGCGAGATCCCTCCAAAATC TGTGGTCATGAGTCCTTCCA	50	296
ACTB F ACTB R	GGACTTCGAGCAAGAGATGG AGCACTGTGTTGGCGTACAG	55	234



**Table 3.4.** List of synthetic oligonucleotide primers designed for amplification of vigilin, *TRAF6* and *BNIP1L2* in mutational analysis

Primer name	Sequence (5' to 3')	Ta (°C)	Expected Product size (bp)
Vig_1 F Vig_1 R	ACGGACCTTCTGGCTACTGA GGAGACGGTGAAGCTATTGG	62	1169
Vig_2 F Vig_2 R	CCATTGCAGTGGAAGTGAAG GAGCTGCTTCTTGGCCTTCT	62	1259
Vig_3 F Vig_3 R	TCGACCTTCCAGCAGAGAAT TGGTTCCCATCGTCCTTATC	62	1444
Vig_4 F Vig_4 R	AAGGAAGCTCTGGAGGCATT AACAATTTACGGAGGGTCCA	62	1020
TRAF6_1F TRAF6_1R	CAGTGTCTGTGTCCGTCCTC AGGCGACCCTCTAACTGGTG	58	1135
TRAF6_2F TRAF6_2R	GGATTGTCCAAGGAGACAGG TGAGAACAGGGCAAGGAAAG	58	1096

**Table 3.5.** List of synthetic oligonucleotide primers designed for amplification of vigilin, *TRAF6*, and *GAPDH* in quantitative PCR

Primer name	Sequence (5' to 3')	Ta (°C)	Expected Product size (bp)
Gap_Q1 F Gap_Q1 R	AAGGTGAAGGTCGGAGTCAA AATGAAGGGGTCATTGATGG	60	108
TRAF6_Q3F TRAF6_Q3R	AGATGATAGTGTGGGTGGAAC GATGGGGCATTCTACTTGCTT	60	121
Vig_Q1 F Vig_Q1 R	GAAAGCTCGGAAGGACATTG GCCAATAACAAAGCGATGGT	60	91

### **3.3 Semi-quantitative RT-PCR**

#### **3.3.1 Preparation of first strand cDNA templates**

Total RNA (2 µg) from local biopsy samples were reverse transcribed using 200 units of Moloney Murine Leukemia Virus (MMLV) RT enzyme (Promega, USA) in the presence of 0.5 µg Oligo(dt)15 primer (Promega, USA), 1 X MMLV buffer, 25 units of RNasin® Plus RNase Inhibitor, 0.5 mM dNTPs and sterile nuclease-free water to a final reaction volume of 25 µl. The mixture was preheated at 70°C for 10 min to denature secondary structures, followed by 1 hour incubation at 42°C for reverse transcription. The reaction was terminated by heating at 70°C for 15 min. The cDNA stock was stored at -20°C.

#### **3.3.2 Polymerase Chain Reaction (PCR)**

One microliter of freshly prepared first strand cDNA templates was amplified in a total 25 µl PCR reaction volume. The PCR reaction was performed using PTC-200 Peltier Thermal Cycler (MJ Research, USA). The PCR products were electrophoresed on the ethidium bromide pre-stained agarose gel in 1 X TAE buffer and were visualized under ultraviolet light. Images were acquired using Red™ Imaging System (Alpha Innotech, USA). Details of the PCR components setup and cycling conditions are listed in Table 3.6 and 3.7.



**Table 3.6** Conventional PCR reaction setup

Component	volume/reaction	Final concentration
5x Taq buffer	5ul	1x
MgCl <sub>2</sub>	1.5ul	1.5mM
dNTP	0.5ul	0.2mM each
Primer (For)	1ul	1uM
Primer (Rev)	1ul	1uM
Taq	0.125ul	0.625 units
Template cDNA	1ul (3.2ng/ul)	≤10ng/ul
RNase-free water	14.875ul	
Total reaction volume	25ul	

**Table 3.7** Conventional PCR cycling conditions

Step	Time	Temperature	Number of cycles
Initial denaturation	2min	95°C	1 cycle
Denaturation	50 s	95°C	25-35 cycles
Annealing	50s	x°C	
		(refer Table 3.3 and 3.4)	
Extension	50 s	72°C	1 cycle
Final extension	7min	72°C	



### **3.3.3 PCR products verification**

Purified PCR products were sent to FirstBase Laboratory for sequencing procurement. After verification, quantification and statistical analyses were carried out.

### **3.3.4 Statistical analysis**

The RT-PCR images were captured using Red™ Imaging System (Alpha Innotech, USA ) and quantification of the bands intensity in ng unit was performed using AlphaEase®FC Stand Alone software. The 100 bp DNA marker (Fermentas, Lithuania) in each gel picture was used as the reference marker. Marker bands with known concentrations (ng) were used to plot the standard curve. The intensity of each spot, quantified after background correction, was normalised for the amount of template added by comparison relative to the housekeeping gene. For quantitative statistical analysis, the values for genes of interest and normaliser gene were averaged from 2 replicates. Statistical values were analysed using SPSS Paired Sample t-test to check for significant differences between normal and tumor samples (p-value < 0.05 is considered significant).

## **3.4 Quantitative PCR**

### **3.4.1 DNase treatment**

To degrade any DNA contamination in a sample of RNA, 1 unit of RQ1 RNase-Free DNase was used per ug of RNA. For smaller amounts of RNA, 1 unit of RQ1 RNase-Free DNase per reaction was used. The reaction was set up with 1x reaction buffer and topped up with Nuclease-free water to a final volume of 10ul and incubated at 37°C for 30 minutes to 1 hour. One microlitre of RQ1 DNase Stop Solution was added to terminate the reaction and left incubated at 65°C for 10 minutes to inactivate the DNase.



### **3.4.2 Purification**

DNase treated total RNA was purified using Trizol method. 10-20ul of treated RNA was added to 1ml TRIzol (GIBCO BRL). Two hundred microlitres of chloroform was then added and shaken vigorously for 15 seconds and left for incubation at room temperature for 10 minutes. It was then centrifuged at 14,000 rpm for 15 minutes at 4°C. The aqueous phase was then transferred to a clean 1.5ml eppendorf tube and 500ul isopropanol was added and stored at room temperature for 10 minutes. This was followed by centrifugation at 14, 000 rpm at 4°C for 8 minutes. The pellet was washed with 1ml of 70% ethanol and centrifuged at 12, 000 rpm for 5 minutes, 4°C. Ethanol wash was removed and the pellet air-dried for 3-5 minutes.

### **3.4.3 Preparation of first strand cDNA templates**

The same as previously described (section 3.3.1, page 38)

### **3.4.4 Quantitative PCR amplification**

2x Rotor-Gene SYBR Green PCR Master Mix were thawed and template cDNA, primers, and RNase-free water were added. The reaction mix was mixed thoroughly, and was dispensed in appropriate volumes into PCR tubes. Template cDNA ( $\leq 100$  ng/reaction) was added to the individual PCR tubes containing the reaction mix. The Rotor-Gene cycler (Qiagen) was programmed according to the program outlined in Table 3.9. PCR tubes were placed in the Rotor-Gene cycler, and the cycling program started. Melting curve analysis of the PCR products was performed to verify their specificity and identity. Melting curve analysis is an analysis step built into the software of the Rotor-Gene cycler.

**Table 3.8:** Quantitative PCR cycling conditions

Step	Time	Temperature
PCR initial activation step	5min	95°C
Denaturation	5 s	95°C
Combined annealing/extension	10 s	60°C
Number of cycles	40	

**3.4.5 Efficiency test**

For quantitative PCR reactions in this study, 50ng RT product was used as the highest template mass point for the standard curve. The other standard curve points were prepared from subsequent 5x serial dilutions with two replicates for each point. Therefore, the five points were 50ng, 10ng, 2ng, 0.4ng, and 0.08ng. The slope (M) of a reaction (shown in the standard curve window) was used to determine the exponential amplification and efficiency of a reaction. The slope is calculated by the Rotor-Gene software of being the change in  $C_T$  divided by the change in log input. Amplification efficiencies of the gene of interest and housekeeping/normalizer gene were validated.

**3.4.6 Delta Delta  $C_T$  Relative Quantitation**

This method does not require the generation of standard curves in each test. Each sample was first normalised for the amount of template added by comparing with the housekeeping gene *GAPDH* (endogenous control). These normalised values were further normalised relative to a calibrator treatment. The calibrator in this study is the human normal nasopharyngeal tissues. The  $C_T$ 's for the Gene of Interest analysis (GOI  $C_T$ ), the Normaliser Gene (Norm.  $C_T$ ), the Delta  $C_T$ , Delta Delta  $C_T$  and Relative Concentration (Relative Conc.) were calculated by Rotor-Gene 6000 Series Software. The expression is relative to the Calibrator sample which is assigned a relative expression of 1.



### **3.5 Cloning, screening and sequencing for mutational analysis**

PCR products were gel-excised and purified using Gel-M extraction system (Viogene, USA). Purified PCR fragments were cloned using Promega pGEM®-T Easy Vector System II. The total of 10 µl ligation volume contained 1 X ligation buffer, 1 unit of each T4 DNA ligase and pGEM®-T Easy Vector, and 3 µl of purified PCR amplicons. After incubation at room temperature for 1-2 hours, 3 µl of ligated products were transformed using heat-shock method (42°C for 45 seconds) into chemically competent *E. coli* JM109 (Promega, USA). Transformants were grown on LB agar with Ampicillin, IPTG and X-gal for selection purpose. White colonies were screened via PCR approach using T7 and SP6 promoter primers and were further confirmed using gene specific primer. The positive clones that carry insert of interest were subcultured overnight. Plasmid DNA isolation was performed the next day using Wizard® Plus Minipreps DNA Purification Systems (Promega, USA) according to the manufacturer's protocol. Purified plasmid DNAs were sent to FirstBase Laboratory for sequencing procurement. After verification, clones of interest were made into glycerol stocks by mixing bacteria culture broth with pure glycerol in a ratio of 8:2 and stored at -80°C.

### **3.6 Protein analysis**

#### **3.6.1 Protein isolation using Nonidet P-40 lysis buffer analysis**

All works were carried out either on ice or in a cold room. 1mM phenylmethylsulfonyl fluoride (PMSF) (Protease inhibitor) was added to 1% Nonidet P-40 (NP-40) lysis buffer prior to use. Detergent lysis buffer was prepared by mixing 1% NP-40 (Roche, Germany), 20mM Tris-HCl pH 8.0, 137mM NaCl, 10% Glycerol and 2mM EDTA pH 7.4. NP Cell culture (Table 3.2) flask was placed on ice. The media was discarded and the cells washed with ice cold phosphate buffered saline (PBS), prior to addition of ice cold lysis buffer (1ml

per 75cm<sup>2</sup> flask and 0.5ml per 25 cm<sup>2</sup> flask). Adherent cells were scraped off using a cold plastic cell scraper. The suspension was then transferred into a cooled microcentrifuge tube and agitated constantly for 30 minutes. After half an hour, the suspension was centrifuged at 12,000 rpm, at 4°C for 20 minutes. The supernatant (protein) was aspirated and placed in a pre-cooled fresh tube and kept at -80°C and the pellet (cell debris) was then discarded.

### **3.6.2 Protein quantification using Bradford assay**

#### **3.6.2.1 Reagents and standard curve preparation**

Bradford reagent was prepared according to the protocols by Bradford (1976). Coomassie Blue G-250 (Sigma, USA) (100 mg) was dissolved in 50 ml 95% ethanol, and mixed with 100 ml 85% phosphoric acid. The solution was topped up with dH<sub>2</sub>O to 1L, and filtered using no. 1 filter paper (Whatman, England). The filtered solution was stored in the dark at 4°C. Bovine serum albumin (BSA) (Amresco, USA) was used as the standard protein to plot the standard curve. Stock standards (5 mg/ml) was prepared by dissolving BSA into water. A series of standards of known concentration of BSA ranging from 0.5mg to 2mg was prepared by diluting stock standards with water. Half a milliliter of BSA standards from each concentration was mixed with 1.5 ml of Bradford reagent, and left for 5 minutes at room temperature before proceeding with determination of the absorbance reading at 595nm (A<sub>595</sub>) using a 1 cm-path-length (1 ml) microcuvette (Eppendorf, Germany). Standard curve of absorbance versus concentration for each standard was plotted.



### **3.6.2.2 Protein quantification**

All conditions under which standards and unknowns were prepared were kept identical. Protein samples (unknown concentration) were diluted from the stock in distilled water to a total volume of 0.5ml and mixed with 1.5 ml of Coomassie brilliant blue solution. After 5 minutes of incubation,  $A_{595}$  was determined using Amersham Pharma Ultrospec® 1100 *pro* UV/Visible Spectrophotometer (Biochrom, England). Using the  $A_{595}$  values, the protein concentration was determined based on the standard curve.

### **3.6.3 Western blot**

#### **3.6.3.1 Preparing SDS-PAGE**

Bio-Rad Mini-Protean III gel electrophoresis system was used according to the manufacturer's recommendation. Two clean glass plates and two 1.0-mm spacers were locked to the gel-casting stand. The resolving gel and stacking gel were prepared as shown in Table 3.10. Lower percentage resolving gel (7.5%) was used to resolve high molecular weight proteins (vigilin), while much higher percentages (10%) was used to resolve smaller proteins (TRAF6). The resolving gel solution was loaded into the glass-plate sandwich using pipet tips until the height of the solution is approximately 1 cm below the sample-loading well. The top of the gel was overlayed with  $dH_2O$  to inhibit polymerization and allows a flat interface to form during gel formation. The gel was then allowed to polymerize at room temperature for 30 minutes. The  $dH_2O$  overlay was discarded and the stacking gel solution was prepared. The stacking gel was added slowly until the height of the glass plate. Gently, the 1.0 mm comb was carefully inserted into the layer of the stacking gel solution. The gel was allowed to polymerize at room temperature for another 30 minutes.

**Table 3.9:** Recipe for resolving and stacking gels for SDS-PAGE

Stock solution	Resolving gel (10%)	Resolving gel (7.5%)	Stacking gel (4%)
30% Acrylamide	1.667ml	1.25ml	0.333ml
1.5M Tris pH 8.8	1.25ml	1.25ml	-
0.5M Tris pH 6.8	-	-	0.625ml
dH <sub>2</sub> O	2.003ml	2.41ml	1.502ml
20% SDS	25ul	25ul	12.5ul
10% APS	50ul	50ul	25ul
TEMED	5ul	5ul	2.5ul
Total	~5ml	~5ml	~5ml

**3.6.3. 2 Preparing samples, gel-loading and running the gel**

For protein samples preparation, protein sample from -80°C was thawed and diluted with dH<sub>2</sub>O to a desired concentration and mixed with 5 x loading buffer. The sample mixture was heated at 99°C on a heater block for 3 minutes and allowed to cool at room temperature for 2 minutes. Protein was loaded in equal amounts and equal volumes (10 µg in 15 µl) into the 1 mm thick well mini-gel systems. Five microlitres of prestained protein ladder (FERMENTAS) and unstained protein ladder (FERMENTAS) were loaded at each end.

The comb was removed gently. The mini tank assembly was set up according to the manufacturer’s instruction. Inner chamber was filled with ~125ml of 1 X running buffer until the level reaches halfway between the tops of the taller and shorter glass plates of the gel cassettes while the outer buffer chamber was filled with ~200ml of 1 X running buffer. The unit was reassembled if leakages were observed. Subsequently, protein samples were loaded using 200 µl PAGE gel-loading tips into one or more wells slowly and carefully in order not to disperse the samples into the other lanes. The remaining buffer was added to the top to submerge the upper electrode. Electrophoresis was carried out at 200 V for ~35 minutes until the bromophenol blue dye exit the bottom of the gel. The gel was then carefully removed



from the lower glass plate using a gel cutter and rinsed with dH<sub>2</sub>O. At this stage, the gel was ready to be used for electroblotting.

### **3.6.3.3 Electrophoretic blotting**

Electrophoretic transfer was performed using Mini Trans-blot Cell (Bio-Rad, USA). After electrophoresis, the gel sandwich was disassembled and the stacking gel was removed. The resolving gel was rinsed with dH<sub>2</sub>O and equilibrated in transfer buffer at room temperature for 15-30 minutes. In a large tray, transfer cassette together with sponge, 3 MM filter paper (Bio-Rad, USA) and gel were soaked in transfer buffer. Immobilon-P polyvinylidene fluoride (PVDF) membrane (Millipore, USA) was cut to the size of the gel (9 cm x 5 cm) and was slowly placed into 100% methanol for 15 seconds to pre-wet the membrane. The membrane was soaked into dH<sub>2</sub>O for 2 minutes, and later left to equilibrate in transfer buffer for 5 – 10 minutes. The pre-wetted membrane was placed directly on top of the gel and all air bubbles were rolled out using a glass roller. The transfer sandwich was checked for correct orientation with the cathode (negative) gel cassette holder at the bottom, followed by stacking of sponge, filter paper, gel, membrane, filter paper, sponge and the anode (positive) gel cassette holder. The assembled transfer sandwich was placed in a transfer tank and the tank was filled up with cold transfer buffer until the level of the electrode panels. Bio-ice cooling unit and a magnetic stirrer were also included to maintain the low temperature of the buffer and to disperse the heat evenly throughout the transfer process. The transfer was performed at 100 V, 350mA for 1 hour in the cold room. After transfer, the apparatus was disassembled and the gel and the membrane were rinsed with dH<sub>2</sub>O prior to gel staining and membrane blocking.

#### **3.6.3.4 Coomassie blue staining**

After electroblotting, the gel was stained to ensure that the protein has been successfully transferred from the gel to the membrane. The gel was first washed with dH<sub>2</sub>O by gentle agitation in a rocker for 15 minutes to remove methanol residues. The water was removed and the gel was stained with Imperial<sup>™</sup> protein stain (Pierce, Belgium) for 5-10 minutes. Excess dye was removed and the gel was rinsed in dH<sub>2</sub>O for 5 minutes and the rinsing process was repeated 3 times.

#### **3.6.3.5 Blocking and immunoprobng**

BSA (3%) was used as blocking reagent by dissolving BSA powder (Amresco, USA) in PBST buffer (PBS with 0.05% Tween 20) prior to use. PVDF membrane with transferred proteins was sealed in plastic bag with ~6 ml blocking reagent and agitated at room temperature for 1 hour. The membrane was then washed with water for 5 minutes at room temperature before incubated with 5– 6 ml of diluted primary antibody and agitated for 1 hour at room temperature. The blot was washed in 30 – 40 ml of PBST 3 times, with 10 minutes each wash in a modified T75 flask. Subsequently, the blot was exposed to secondary antibody in a sealed bag for another 1 hour at room temperature. A second round of washing was performed as previously mentioned. Primary and secondary antibodies were determined empirically and optimized dilutions were as stated in Table 3.10.



**Table 3.10:** Primary and secondary antibody dilutions

Type of Polyclonal antibody (Santa Cruz, USA)	Primary antibody	Secondary antibody (donkey anti-goat IgG-HRP sc-2020)
GAPDH (I-19:sc-48166)	1:200	1:2000
Vigilin (N-16:sc-51016)	1:200	1:2000

**3.6.3.6 Chemiluminescent detection**

After the second round of washing, the blot was incubated with SuperSignal® West Pico Chemiluminescent Substrate (Pierce, Belgium) for 5 minutes. Excess substrate was drained off and the blot was wrapped in plastic cling wrap. Detection was performed using ImageQuant 400 Imager (GE Healthcare) and quantitation of the band was analysed with ImageQuant TL software.

**3.6.3.7 Membrane stripping by low pH**

Stripping solution consisted of 25 mM glycine-HCl, pH 2, and 1% (w/v) SDS. The visualized blot was placed in stripping solution and agitated for 30 minutes. Next, the blot was washed twice with PBS buffer for 10 minutes. The blot was used for subsequent rounds of immunodetection.

## CHAPTER FOUR

### EXPRESSION ANALYSIS OF *TRAF6*, *VIGILIN*, *BNIP2*, *MIF* AND *GFER* IN NASOPHARYNGEAL CARCINOMA VIA CONVENTIONAL REVERSE TRANSCRIPTION (RT) PCR

#### 4.1 Introduction

Cao *et al.* (1996) showed that when overexpressed in cultured human cells, TRAF6 activates NF- $\kappa$ B. NF- $\kappa$ B plays a well known function in the regulation of immune responses and inflammation, but growing evidences support a major role in oncogenesis (Dolcet *et al.*, 2005).

Based on the finding by Cunningham *et al.* (2000), vigilin induces the stabilization of vitellogenin mRNA. This role of vigilin in cytoplasmic mRNA metabolism has also been suggested by Goolsby *et al.* (2003). Aberrant expression of RNA-binding proteins (RNA-BP) has been reported in diverse cancer types and are often correlated with advanced stage and grade of tumors, resulting in misregulation of genes involved in cancer progression (Wang *et al.*, 2000; Gouble *et al.*, 2002; Audic and Hartley., 2004).

BNIP2 was reported to interact with two proteins which are MIF and GFER via yeast two-hybrid system (Shen *et al.*, 2003). The interactions were confirmed by glutathione S-transferase pull-down assay *in vitro* and co-immunoprecipitation assay *in vivo*. Shang *et al.* (2003) reported that the overexpression of BNIP2 increased cell migration and invasion *in vitro* and promoted the metastasis of hepatocellular carcinoma (HCC) cells *in vivo*. BNIP2



overexpression in human hepatoma cell line has been reported to upregulate genes involved in growth inhibition (*IGFBP-1*, *TGF- $\beta$* ) or cell apoptosis (p21, E2A) (Xie *et al.*, 2004).

There have been several studies reporting the increased expression of MIF in pre-cancerous, cancerous and metastatic tumours (Mitchell, 2003). Prostate, breast, colon, brain, skin and lung-derived tumours have all been shown to contain significantly higher levels of *MIF* mRNA and protein than their non-cancerous cell counterparts (Meyer-Siegler *et al.*, 1998; Takahashi *et al.*, 1998; Shimizu *et al.*, 1999; Kamimura *et al.*, 2000; Markert *et al.*, 2001; Bando *et al.*, 2002; Tomiyasu *et al.*, 2002).

Quantitative mRNA analysis of *GFER* by Thasler *et al.* (2006) revealed significantly increased *GFER* expression in cirrhosis compared with normal liver tissue. Based on another finding by Zheng *et al.* (2004), *GFER* was similarly found to be overexpressed in epithelial ovarian cancer via microarray approach.

Preliminary data (Sim *et al.*, 2008) has detected differential expression of vigilin and *TRAF6* via GeneFishing<sup>TM</sup> Differential Expressed Genes (DEG) analysis techniques. Previous unpublished microarray data by another member in our group revealed *BNIP2* under expression (0.176 fold change) in NPC tumor sample. Shen *et al.* (2003) reported interaction of *BNIP2* with MIF and *GFER* via yeast two-hybrid system. These observations suggest that many more genes may be involved in the multistep progression of NPC. Like most types of cancer, the occurrence of NPC is probably multifactorial in origin and multigenic in mechanism. Therefore, the study in this chapter aimed to establish selected genetic associative factors that have been previously suspected to be involved in NPC.

## 4.2 General methodology

Total RNA was isolated from biopsy samples and cell lines using TRIzol solution (GIBCO-BRL) according to the manufacturer's specifications as outlined in Section 3.1.2. The RNA quality was checked by 1.0% agarose gel electrophoresis, stained with 1 ug/ml ethidium bromide (Figure 4.1 and Figure 4.2).

A two-step conventional RT-PCR method was used to measure gene expression of *TRAF6*, *vigilin*, *BNIP2*, *MIF* and *GFER*. For first strand synthesis, 2µg of total RNA was reverse transcribed using MMLV reverse transcriptase and Oligo(dt) primer. One microliter out of 25 µl cDNA synthesized was used as template for subsequent PCR amplification. The PCR mixture was prepared in a total reaction volume of 25 µl as described earlier in Section 3.3.2 and the optimal conditions were set according to the parameters listed in Table 3.7. PCR amplification of each gene was performed using the primers listed in Table 3.3 and 3.4.

Ten microliters of RT-PCR products were resolved on 2% ethidium bromide incorporated agarose gels and documented using Red™ Imaging System (Alpha Innotech, USA). The quantity and base pair size of the PCR generated DNA fragments were estimated relative to DNA ladder standards. Quantification of the bands intensity in ng unit was performed using AlphaEase®FC Stand Alone software. RT-PCR values are presented as a ratio of the target gene's signal divided by the housekeeping signal. Two housekeeping genes (*GAPDH* and *ACTB*) were used as internal standards to reduce normalization errors.



## **4.3 Results**

### **4.3.1 Total RNA samples assessment**

Expression analysis of *TRAF6*, *vigilin*, *BNIP1L2*, *MIF* and *GFER* mRNA was performed for total RNA that were extracted from local paired normal and tumor nasopharyngeal (NP) biopsy tissues. Only *TRAF6* transcript expression was further investigated in cell lines. This was because at the later stage of the study, TRAF6 protein was not detected in all the cell lines via Western blot. Thus, its detection at the transcript level was checked via conventional PCR.

The descriptions of these samples were indicated in Section 3.1.1, Table 3.1 and Table 3.2. Total RNA for the samples were determined on 1% agarose gel before they were used for expression analysis (Figure 4.1 and Figure 4.2).

As shown in Figure 4.1 and Figure 4.2, 28 S and 18 S ribosomal RNA bands were observed for all samples. Our initial agarose gel electrophoresis step is necessary to ensure that the RNAs are in good conditions before proceeding to conventional PCR.



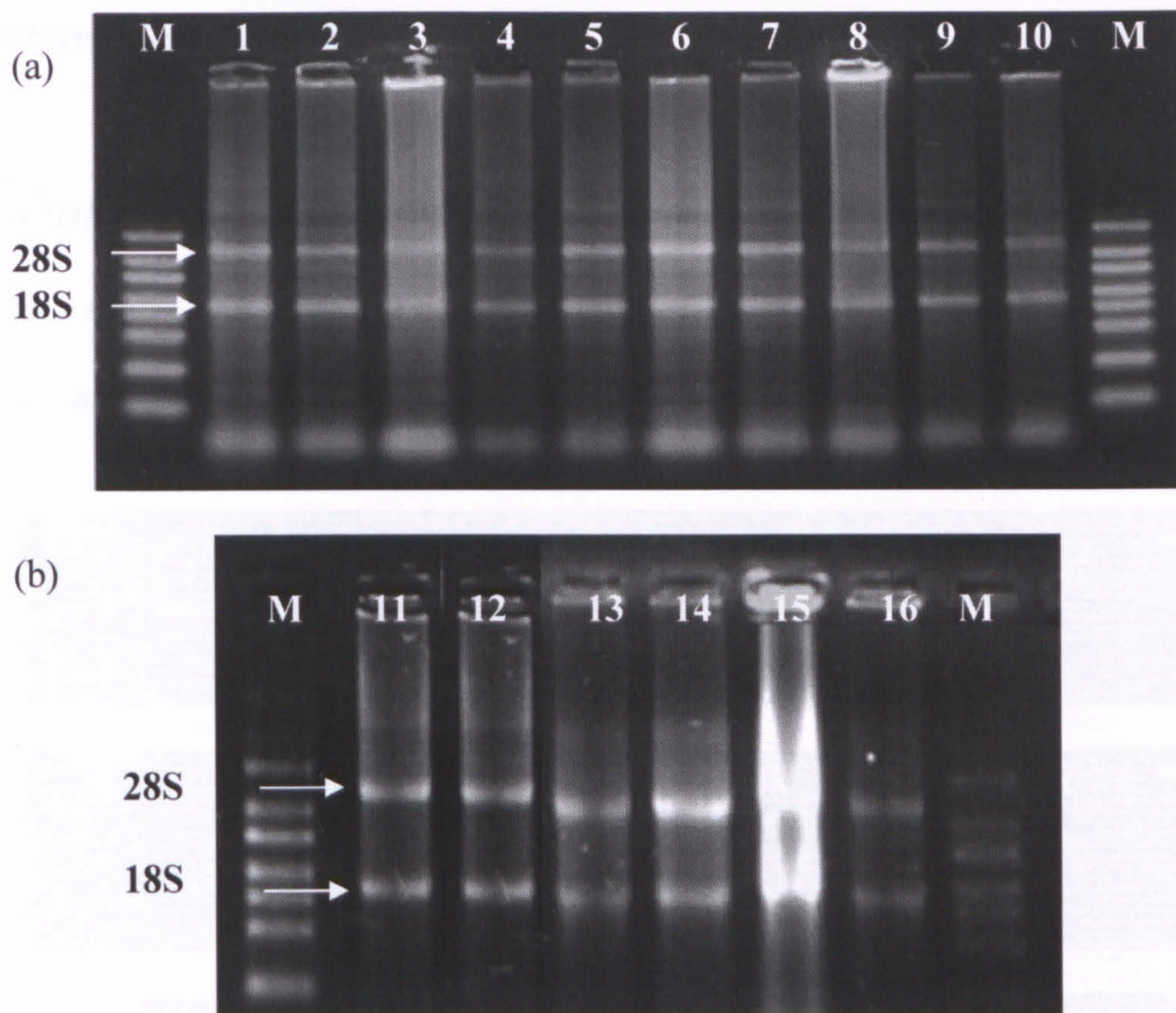


**Figure 4.1:** Total RNA isolated from paired biopsy samples using Trizol method. RNA was displayed on a 1% x TAE agarose gel ( $\sim 1 \mu\text{g}$  per lane). (a) Lane 1 – 10: T20, N20, T22, N22, T24, N24, T27, N27, T41, N41 (b) lane 11 – 16: T48, N48, T67, N67, T96, N96; Lane M: RNA ladder, High Range, 200-6000 bases (Promega, USA),

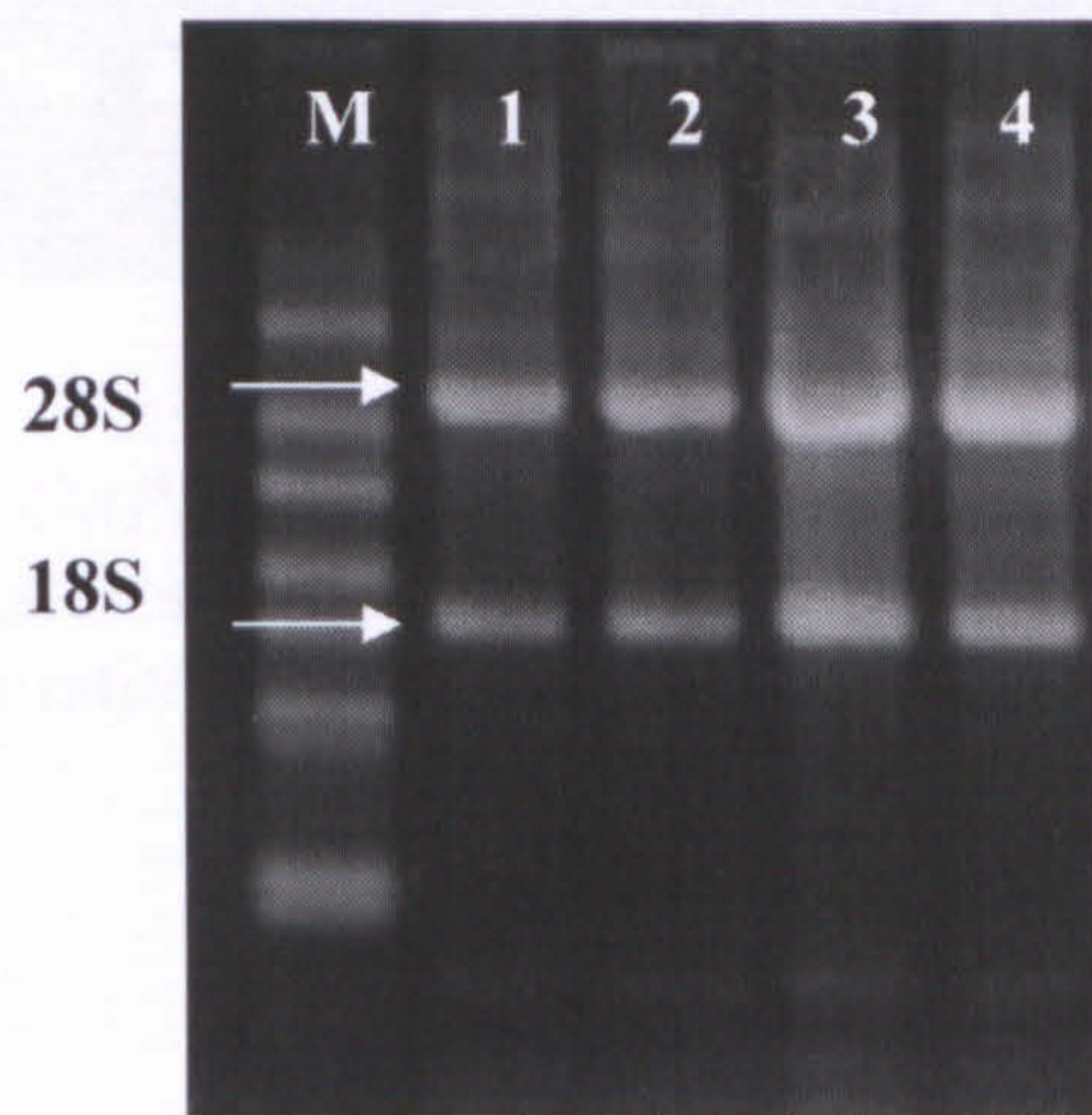


**Figure 4.2:** Total RNA isolated from nasopharyngeal cell lines using Trizol method. RNA was displayed on a 1% x TAE agarose gel ( $\sim 1 \mu\text{g}$  per lane). lane 1-3: NPC cell line HONE1, HK1 SUNE1; lane 4: normal NP69 cell line ; Lane M: RNA ladder, High Range, 200-6000 bases (Promega, USA)



4.3.2 Internal Control

The *GAPDH* and *ACTB* genes were used as internal control for all samples studied in this expression study. The observed expression of *GAPDH* and *ACTB* in all samples is shown in Figure 4.3 and Figure 4.4.

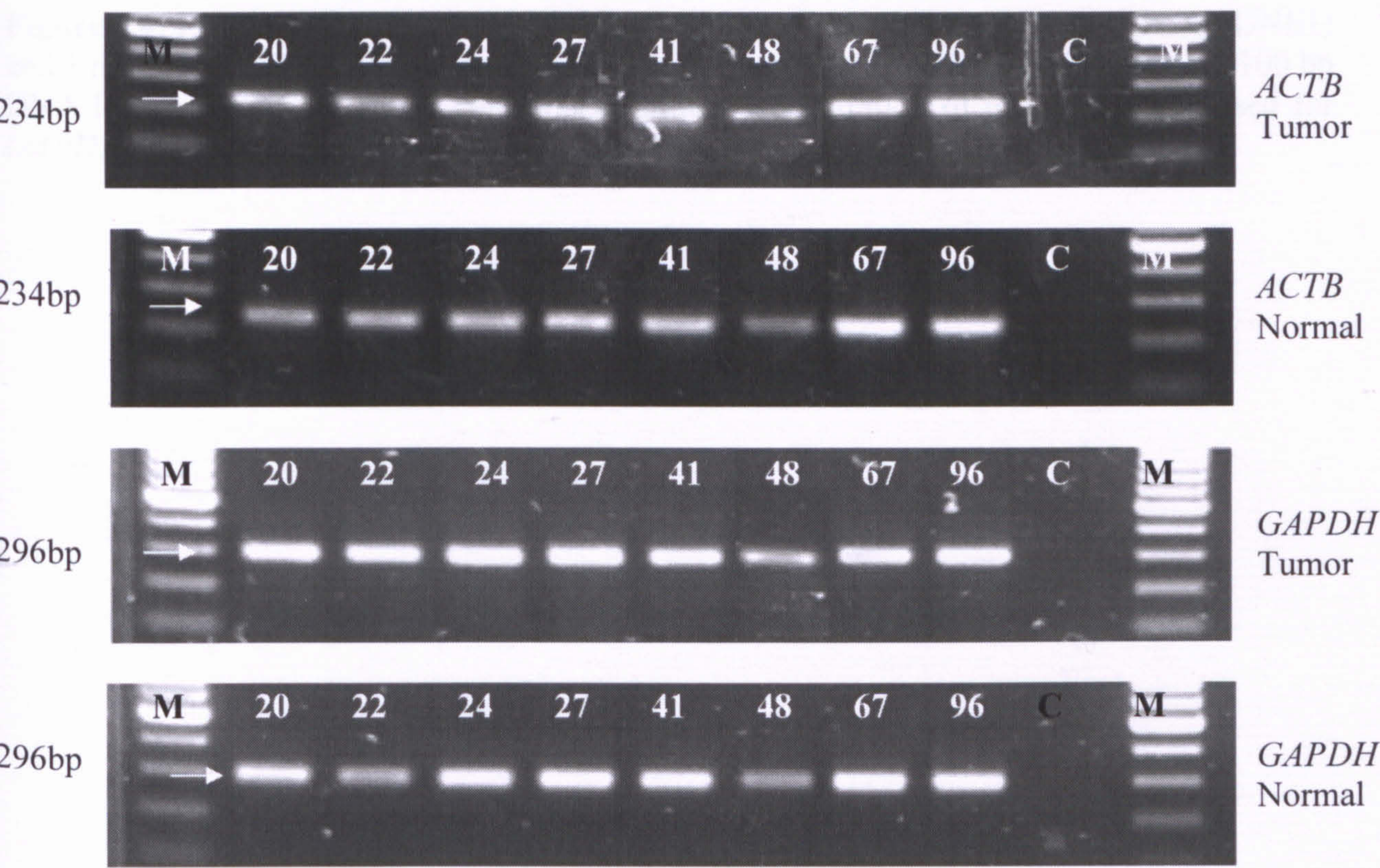


**Figure 4.3:** Expression of *GAPDH* and *ACTB* in all nasopharyngeal biopsy samples screened. Number above lane indicates sample code. lane M: 100 bp DNA ladder, lane C: negative control. Equimolar concentration of total RNA was used for *GAPDH* and *ACTB* analysis.



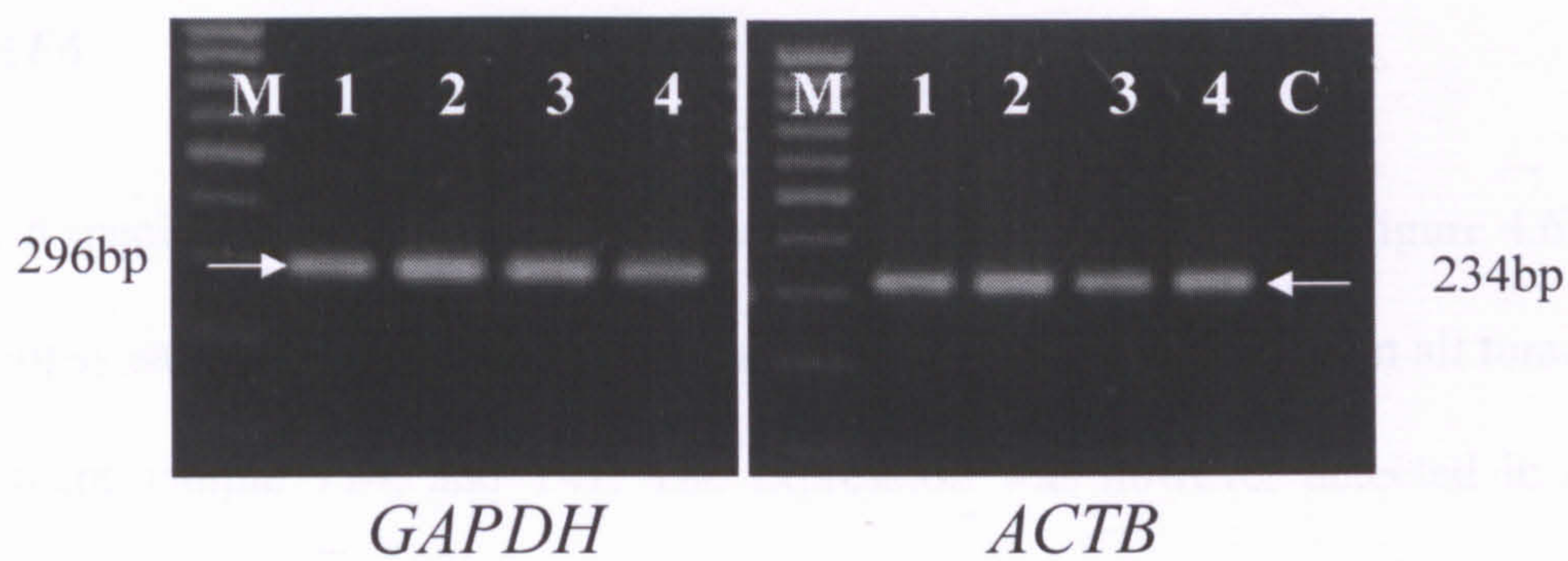


**Figure 4.4:** Expression of *GAPDH* and *ACTB* in three NPC cell lines (HONE1, HK1, SUNE1) and 1 normal NP (NP69) cell line. lane 1-4:; HONE1, TWO1, SUNE1, NP69; lane M: 100 bp DNA ladder, lane C: negative control. Equimolar concentration of total RNA was used for *GAPDH* and *ACTB* analysis.



### 4.3.3 *TRAF6*

The *TRAF6* specific primers amplified a region of 262bp (Figure 4.5 and Figure 4.6). Out of 8 pairs of biopsy samples screened, the expression of *TRAF6* was observed in all tumor samples studied except sample T24, and T41. The expression was however detected in all normal biopsy samples. *TRAF6* transcript expression was also detected in three NPC cell lines (HONE1, HK1, SUNE1) and one normal NP69 cell line. Expression levels were determined using AlphaEase®FC Stand Alone software and the normalized target expressions are shown in Figure 4.5 and Figure 4.6. Table 4.1 and Table 4.2 are summary of *TRAF6* expression in fold change in biopsy samples and cell lines respectively. The fold change is calculated based on expression of tumour sample relative to its paired normal sample. Expression fold change >2 is considered as significant. The SPSS Paired Sample t-test was used to check for significance of overall differential expression between the normal and tumor samples (p-value < 0.05 is considered significant).

Out of 8 paired biopsy samples normalized with both *ACTB* and *GAPDH*, 5 showed *TRAF6* underexpression pattern in tumor (sample 22, 24, 27, 41 and 96) with 3 samples (22, 24 and 41) having significant underexpression fold (Table 4.1). The other 3 biopsy samples (20, 48 and 67) showed higher *TRAF6* expression in tumor with only sample 48 having significant overexpression. Dependent (Paired Samples) T-test revealed that the average *TRAF6* expression in tumor samples did not differ significantly from normal samples normalized with *ACTB* (n=8,  $p \geq 0.05$ ) and *GAPDH* (n=8,  $p \geq 0.05$ ).

Out of 3 NPC cell lines (HONE1, TWO1, SUNE1) and 1 normal cell line (NP69) normalized with *ACTB* and *GAPDH*, all showed *TRAF6* underexpression in tumor cell lines but the

underexpression fold is not significant (Table 4.2). The average *TRAF6* expression in NPC cell lines did not differ significantly from normal NP cell line (n=3,  $p \geq 0.05$ ).



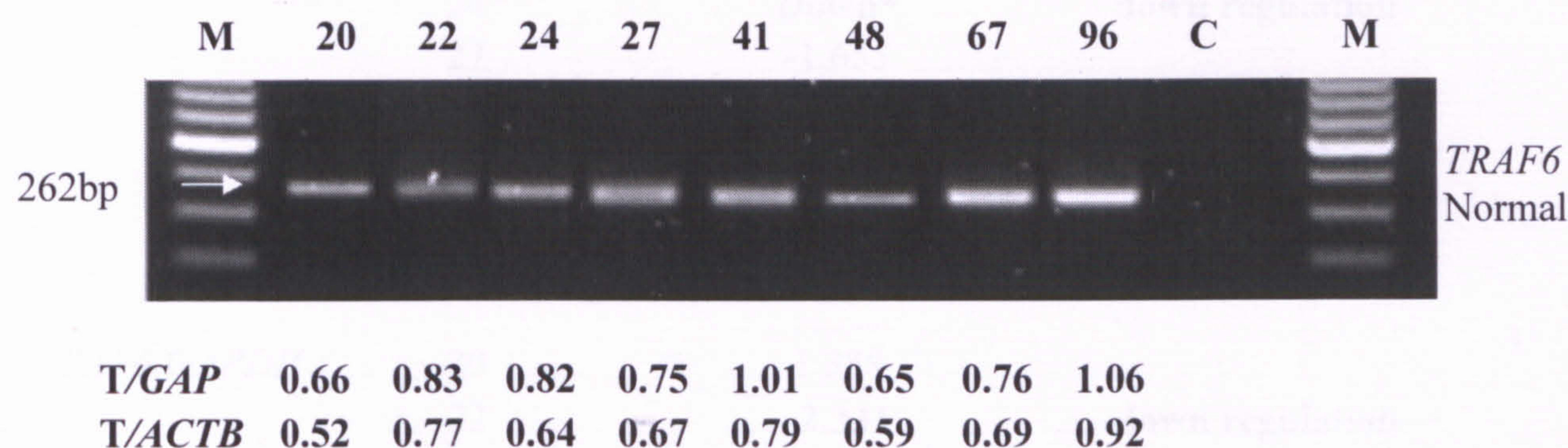
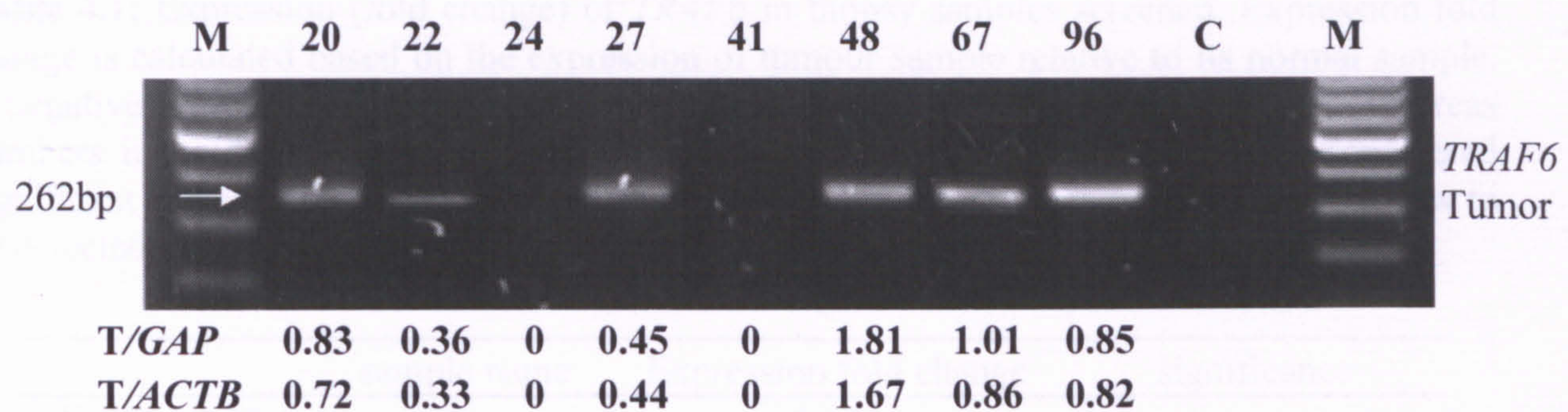


**Figure 4.5:** Expression of *TRAF6* in eight paired samples from local biopsies on 2.0% (w/v) agarose gel. The ratios indicate expression level of the target (T) amplification product after normalized to internal control (*GAPDH* and *ACTB*). lane C: negative control, lane M: 100 bp DNA ladder

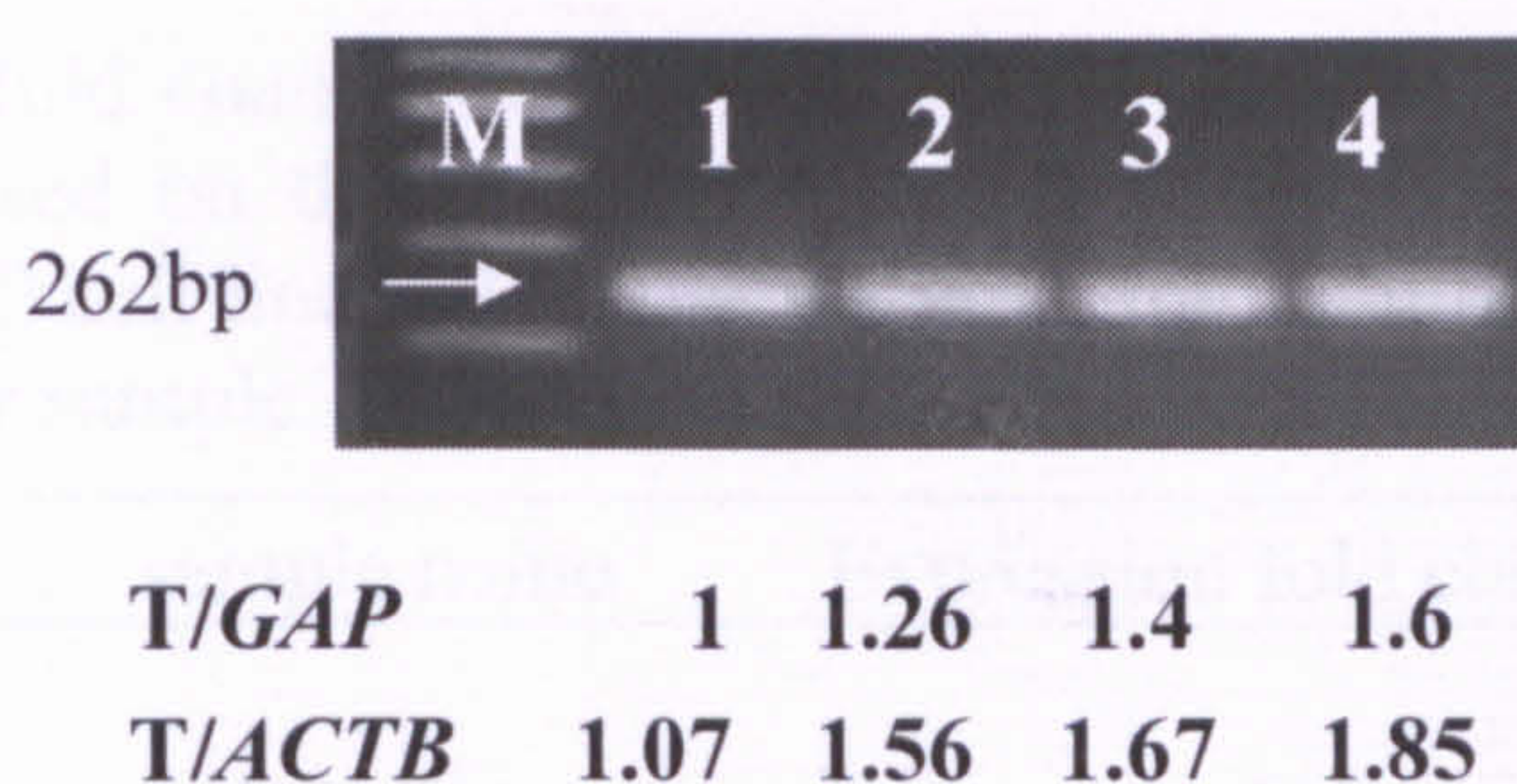


**Figure 4.6:** Expression of *TRAF6* in three NPC cell lines (HONE1, HK1, SUNE1) and one normal cell line (NP69) on 2.0% (w/v) agarose gel. The ratios indicate expression level of the target (T) amplification product after normalized to internal control (*GAPDH* and *ACTB*). lane 1-4: HONE1, HK1, SUNE1, NP69; lane M: 100 bp DNA ladder.



**Table 4.1:** Expression (fold change) of *TRAF6* in biopsy samples screened. Expression fold change is calculated based on the expression of tumour sample relative to its normal sample. A negative fold number indicates the expression is downregulated in tumour sample whereas numbers in bold are expression folds that are considered significant (>2). \* is considered significant because the expression level of *TRAF6* in the sample's counterpart was too low to be detected by RT-PCR.

	sample name	Expression fold change	significance
<i>TRAF6 /ACTB</i>	20	1.271	
	22	<b>-2.307</b>	<b>down regulation</b>
	24	<b>Down*</b>	<b>down regulation</b>
	27	-1.655	
	41	<b>Down*</b>	<b>down regulation</b>
	48	<b>2.799</b>	<b>up regulation</b>
	67	1.339	
	96	-1.249	
<i>TRAF6/GAPDH</i>	20	1.388	
	22	<b>-2.331</b>	<b>down regulation</b>
	24	<b>Down*</b>	<b>down regulation</b>
	27	-1.518	
	41	<b>Down*</b>	<b>down regulation</b>
	48	<b>2.813</b>	<b>up regulation</b>
	67	1.249	
	96	-1.125	

**Table 4.2:** Expression (fold change) of *TRAF6* in nasopharyngeal cell lines. Expression fold change is calculated based on the expression of NPC cell lines (HONE1, HK1, SUNE1) relative to one normal NP cell line (NP69). A negative fold number indicates the expression is downregulated in tumour sample. Expression folds that are >2 is considered significant.

	sample name	Expression fold change	significance
<i>TRAF6 /ACTB</i>	HONE1	-1.395	-
	HK1	-1.19	-
	SUNE1	-1.075	-
<i>TRAF6/GAPDH</i>	HONE1	-1.335	-
	HK1	-1.134	-
	SUNE1	-1.019	-



#### 4.3.4 Vigilin

Expression study was performed on 8 pairs of nasopharyngeal biopsy tissues. The reverse transcription PCR product for vigilin was observed as a band of about 336bp in size on agarose gel and its normalized expression ratio was shown in Figure 4.7. Expression of vigilin was detected in all tissues except for T48. Table 4.3 is a summary of vigilin expression in fold change. Five samples (20, 24, 27, 48 and 96) out of eight samples showed vigilin underexpression in tumor with only sample 48 having significant underexpression fold due to non detection in the expression level in tumor sample 48 (Table 4.3). Three samples (22, 41 and 67) showed vigilin was expressed only slightly higher (not significant) in the tumor (Table 4.3). Statistical analysis revealed that average decrease of vigilin expression in tumor samples was not significant in both *GAPDH* (n=8,  $p \geq 0.05$ ) and *ACTB* (n=8,  $p \geq 0.05$ ) normalized samples.



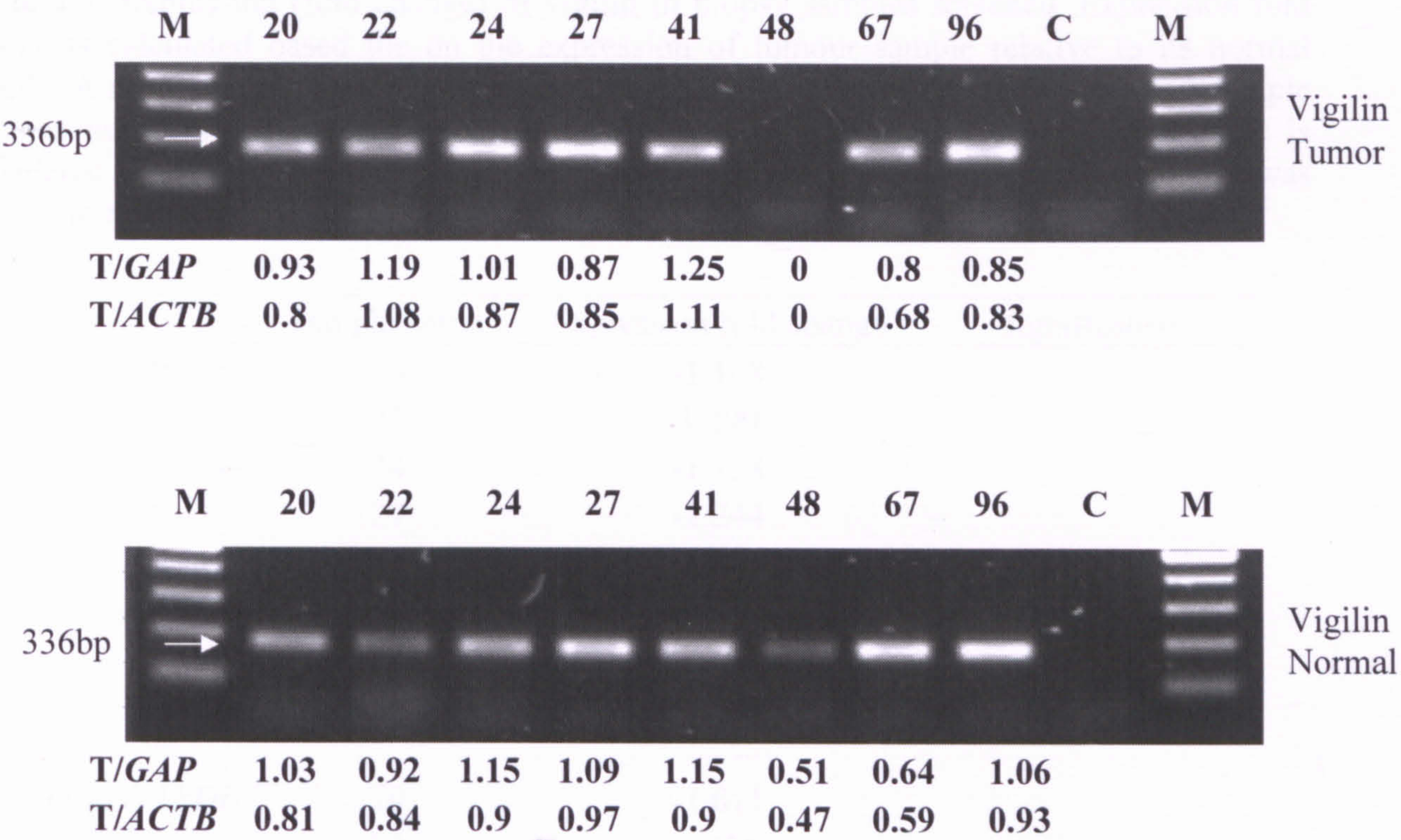


**Figure 4.7:** Expression of vigilin in eight paired samples from local biopsies on 2.0% (w/v) agarose gel. The ratio indicates the expression level of the target (T) amplification product after normalized to internal control (*GAPDH* and *ACTB*). lane C: negative control, lane M: 100 bp DNA ladder



**Table 4.3:** Expression (fold change) of vigilin in biopsy samples screened. Expression fold change is calculated based the on the expression of tumour sample relative to its normal sample. A negative fold number indicates the expression is downregulated in tumour sample whereas numbers in bold are expression folds that are considered significant (>2). \* is considered significant because the expression level of vigilin in the sample’s counterpart was too low to be detected by RT-PCR.

	sample name	Expression fold change	significance
vigilin/ <i>ACTB</i>	20	-1.108	
	22	1.299	
	24	-1.138	
	27	-1.244	
	41	1.088	
	48	<b>Down*</b>	<b>down regulation</b>
	67	1.247	
	96	-1.245	
vigilin/ <i>GAPDH</i>	20	-1.011	
	22	1.285	
	24	-1.036	
	27	-1.144	
	41	1.236	
	48	<b>Down*</b>	<b>down regulation</b>
	67	1.165	
	96	-1.123	

#### 4.3.5 *BNIP2*

The expected RT-PCR product for *BNIP2* is 277bp. Expression levels were determined and the normalized target expression is shown (Figure 4.8). *BNIP2* was expressed in all samples studied except for sample N20, T22, T24 and T48 in which the expression was too low to be detected by RT-PCR. Out of 8 pairs of samples studied, half of the samples (20, 27, 41 and 67) showed higher *BNIP2* expression pattern in the tumour while the other half of the samples (22, 24, 48 and 96) showed lower expression in the tumor. The expression in fold change was calculated and listed in Table 4.4. Out of the 4 samples that showed *BNIP2* underexpression in the tumor, the underexpression in 3 samples (22, 24 and 48) were significant. Out of the other 4 samples that showed overexpression in tumor, only sample T20 were significantly upregulated. The average *BNIP2* expression in the tumor samples did not differ significantly from normal samples with both *GAPDH* (n=8,  $p \geq 0.05$ ) and *ACTB* (n=8,  $p \geq 0.05$ ).



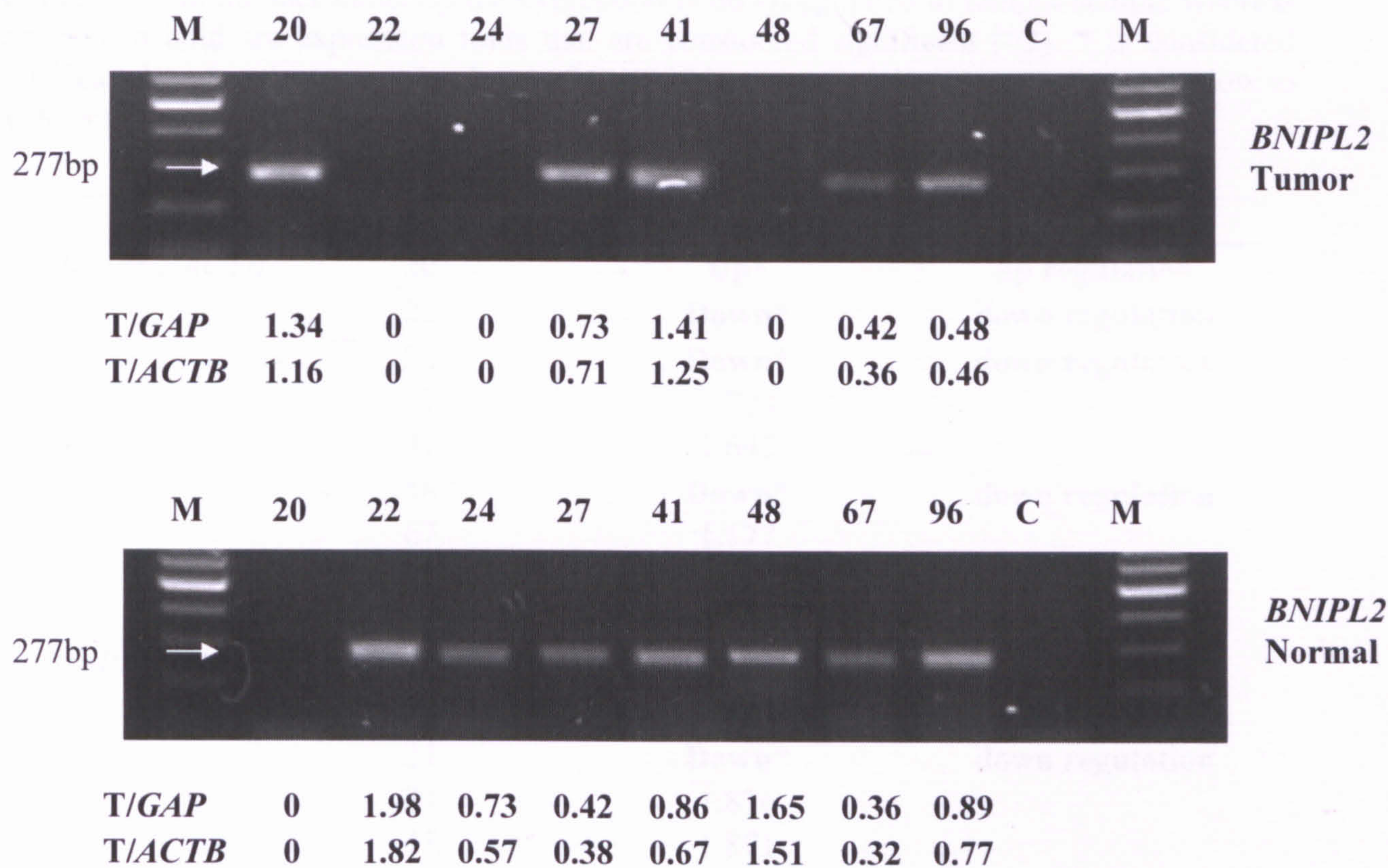


**Figure 4.8:** Expression of *BNIP2* in eight paired samples from local biopsies on 2.0% (w/v) agarose gel. The ratio indicates the expression level of the target (T) amplification product after normalized to internal control (*GAPDH* and *ACTB*). lane C: negative control, lane M: 100 bp DNA ladder



**Table 4.4:** Expression (fold change) of *BNIP2* in biopsy samples screened. Expression fold change is calculated based on the expression in tumour sample relative to its normal sample. A negative fold number indicates the expression is downregulated in tumour sample whereas numbers in bold are expression folds that are considered significant (>2). \* is considered significant because the expression level of *BNIP2* in the sample’s counterpart was too low to be detected by RT-PCR.

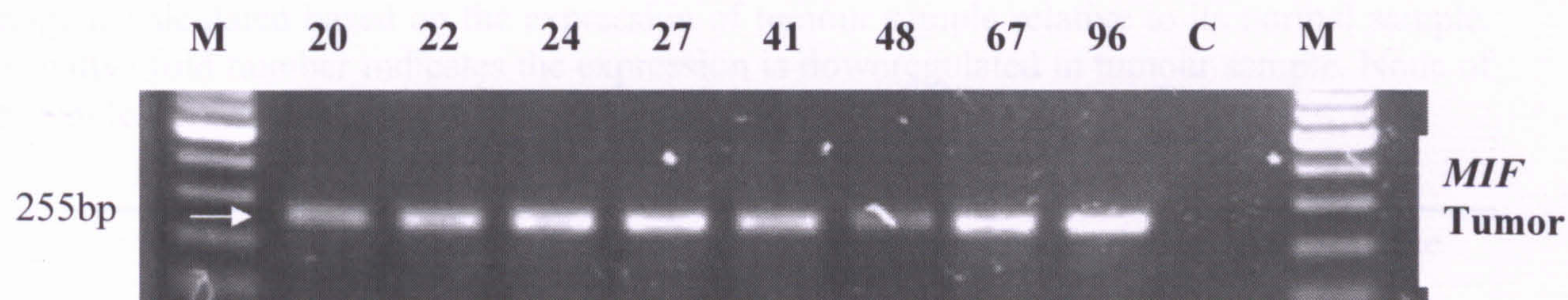
	sample name	Expression fold change	significance
<i>BNIP2/ACTB</i>	20	<b>Up*</b>	<b>up regulation</b>
	22	<b>Down*</b>	<b>down regulation</b>
	24	<b>Down*</b>	<b>down regulation</b>
	27	1.723	
	41	1.645	
	48	<b>Down*</b>	<b>down regulation</b>
	67	1.177	
	96	-1.851	
<i>BNIP2/GAPDH</i>	20	<b>Up*</b>	<b>up regulation</b>
	22	<b>Down*</b>	<b>down regulation</b>
	24	<b>Down*</b>	<b>down regulation</b>
	27	1.876	
	41	1.871	
	48	<b>Down*</b>	<b>down regulation</b>
	67	1.099	
	96	-1.67	



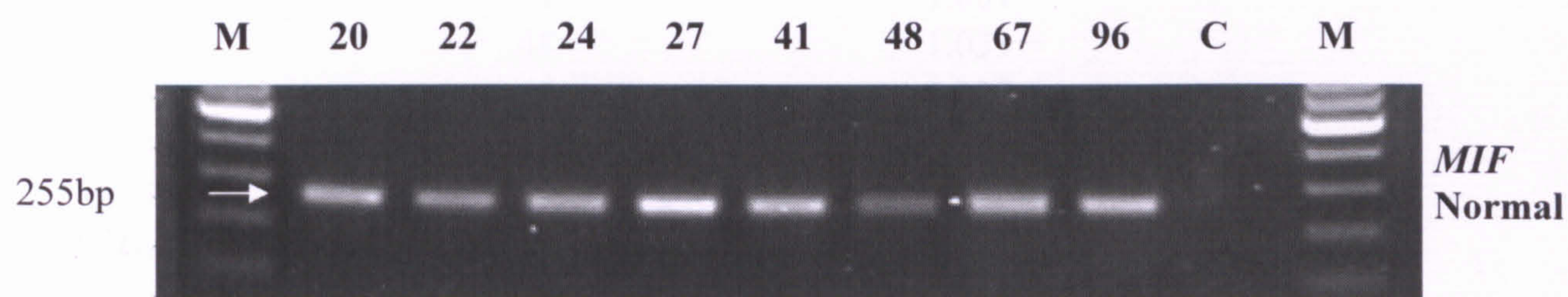
#### 4.3.6 *MIF*

Expression study was performed on 8 pairs of nasopharyngeal biopsy samples. The RT-PCR product for *MIF* was observed as a band of about 255bp in size on agarose gel (Figure 4.9). Normalized target expression in the samples is shown (Figure 4.9). Expression of *MIF* was detected in all normal and tumor biopsy tissues. Out of 8 samples, none of them showed significant fold differences in expression (Table 4.5). This indicates that *MIF* expression was quite similar between the tumor and normal samples. Statistical analysis revealed that average *MIF* expression in tumor samples did not differ significantly from normal samples when normalized with both *ACTB* (n=8,  $p \geq 0.05$ ) and *GAPDH* (n=8,  $p \geq 0.05$ ).





<b>T/<i>GAP</i></b>	<b>0.99</b>	<b>1.63</b>	<b>1.15</b>	<b>0.9</b>	<b>1.24</b>	<b>1.46</b>	<b>1.29</b>	<b>0.87</b>
<b>T/<i>ACTB</i></b>	<b>0.85</b>	<b>1.48</b>	<b>0.98</b>	<b>0.87</b>	<b>1.1</b>	<b>1.35</b>	<b>1.1</b>	<b>0.85</b>



<b>T/<i>GAP</i></b>	<b>1.7</b>	<b>1.69</b>	<b>1.69</b>	<b>1.07</b>	<b>1.24</b>	<b>1.41</b>	<b>1.05</b>	<b>1.16</b>
<b>T/<i>ACTB</i></b>	<b>1.35</b>	<b>1.55</b>	<b>1.32</b>	<b>0.96</b>	<b>0.97</b>	<b>1.29</b>	<b>0.96</b>	<b>1.02</b>

**Figure 4.9:** Expression of *MIF* in eight paired samples from local biopsies on 2.0% (w/v) agarose gel. The ratio indicates the expression level of the target (T) amplification product after normalized to internal control (*GAPDH* and *ACTB*). lane C: negative control, lane M: 100 bp DNA ladder



**Table 4.5:** Expression (fold change) of *MIF* in biopsy samples screened. Expression fold change is calculated based on the expression of tumour sample relative to its normal sample. A negative fold number indicates the expression is downregulated in tumour sample. None of the samples showed significant fold differences (>2).

	sample name	Expression fold change	significance
<i>MIF/ACTB</i>	20	-1.728	-
	22	1.020	-
	24	-1.477	-
	27	-1.199	-
	41	1.001	-
	48	1.039	-
	67	1.227	-
	96	-1.333	-
<i>MIF/GAPDH</i>	20	-1.580	-
	22	1.009	-
	24	-1.344	-
	27	-1.100	-
	41	1.138	-
	48	1.045	-
	67	1.146	-
	96	-1.201	-

#### 4.3.7 *GFER*

The RT-PCR product for *GFER* is a band of about 351bp. Normalized target expression level in the samples is depicted in Figure 4.10. *GFER* was expressed in all samples studied except in sample T48 in which the expression was not detected by RT-PCR. Table 4.6 shows the expression fold of *GFER* in biopsy samples screened. Out of the 8 pairs of samples studied, half of the samples showed *GFER* underexpression in tumor (20, 48, 67 and 96) with only sample 48 having significant underexpression fold. In samples 22, 24, 27 and 41, *GFER* expression was detected to be slightly higher (not significant) in the tumor (Table 4.6). Statistical analysis revealed that the average *GFER* expression in tumor samples did not differ significantly from normal samples with *GAPDH* (n=8,  $p \geq 0.05$ ) and *ACTB* (n=8,  $p \geq 0.05$ ).



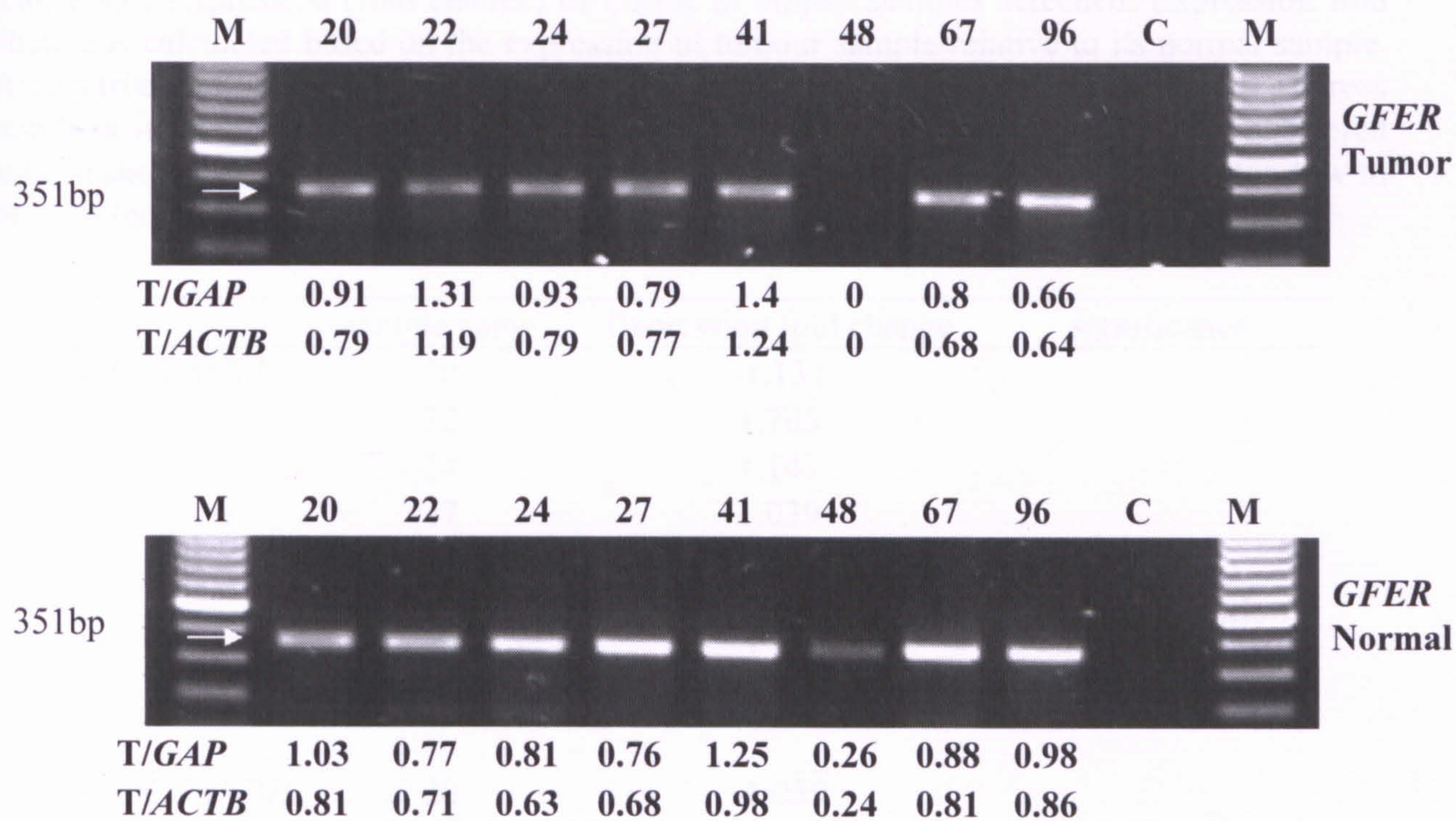


**Figure 4.10:** Expressions of *GFER* in eight paired samples from local biopsies on 2.0% (w/v) agarose gel. The ratio indicates the expression level of the target (T) amplification product after normalized to internal control (*GAPDH* and *ACTB*). lane C: negative control, lane M: 100 bp DNA ladder



**Table 4.6:** Expression (fold change) of *GFER* in biopsy samples screened. Expression fold change is calculated based on the expression of tumour sample relative to its normal sample. A negative fold number indicates the expression is downregulated in tumour sample whereas numbers in bold are expression folds that are considered significant (>2). \* is considered significant because the expression level of *GFER* in the sample’s counterpart was too low to be detected by RT-PCR.

	sample name	Expression fold change	significance
<i>GFER/ACTB</i>	20	-1.131	
	22	1.705	
	24	1.147	
	27	1.039	
	41	1.117	
	48	<b>Down*</b>	<b>down regulation</b>
	67	-1.104	
	96	-1.487	
<i>GFER/GAPDH</i>	20	-1.039	
	22	1.685	
	24	1.251	
	27	1.132	
	41	1.271	
	48	<b>Down*</b>	<b>down regulation</b>
	67	-1.18	
	96	-1.34	



#### 4.4 Discussion

Our study on *TRAF6* expression revealed its significant underexpression in 3 tumor cases out of 8 samples. In another 2 biopsies and in all NPC cell lines, *TRAF6* expression was also found lower in tumor but the underexpression was not significant (Table 4.1 and Table 4.2). Although there have been reports on *TRAF6* overexpression as crucial for NF- $\kappa$ B activation (Darnay *et al.*, 1999) and NF- $\kappa$ B activation linking with development of several cancers (Nakshatri *et al.*, 1997; Marker and Woodworth, 2006), interestingly, there has also been report on *TRAF6* overexpression and suppression of *oriP* activity (Shirakata *et al.*, 2001). *OriP* is the origin of DNA synthesis for episomal EBV DNA in latently infected cells (Sugden *et al.*, 1994; Yates, 1996). *OriP* allows for the proper segregation of replicated EBV episomes to daughter cells, upon cell division (Sugden *et al.*, 1994; Yates, 1996). Thus, *oriP* is needed to maintain EBV genome during latent infection.

EBV has been linked to Burkitt's lymphoma, T-cell lymphoma, gastric carcinoma, infectious mononucleosis and opportunistic lymphoma in immunosuppressed patients (Pattle and Farrell, 2006), but this is especially an important consideration in NPC where EBV is an aetiological agent (Tao and Chan, 2007). Our results of *TRAF6* underexpression observed in some of the samples suggested that this gene may be associated with NPC as tumor suppressor by suppressing *oriP* activity. Mutational analysis on *TRAF6* (appendix) reveal no mutations in the cDNA coding region. *TRAF6* expression was further tested via quantitative PCR approach which are described and discussed in Chapter Five.

The exact role of vlglin in human cell is still unclear, but it has been suggested to be involved in mRNA stabilization due to its numerous KH RNA binding domains (Siomi *et al.*, 1993)

and has been shown to bind mRNA (Dodson and Shapiro, 1997). Aberrant expression of RNA-BP can modify the regulation of a given mRNA as can modulation of signalling pathways that post-translationally modify RNA-BPs or other associated proteins (Audic and Hartley, 2004). These alterations have been reported in diverse cancer types and are often correlated with advanced stage and grade of tumors, resulting in misregulation of genes involved in cancer progression (Wang *et al.*, 2000; Gouble *et al.*, 2002; Audic and Hartley, 2004).

Recently Woo *et al.* (2010) showed that down-regulation of vigilin resulted in increased expression of *c-fms* proto-oncogene mRNA and protein. Vigilin over-expression reduced the level of *c-fms* mRNA and also suppressed translation of *c-fms* mRNA (Woo *et al.*, 2010). *C-fms* was expressed by the tumor epithelium in several human epithelial cancers (Chambers, 2009; Dai *et al.*, 2009) and its overexpression in breast cancer conferred invasive and metastatic properties (Lin *et al.*, 2001; Toy *et al.*, 2005). In addition, directed motility and invasion assays using human breast cancer cell lines showed that vigilin suppressed cellular motility and invasion (Woo *et al.*, 2010). This is the first demonstration linking vigilin to cancer functioning as a tumor repressor through binding to 3'UTR sequence in *c-fms* mRNA.

In our study, we found vigilin to be significantly underexpressed in 1 tumor biopsy (refer Table 4.3). Although there was only 1 sample that showed significant down regulation, but overall there were more samples (5 out of 8 samples) that showed the downexpression trend. Our results indicate that vigilin may have tumor suppressor role as well in the context of NPC. Our mutational analysis on vigilin (appendix) found no mutations in the cDNA coding region.



Studies by Shen *et al.* (2003) and Xie *et al.* (2004) indicated a tumor suppressive role of *BNIP2* but oncogenic role of this gene has also been reported (Xie *et al.*, 2007). In our study, *BNIP2* was significantly underexpressed in 3 tumour biopsies when compared to their normal counterparts (Table 4.4). This preliminary data indicates that this gene may be associated with the development of NPC.

In a study by Fang *et al.* (2008), *MIF* was found to be overexpressed in NPC samples from Southern China via cDNA microarray approach. Our findings did not show a specific *MIF* alteration pattern (Table 4.5) which may be due to disparities between ethnic groups used in the study in addition to geographical locations. A majority of the biopsy samples in our study were not Chinese, 2/8 are Ibans, 3/8 are Bidayus and 2/8 are Malays (Section 3.1.1, Table 3.1).

A number of recent studies imply that *MIF* could be centrally involved in processes regulating cell proliferation and tumor angiogenesis (Takahashi *et al.*, 1998; Chesney *et al.*, 1999; Shimizu *et al.*, 1999; Vecchio *et al.*, 2000; Yang *et al.*, 2000). Chesney *et al.* (1999) however demonstrated that although neutralization of *MIF* dramatically reduced the initial outgrowth of lymphoma cells in tumor-bearing mice, it did not significantly affect the growth of established tumors. The authors thus suggested an early primary effect for *MIF*. Interestingly, del Vecchio and colleagues (2000) studied *MIF* levels in different stages of prostatic adenocarcinomas and found that *MIF* expression was stronger in low-grade than in high-grade adenocarcinomas. In fact, the observation by del Vecchio and colleagues is consistent with the proposed early primary effect of *MIF* on tumor cell proliferation indicated by the study of Chesney *et al.* (1999). A direct tumorigenic and/or proangiogenic effect of overexpressed or

exogenously added recombinant human *MIF* (r*MIF*) alone has not been reported. In one study, r*MIF* failed to have the expected proliferative effect (Ogawa *et al.*, 2000). Together, the available evidences suggest that *MIF* is centrally involved in the initial phase of tumorigenesis and promotes angiogenesis, while its role in later tumor stages is unclear. If *MIF* is centrally involved in the initial phase of tumorigenesis, this may explain why *MIF* expression in our study did not show any significant deregulation in expression as our tumor samples were of late stage NPC. This is especially true for cancer like NPC as most NPC victims have had metastasis when first diagnosed due to its deep location and vague symptoms. However, whether *MIF* is playing some role in initiating NPC is not known.

*GFER* has been shown to be mainly involved in the process of liver regeneration (Pawlowski and Jura, 2006). The status of *GFER* overexpression and cancer has been reported previously (Zheng *et al.*, 2004; Thasler *et al.*, 2005). This gene has been identified in our NPC samples to be significantly underexpressed in 1 sample (Table 4.6). Overall expression pattern revealed underexpression of *GFER* in half of the samples and overexpression in the other half of the samples. Our data suggest that *GFER* may not be directly involved in the pathogenesis of NPC.



## CHAPTER FIVE

### EXPRESSION ANALYSIS OF *TRAF6* AND VIGILIN IN NASOPHARYNGEAL CARCINOMA VIA QUANTITATIVE PCR

#### 5.1 Introduction

When overexpressed in cultured human cells, TRAF6 activates NF- $\kappa$ B (Cao *et al.*, 1996). Recent evidences suggest that activation of NF- $\kappa$ B contributes to the development of several types of human cancers, including cancers of the blood and certain breast cancers (Nakshatri, *et al.*, 1997; Marker and Woodworth, 2006). It was reported that *Helicobacter pylori* induced NF- $\kappa$ B activation through an intracellular signaling pathway that involved TRAF6 in gastric cancer cells (Maeda *et al.*, 2000). Overexpression of TRAF6 has been found to suppress *oriP* activity of Epstein-Barr virus (EBV) (Shirakata, 2001). During latent infection, EBV genome is maintained by the region *oriP* containing an origin of bidirectional DNA replication (Yates, 1996). TRAF6 was found to play a role in cell growth and carcinogenesis through Akt activation (Yang *et al.*, 2009). TRAF6 depletion in prostate cancer cells reduced Akt activation and mice with *TRAF6* knocked down developed smaller prostate cancer tumors than those with active *TRAF6* (Yang *et al.*, 2009). *TRAF6* is believed to be a previously unrecognized oncogene and is a new potential target for treating human cancers (Yang *et al.*, 2009).

K Homology (KH) protein family member vigilin known as the high density lipoprotein-binding protein (Fidge, 1999; McKnight *et al.*, 1992), contains 15 tandemly arranged KH domains for RNA binding (Gherzi, 2004) and has been shown to bind to the non-ARE-containing *Xenopus* vitellogenin mRNA 3'UTR 3 (Dodson and Shapiro, 1997) and stabilizes

its mRNA. The yeast vigilin homolog Scp160p was found in polysome-bound Mrnp (messenger ribonucleoprotein) complexes which also includes PABPs (Poly(A)-binding proteins (Lang, and Fridovich-Keil, 2000). This suggests a role for vigilin in regulation of mRNA metabolism and translation.

Woo *et al.* (2010) showed that vigilin binds to the same 69nt sequence in the *c-fms proto-oncogene* mRNA 3'UTR, to which HuR binds. They reported that when vigilin expression was down regulated, *c-fms* mRNA and protein expression was increased. In addition, it was observed that vigilin suppressed cellular motility and invasion in human breast cancer cell lines (Woo *et al.*, 2010). Their work suggested that vigilin may have a role in cancer by functioning as a tumor repressor through competing with HuR for binding to a novel 69nt non-ARE containing 3'UTR sequence in *c-fms* mRNA.



## 5.2 General methodology

Tri reagent (Molecular Research Center) was used in total RNA isolation as described in chapter 3, section 3.1.2. The biopsy sample was homogenized in the Ambion<sup>®</sup> TRI Reagent, mixed with chloroform and the mixture was separated into three phases by centrifugation. The RNA was then precipitated from the aqueous phase with isopropanol. RNA was DNase treated prior to reverse transcription.

A two-step Reverse Transcription PCR (RT-PCR) was employed, where reverse transcription and quantitative PCR were carried out in separate tubes. The expression analysis was performed on nine paired local biopsies samples (20, 22, 24, 27, 41, 48, 55, 67 and 96).

Rotor-Gene SYBR Green PCR Kit was used in our quantitative PCR study. The components of 2x Rotor-Gene SYBR Green PCR Master Mix include HotStarTaq *Plus* DNA Polymerase, Rotor-Gene SYBR Green PCR Buffer, and SYBR Green I. Approximately 10ng cDNA template was used in the PCR reaction. The amplification was carried out in Rotor-Gene 6000 real-time PCR cycler. PCR tubes were placed into the rotor which spins tubes past the same excitation light source and the same detector in a chamber of moving air.

A minus-reverse transcriptase control ("No Amplification Control" or NAC) was included in quantitative PCR experiments to check for the presence of DNA contamination. The NAC is a mock reverse transcription containing all the RT-PCR reagents, except the reverse transcriptase. Besides, a "No Template Control" (NTC) was also included in the run to rule

out cross contamination of reagents and surfaces. The NTC includes all of the RT-PCR reagents except the RNA template whereby RNA was substituted with nuclease-free water.

Dissociation (melting) curves were performed to check specificity of products. Primer sets were designed to specifically amplify cDNA sequences derived from mRNA transcripts. This prevents amplification of contaminating genomic DNA. The comparative  $C_T$  Method, also referred to as  $\Delta\Delta C_T$  method was used for relative quantitation of gene expression. Target(s) and endogenous control were ensured to have similar or relatively equivalent PCR efficiencies. Using the  $\Delta\Delta C_T$  method, the data was presented as the fold change in gene expression of target amplicons in NPC samples normalized to an endogeneous reference gene and relative to the normal control.



5.3 Results

5.3.1 Total RNA samples assessment

Expression analysis with quantitative PCR for *TRAF6* and *vigilin* mRNA was performed for total RNA extracted from nine paired normal and tumor NP tissue (20, 22, 24, 27, 41, 48, 55, 67 and 96). Out of these 9 samples, 8 samples were previously used with conventional PCR except for paired sample 55 which were only collected and added at a later stage of this study. The RNA gels of the previous 8 samples were shown in Figure 4.1. Ribosomal RNA bands for paired sample 55 were shown in Figure 5.1 below.

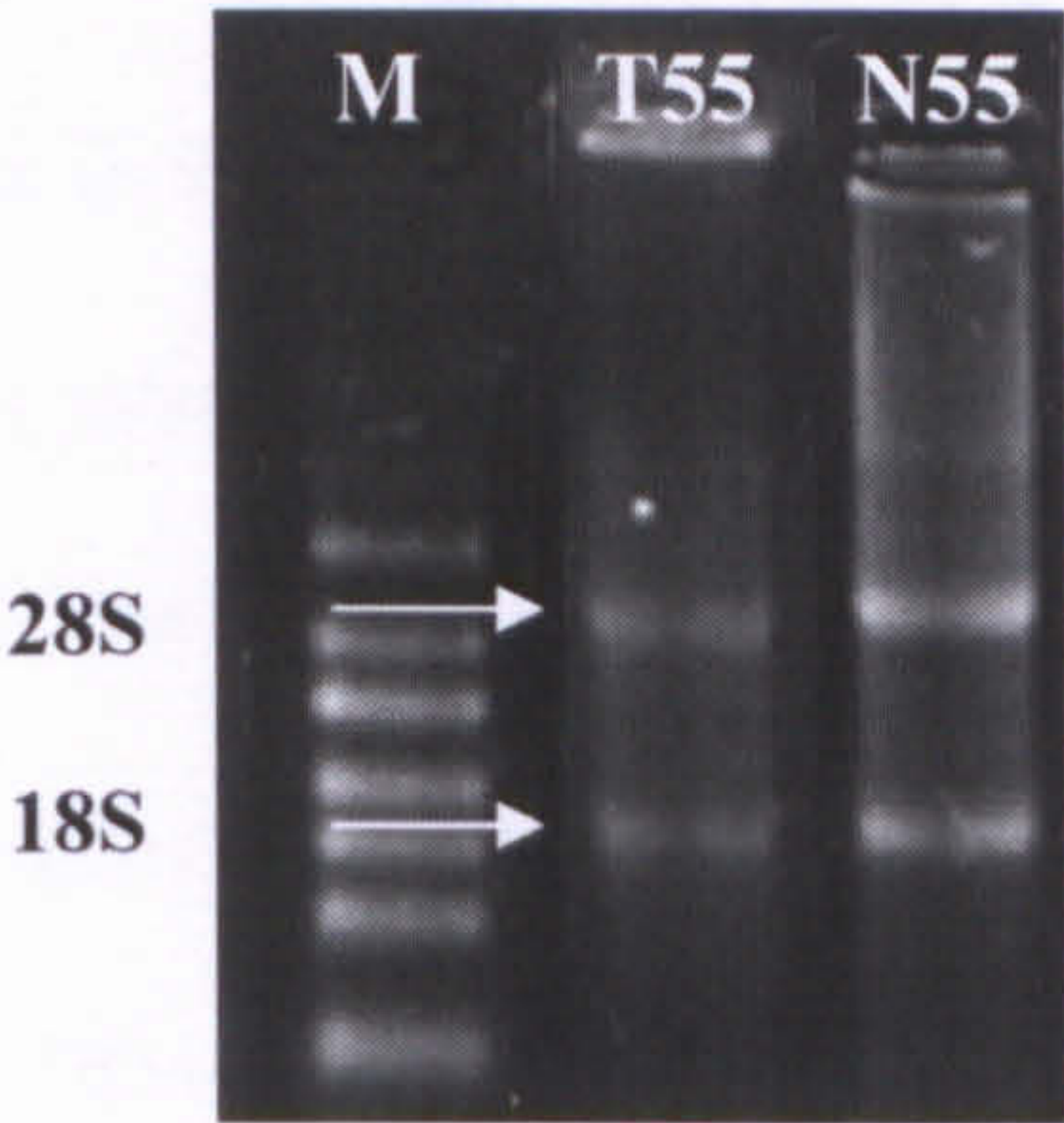


**Figure 5.1:** Total RNA isolated from paired biopsy sample 55 using Trizol method. RNA was displayed on a 1% x TAE agarose gel (~1 µg per lane). Lane M: RNA ladder, High Range, 200-6000 bases (Promega, USA)



### 5.3.2 Validation of Target and Control Genes for the Comparative C<sub>T</sub> Method

The Comparative C<sub>T</sub> Method, also referred to as the  $\Delta\Delta C_T$  Method, is similar to the Relative Standard Curve Method, except it uses arithmetic formulae to achieve the result for relative quantitation. It is possible to eliminate the use of standard curves and to use the  $\Delta\Delta C_T$  Method for relative quantitation as long as the PCR efficiencies between the target(s) and endogenous control(s) are relatively equivalent.

The slope (M) of a reaction (calculated by Rotor-Gene 6000 Software and shown in the standard curve window) (Figure 5.2) was used to determine the exponential amplification and efficiency for *GAPDH*, *TRAF6* and vigilin. The slope was calculated automatically by the software of being the change in C<sub>T</sub> divided by the change in log input. Table 5.1-5.3 shows the standard curve C<sub>T</sub> values involving five input cDNA (HONE1, NPC cell line) from a 5-fold serial dilution: 50, 10, 2, 0.4, 0.08 (ng) with two replicates at each point. Standard curve for *GAPDH*, *TRAF6* and vigilin is shown in Figure 5.3. Ideally, the dilution series will produce amplification curves that are evenly spaced.

A 100% efficient amplification means a doubling of amplification product in each cycling resulting in a reaction efficiency of 1. Reaction efficiency was calculated by the software with the formula  $[10(-1/M)] - 1$ . Given an M value of -3.322, the calculation is as follows:  $[10(-1/-3.322)] - 1 = 1$  (Corbett Research, 2006). The calculated reaction efficiency for *TRAF6*, vigilin and *GAPDH* is displayed in Table 5.4. The amplification efficiency of the gene of interest (*TRAF6* and vigilin) and normalizer (*GAPDH*) are relatively similar, thus the  $\Delta\Delta C_T$  calculation for the relative quantification of target was used in this study.



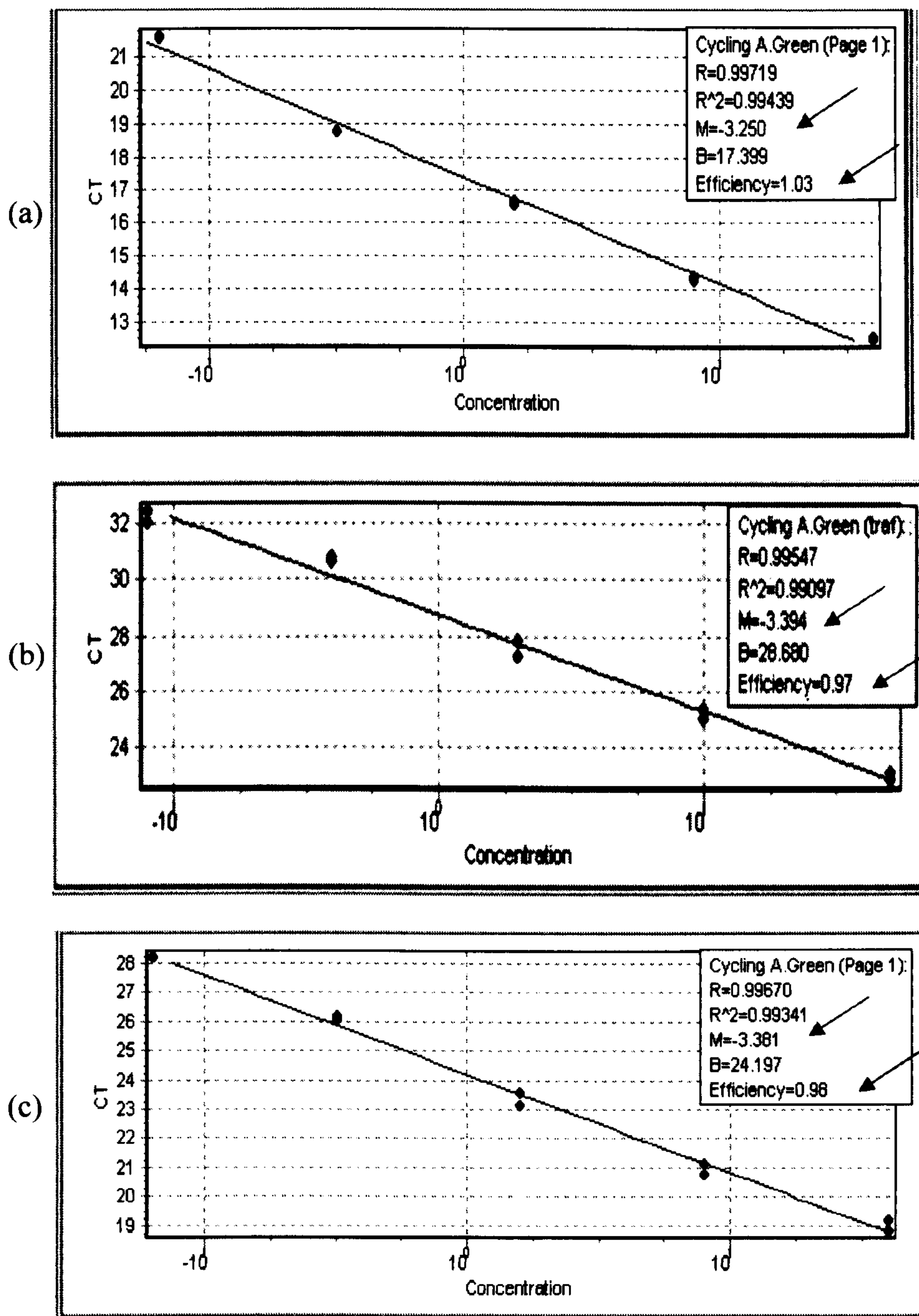


**Figure 5.2:** Standard curve plots: log of input cDNA (HONE1, NPC cell line) from a 5-fold serial dilution: 50, 10, 2, 0.4, 0.08 (ng) versus  $C_T$  value obtained during amplification of each dilution (a) *GAPDH* (b) *TRAF6* (c) *vigilin*

**Table 5.1:** *GAPDH* standard curve involving five-fold dilutions: 50, 10, 2, 0.4, 0.08 (ng) with two replicates at each point.

Type	C <sub>T</sub>	Conc (Copies)	Rep. C <sub>T</sub>
Standard	12.44	50	12.46
Standard	12.48	50	
Standard	14.35	10	14.29
Standard	14.22	10	
Standard	16.65	2	16.6
Standard	16.56	2	
Standard	18.76	0.4	18.74
Standard	18.73	0.4	
Standard	21.62	0.08	21.59
Standard	21.55	0.08	

**Table 5.2:** *TRAF6* standard curve involving five-fold dilutions: 50, 10, 2, 0.4, 0.08 (ng) with two replicates at each point.

Type	C <sub>T</sub>	Conc (Copies)	Rep. C <sub>T</sub>
Standard	22.99	50	22.97
Standard	22.95	50	
Standard	25.03	10	25.18
Standard	25.34	10	
Standard	27.68	2	27.51
Standard	27.34	2	
Standard	30.77	0.4	30.71
Standard	30.64	0.4	
Standard	32.33	0.08	32.23
Standard	32.13	0.08	

**Table 5.3:** *Vigilin* standard curve involving five-fold dilutions: 50, 10, 2, 0.4, 0.08 (ng) with two replicates at each point.

Type	C <sub>T</sub>	Conc (Copies)	Rep. C <sub>T</sub>
Standard	19.08	50	18.99
Standard	18.9	50	
Standard	20.99	10	21.02
Standard	21.05	10	
Standard	23.11	2	23.33
Standard	23.54	2	
Standard	26.15	0.4	26.1
Standard	26.04	0.4	
Standard	28.89	0.08	28.91
Standard	28.93	0.08	



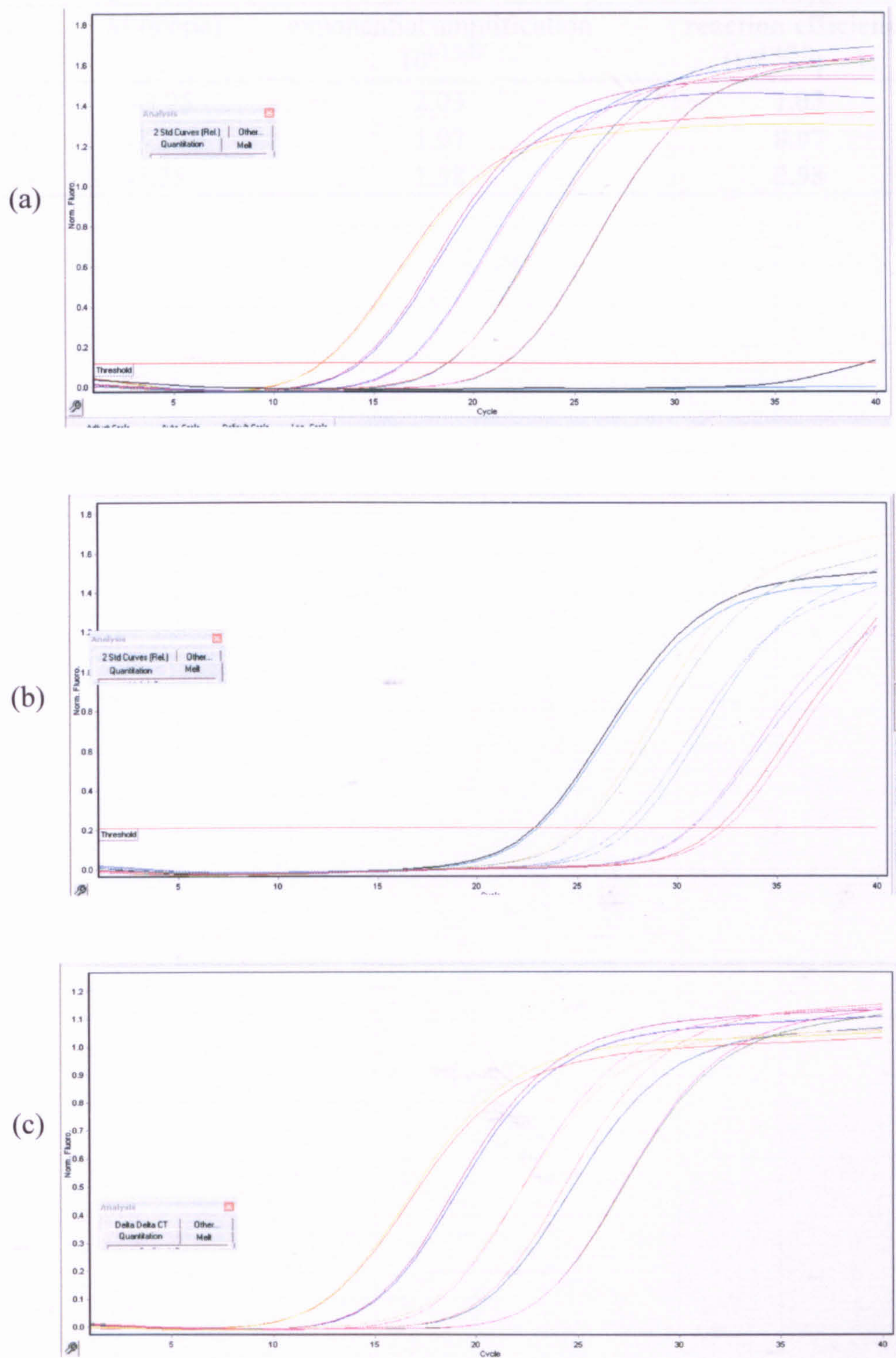


**Figure 5.3:** Standard curve (a) *GAPDH* (b) *TRAF6* (c) *vigilin*



**Table 5.4:** Slope, amplication and reaction efficiency for *GAPDH*, *TRAF6* and vigilin

Gene	M (slope)	exponential amplification $10^{(-1/M)}$	reaction efficiency $[10^{(-1/M)}] - 1.$
<i>GAPDH</i>	-3.25	2.03	<b>1.03</b>
<i>TRAF6</i>	-3.394	1.97	<b>0.97</b>
vigilin	-3.381	1.98	<b>0.98</b>

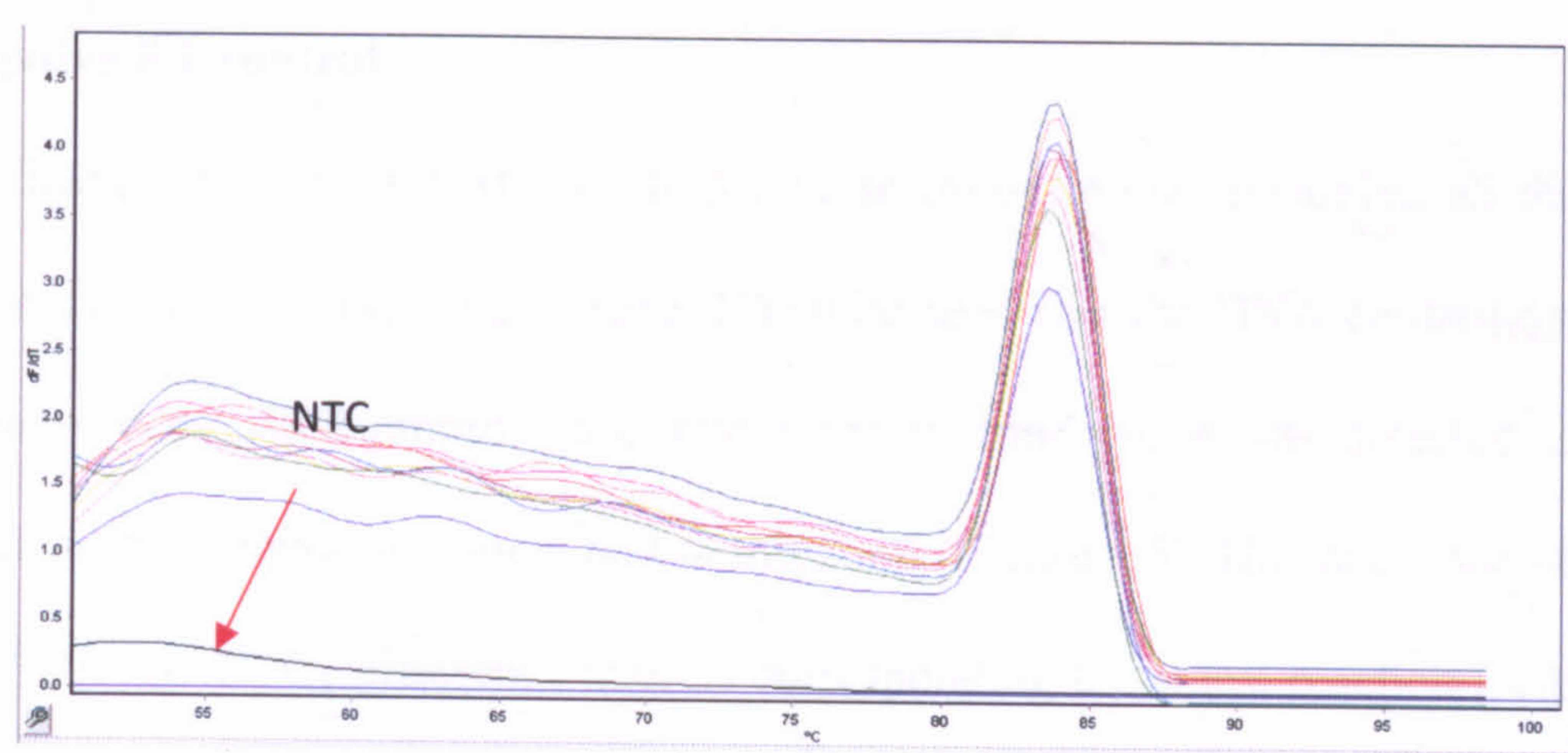


### **5.3.3 Dissociation (melting) curves**

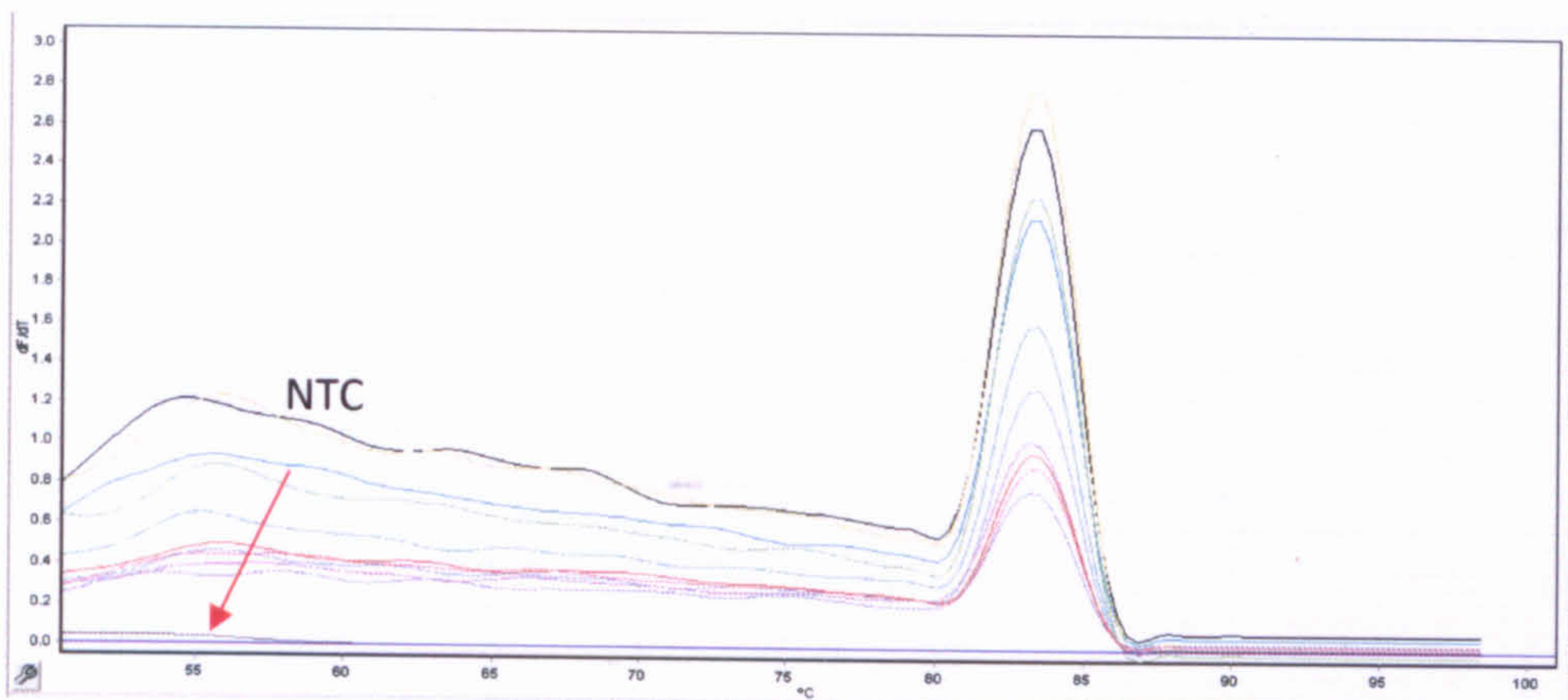
Dissociation (melting) curves were performed for *GAPDH*, *TRAF6* and vigilin as shown in Figure 5.4. The experimental samples gave a sharp peak of dissociation (melting) curves at the melting temperature of the amplicon (*GAPDH*, *TRAF6* and vigilin), whereas NTC did not generate significant fluorescent signal. This result indicates that the products are specific, and that SYBR Green I fluorescence is a direct measure of accumulation of the product of interest.



(a)



(b)



(c)

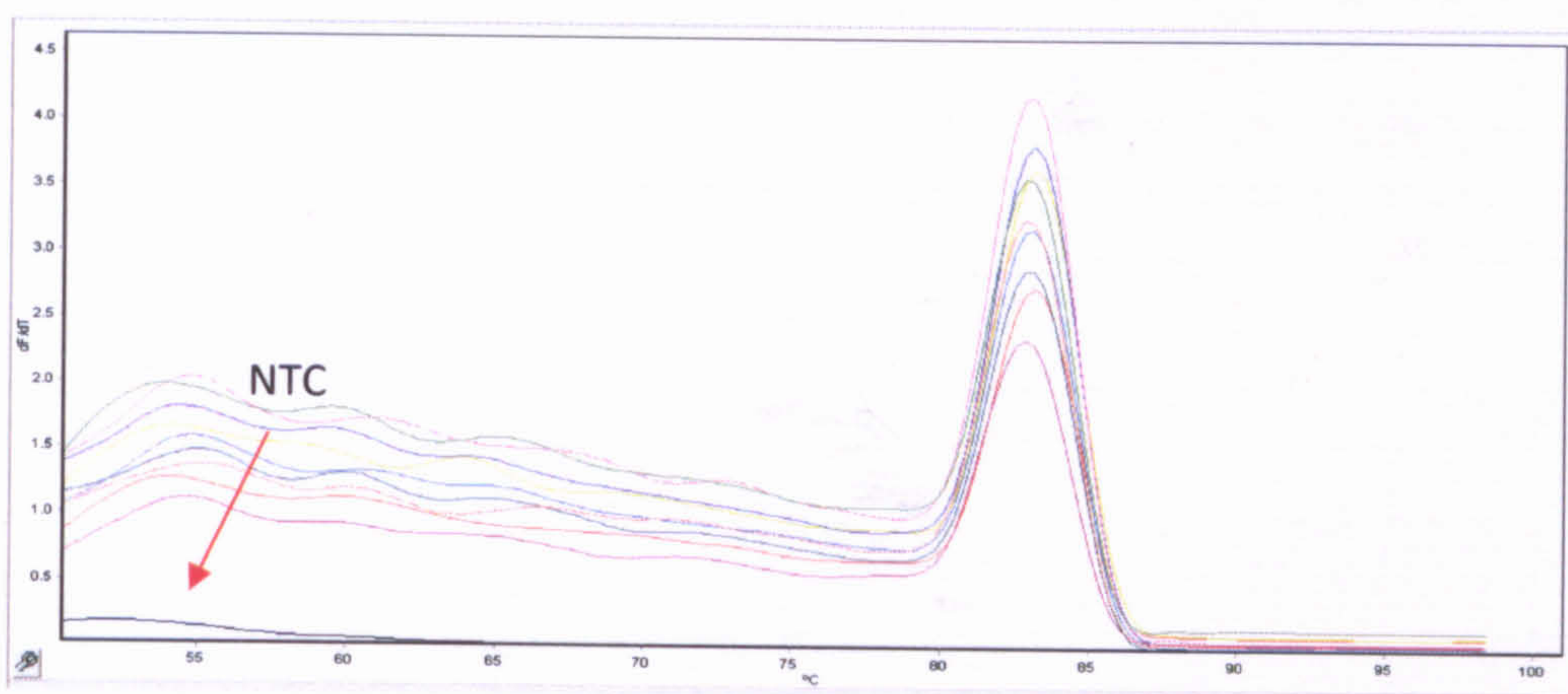


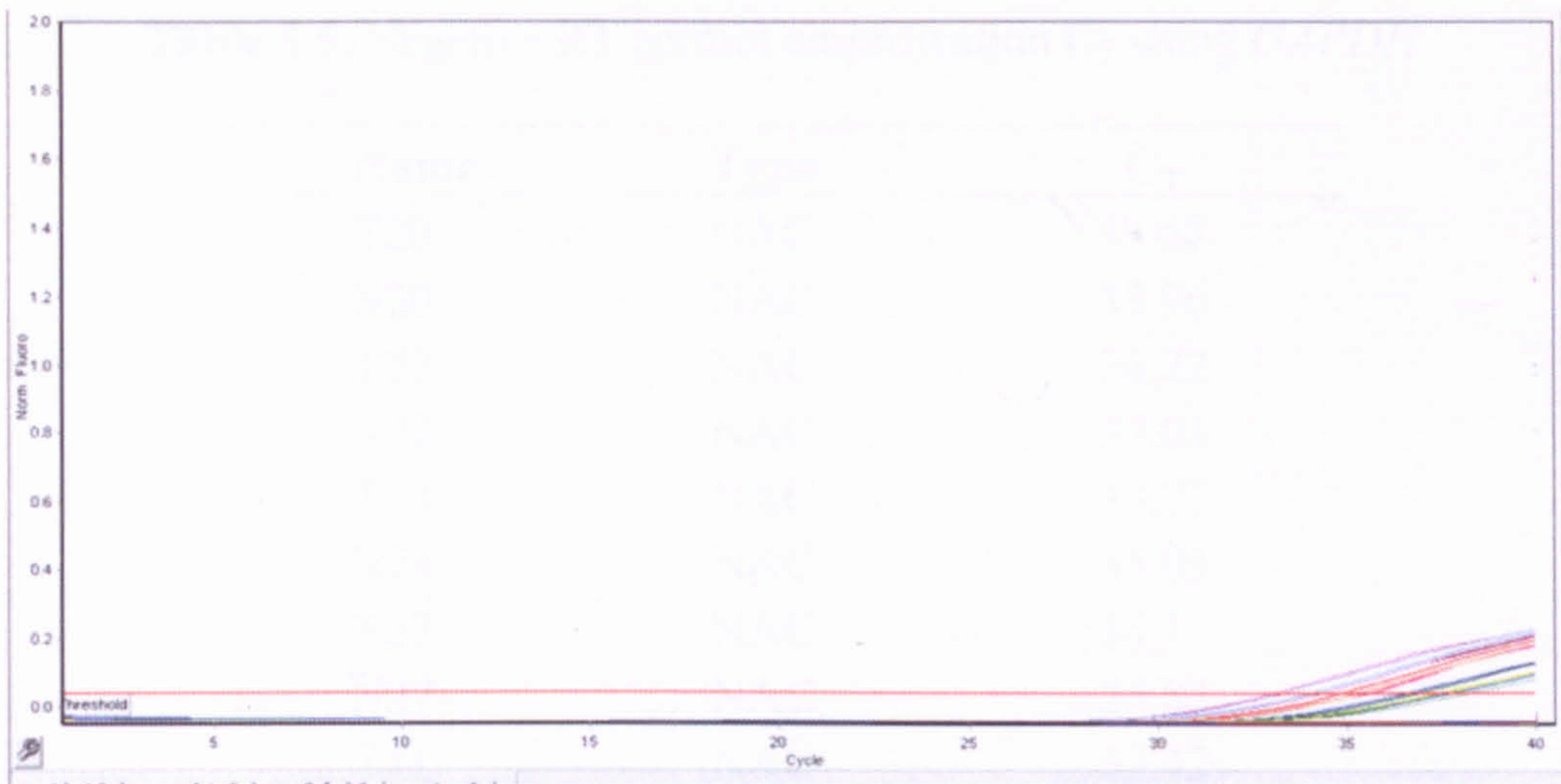
**Figure 5.4:** Melting curve for samples used in quantitative study for (a) *GAPDH* (b) *TRAF6* (c) *vigilin*



#### **5.3.4 Negative RT control**

No amplification control or NAC is a trial reverse transcription containing all the RT-PCR reagents, except the reverse transcriptase. It can be seen that the DNA contamination is not totally removed as small amplification curve and melting curve was detected in the –RT samples even after DNase treatment and purification (Figure 5.5). However, our –RT control using *GAPDH* has 10  $C_T$  difference than its corresponding  $C_T$  in test reaction (refer to Table 5.5 and 5.6).

(a)



(b)

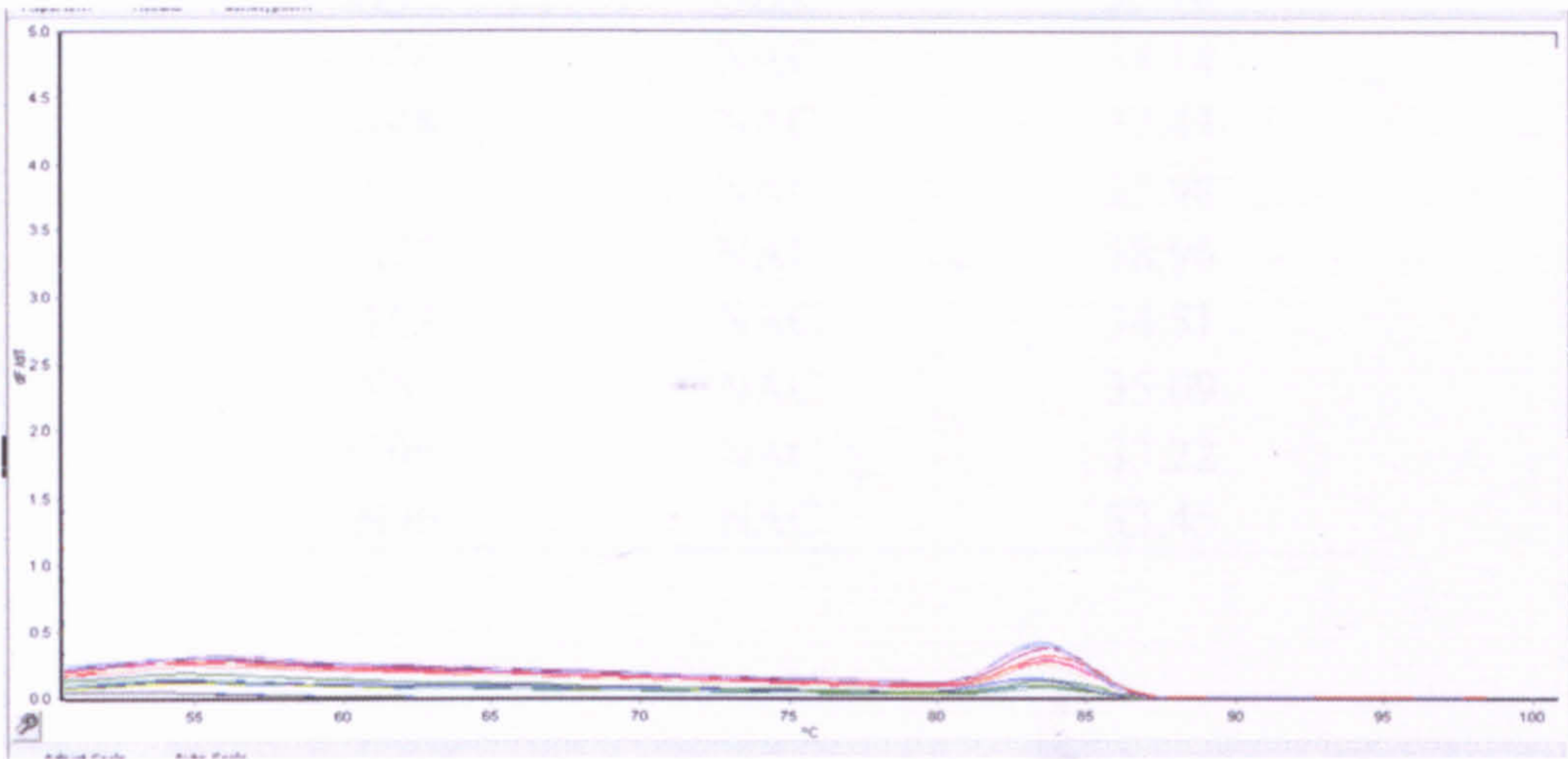


**Figure 5.5:** *GAPDH* (a) NAC amplification curve and (b) NAC melting curve for nine paired biopsy samples



**Table 5.5:** Negative RT control amplification C<sub>T</sub> using *GAPDH*

<b>Name</b>	<b>Type</b>	<b>C<sub>T</sub></b>
T20	NAC	33.58
N20	NAC	33.96
T22	NAC	34.22
N22	NAC	37.01
T24	NAC	33.77
N24	NAC	35.03
T27	NAC	34.17
N27	NAC	34.87
T41	NAC	33.42
N41	NAC	33.18
T48	NAC	38.14
N48	NAC	37.44
T55	NAC	35.98
N55	NAC	38.96
T67	NAC	34.51
N67	NAC	35.09
T96	NAC	33.22
N96	NAC	33.45

### 5.3.5 Data analysis using the $\Delta\Delta C_T$ (Delta Delta $C_T$ ) Method

Using this method, the amount of target, normalized to an endogenous reference and relative to a calibrator, is given by the formula  $2^{-\Delta\Delta C_T}$ . The calibrator in this study is the paired normal (non-cancer) samples. Each sample was initially normalised for the amount of template added by comparison relative to the housekeeping gene (*GAPDH*) calculated as the  $C_T$  difference of target and housekeeping gene (refer to Table 5.6, delta  $C_T$  column). These normalised values were further normalised relative to a calibrator treatment calculated as  $C_T$  difference of normalized tumor and normal paired samples (refer to Table 5.6, delta delta  $C_T$  column). The expression of target gene is relative to the calibrator sample (normal counterpart) which is assigned a relative expression of 1 calculated by the formula  $2^{-\Delta\Delta C_T}$ . In this study, each sample was performed in two replicates and the mean of relative concentration was calculated.

The threshold (a level of normalized reporter signal that was used for  $C_T$  determination) was determined using the Auto-Find Threshold function of the Rotor-Gene 6000 (Qiagen, USA) that scans the range of threshold levels to obtain the best level.



**Table 5.6:** *TRAF6* and *GAPDH* amplification C<sub>T</sub> of replicate 1

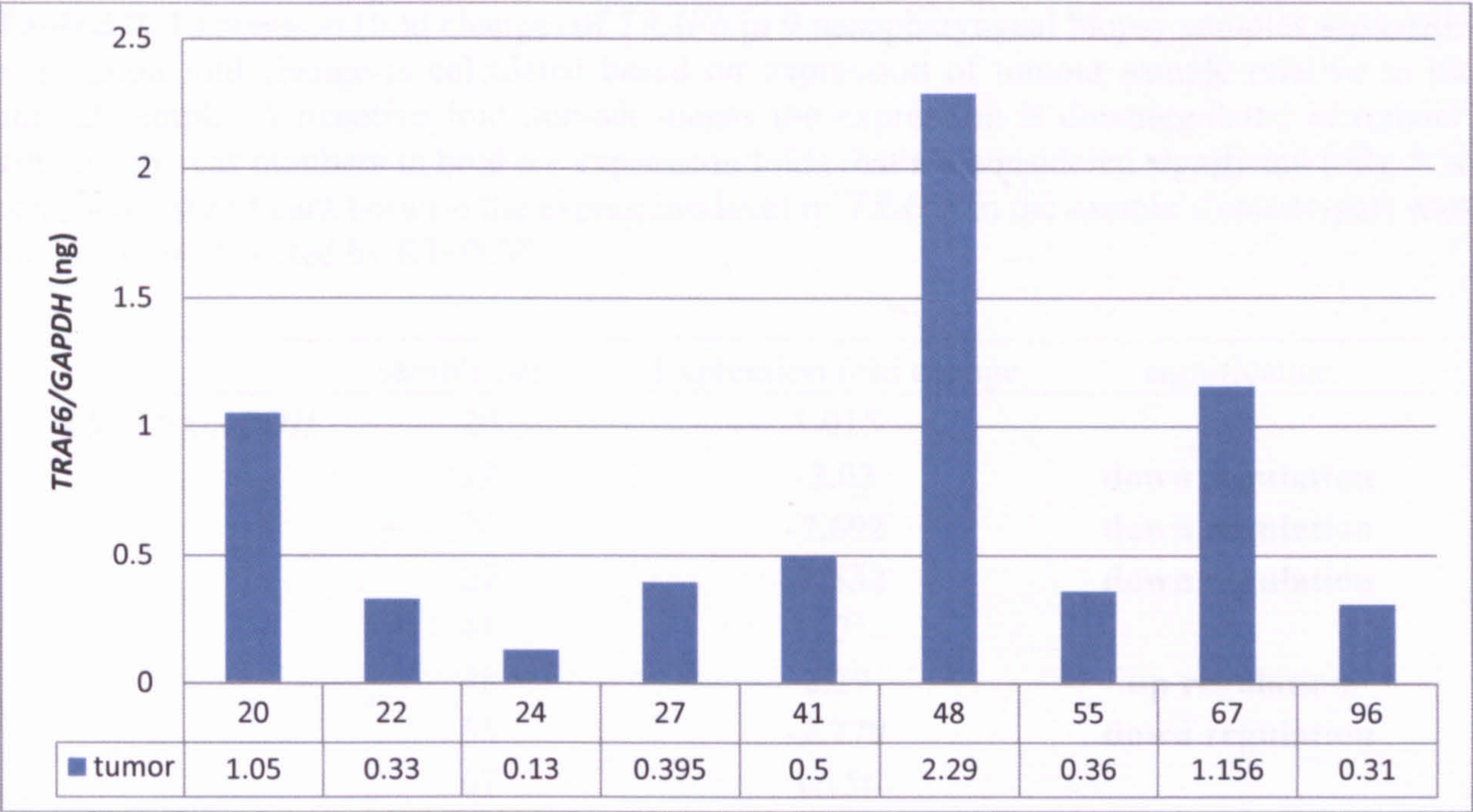
Name	<i>TRAF6</i> C <sub>T</sub>	<i>GAPDH</i> C <sub>T</sub>	Delta C <sub>T</sub>	Delta Delta C <sub>T</sub>	Relative Conc.
T20	31.12	22.68	8.44	-0.33	1.26
N20	32.34	23.57	8.77	0	1
T22	32.75	24.41	8.34	2.84	0.14
N22	31.71	26.21	5.50	0	1
T24	33.95	21.85	12.1	2.56	0.17
N24	32.50	22.96	9.54	0	1
T27	31.93	21.16	10.77	1.18	0.44
N27	30.92	21.33	9.59	0	1
T41	34.15	22.9	11.25	2.56	0.17
N41	30.65	21.96	8.69	0	1
T48	31.51	27.32	4.19	-0.76	1.69
N48	32.09	27.14	4.95	0	1
T55	29.66	24.99	4.67	0.89	0.54
N55	32.61	28.83	3.78	0	1
T67	31.11	21.92	9.19	-0.46	1.372
N67	29.82	20.17	9.65	0	1
T96	29.11	19.57	9.54	1.56	0.34
N96	29.36	21.39	7.98	0	1

#### 5.3.5.1 *TRAF6*

The *TRAF6* specific primers amplified a region of 262bp. The relative expression of *TRAF6* depicted in bar chart is shown in Figure 5.6. Table 5.7 is a summary of *TRAF6* expression analysis in fold change by comparing the expression of tumour samples relative to the expression of their normal counterparts. Expression fold change  $>2$  is considered as significant. SPSS Paired Sample t-test was used to check for overall significance of the differential expression between normal and tumor samples (p-value  $< 0.05$  is considered significant).

Out of 9 samples normalized with *GAPDH*, 5 samples (22, 24, 27, 55 and 96) showed significant *TRAF6* underexpression in tumor (Table 5.7). One sample (48) however showed *TRAF6* overexpression in tumor. Overall, 6 out of 9 samples exhibited underexpression pattern. The average *TRAF6* expression (normalized with *GAPDH*) in tumor samples did not differ significantly from normal samples ( $n=9$ ,  $p \geq 0.05$ ).





	Mean	N	Std. Deviation	Std. Error Mean
Normal	1	9	0	0
Tumor	0.72	9	0.68	0.227

**Figure 5.6:** A bar chart showing relative concentration of *TRAF6* in nine paired biopsy samples. The normalized expression is relative to the paired normal sample which is assigned a relative expression of 1. Mean and standard deviation were calculated after normalization to *GAPDH*.



**Table 5.7:** Expression (fold change) of *TRAF6* in 9 nasopharyngeal biopsy samples screened. Expression fold change is calculated based on expression of tumour sample relative to its normal sample. A negative fold number means the expression is downregulated in tumour sample whereas numbers in bold are expression folds that are considered significant (>2). \* is considered significant because the expression level of *TRAF6* in the sample’s counterpart was too low to be detected by RT-PCR.

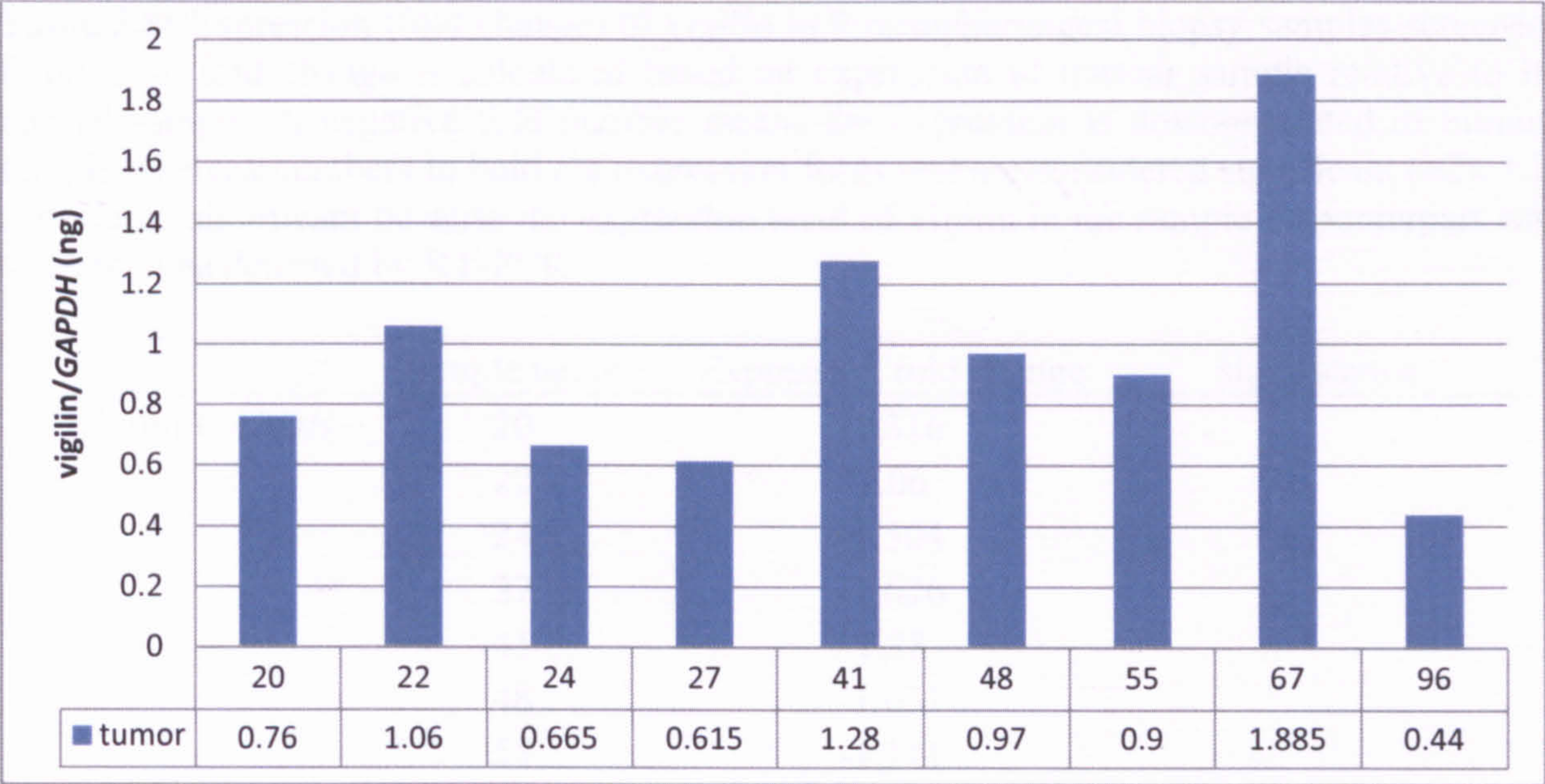
	sample name	Expression fold change	significance
<i>TRAF6/GAPDH</i>	20	1.015	
	22	<b>-3.03</b>	<b>down regulation</b>
	24	<b>-7.692</b>	<b>down regulation</b>
	27	<b>-2.532</b>	<b>down regulation</b>
	41	-2	
	48	<b>2.29</b>	<b>up regulation</b>
	55	<b>-2.778</b>	<b>down regulation</b>
	67	1.156	
	96	<b>-3.226</b>	<b>down regulation</b>



**5.3.5.2 Vigilin**

The relative expression of vigilin in the samples after normalization is depicted as bar chart shown in Figure 5.7. Table 5.8 is a summary of vigilin expression in fold change by comparing the expression in tumour samples relative to their normal counterparts. Out of 9 samples, only 1 sample (96) showed significant underexpression foldchange (Table 5.9). Overall, 6 (20, 24, 27, 48, 55 and 96) out of 9 samples showed vigilin underexpression in tumor. The average vigilin expression in tumor samples did not differ significantly from normal samples (n=9,  $p \geq 0.05$ ).





	Mean	N	Std. Deviation	Std. Error Mean
Normal	1	9	0	0
Tumor	0.953	9	0.431	0.144

**Figure 5.7:** A bar chart showing relative concentration of vigilin in nine paired biopsy samples.. The normalized expression is relative to the paired normal sample which is assigned a relative expression of 1. Mean and standard deviation were calculated after normalization to *GAPDH*.



**Table 5.8:** Expression (fold change) of vigilin in 9 nasopharyngeal biopsy samples screened. Expression fold change is calculated based on expression of tumour sample relative to its normal sample. A negative fold number means the expression is downregulated in tumour sample whereas numbers in bold are expression folds that are considered significant (>2). \* is considered significant because the expression level of vigilin in the sample’s counterpart was too low to be detected by RT-PCR.

	sample name	Expression fold change	significance
vigilin/ <i>GAPDH</i>	20	-1.316	
	22	1.06	
	24	-1.504	
	27	-1.626	
	41	1.28	
	48	-1.031	
	55	-1.111	
	67	1.885	
	96	<b>-2.273</b>	<b>down regulation</b>

### **5.3.6 Comparison of *TRAF6* and vigilin mRNA expression via conventional PCR and quantitative PCR**

Out of the 9 samples screened via quantitative PCR, 5 samples (22, 24, 27, 55, 96) showed significant *TRAF6* underexpression in tumor (Table 5.7). Though the overall (9 samples) underexpression pattern is not significant at  $P=0.05$ , but at least two fold or more of *TRAF6* underexpression was detected in those five samples. Of these five samples, all have the same underexpression pattern/trend seen with previous expression data obtained with conventional PCR except for sample 55 which was only used in quantitative PCR study (Table 5.9). Out of these 4 samples that have consistently shown underexpression pattern (with both conventional PCR and quantitative PCR), 3 samples namely 22, 24 and 96 were of undifferentiated type of NPC.

With vigilin, only sample 96 showed significant underexpression in tumor (Table 5.8). However, 6 out of 9 samples revealed underexpression pattern in tumor namely samples 20, 24, 27, 48, 55 and 96. Of these, all were also showing underexpression pattern as with previous conventional PCR with an exception to sample 55 (Table 5.9). The overall underexpression of vigilin from 9 samples screened was not significant ( $p>0.05$ ), but more samples were observed to show the trend.



**Table 5.9:** Summary of expression analysis of target gene expression (after normalization) in paired tumor and normal nasopharyngeal biopsy samples via conventional and quantitative PCR approach. A negative fold number means the expression is downregulated in tumour sample whereas numbers in bold are expression folds that are considered significant (>2). \* is considered significant because the expression level of target genes in the sample’s counterpart was too low to be detected.

		Conventional PCR		Quantitative	
			significance	PCR	significance
<i>TRAF6/GAPDH</i>	20	1.388		1.015	
	22	<b>-2.331</b>	<b>down</b>	<b>-3.03</b>	<b>down</b>
	24	<b>Down*</b>	<b>down</b>	<b>-7.692</b>	<b>down</b>
	27	-1.518		<b>-2.532</b>	<b>down</b>
	41	<b>Down*</b>	<b>down</b>	-2	
	48	<b>2.813</b>	<b>up</b>	<b>2.29</b>	<b>up</b>
	55			<b>-2.778</b>	<b>down</b>
	67	1.249		1.156	
	96	-1.125		<b>-3.226</b>	<b>down</b>
		Conventional PCR		Quantitative	
			significance	PCR	significance
<i>vigilin/GAPDH</i>	20	-1.011		-1.316	
	22	1.285		1.06	
	24	-1.036		-1.504	
	27	-1.144		-1.626	
	41	1.236		1.28	
	48	<b>Down*</b>	<b>down</b>	-1.031	
	55			-1.111	
	67	1.165		1.885	
	96	-1.123		<b>-2.273</b>	<b>down</b>

## 5.4 Discussions

Our quantitative PCR data further strengthen our observation of *TRAF6* underexpression in tumor. Undifferentiated NPCs are the human malignancy most consistently associated with EBV, regardless of the geographic distribution of cases (Raab-Traub, 2002; Tao *et al.*, 2007). In NPC, EBV infection is predominantly latent (Tao *et al.*, 2007). Latent Epstein-Barr virus (EBV) is maintained by the virus replication origin *oriP* that initiates DNA replication of ebv (Yates, 1996). Overexpression of TRAF6 has been reported to suppress *oriP* activity (Shirakata, 2001).

Our expression study showed consistent underexpression of *TRAF6* in majority tumor via both conventional and quantitative PCR (Table 5.9). This suggests that lower *TRAF6* expression is needed to avoid suppression of *oriP* activity in order to maintain EBV genome. It has also been reported that replication of EBV genome can be initiated in a broad initiation zone distant from *oriP* (Izumi *et al.*, 1999). In other words, replication of EBV genome could occur independently from *oriP*. It was shown *oriP*-independent replication may be preferentially used over *oriP* in lymphomas (Izumi *et al.*, 1999). It was shown that DNA replication by *oriP* requires only the viral *oriP*-binding protein EBNA1 (Shirakata *et al.*, 1999; Hirai and Shirakata, 2001). Studies by Niedobitek *et al.* (1992) showed that EBNA1 was expressed in all NPC cases, and between 38% and 65% of cases showed detectable levels of LMP but no other latent gene products nor lytic cycle antigens were detected. Thus, it is very likely that EBV genome is maintained by *oriP*-dependent and that *TRAF6* underexpression would be an advantage for EBV latent infection in NPC. Hence underexpression of *TRAF6* in this context suggest tumor suppressor role of this gene.



Vigilin underexpression in tumor was detected in only 1 sample with conventional and quantitative PCR (Table 5.9). Earlier studies by Siomi *et al.* (1993) suggested a role of vigilin in mRNA stability due to the presence of 15KH domains for RNA binding. RNA binding proteins together with non-coding regulatory RNAs are now recognized to coordinate both mRNA stability and translation (Morris *et al.*, 2010). It is estimated that more than 50% of genes are regulated on the basis of mRNA stability by RNA binding proteins (Colegrove-Otero *et al.*, 2005). Many post-transcriptional events are regulated by sequences in the 3'-untranslated region (3'UTR) (Audic and Hartley, 2004). Binding of RNA binding proteins to cis-acting mRNA elements can either protect the mRNA from ribonuclease cleavage (e.g., HuR; Fan and Steitz, 1998), or promote degradation (e.g., TTP, Hau *et al.*, 2007; AUF1, Lai *et al.*, 2004; Sarkar *et al.*, 2003), and thereby mediate many of the phenotypic changes related to 3'UTR expression.

Recently, Woo *et al.* (2010) identified *c-fms* oncogenic mRNA 3'UTR sequence as a cellular vigilin target through which vigilin inhibits the expression of *c-fms* mRNA and protein. Their studies showed that vigilin decreased *c-fms* mRNA stability and inhibited *c-fms* translation thus suppresses cellular motility and invasion of breast cancer cells. They have for the first time showed direct evidence suggesting a role for vigilin relating to cancer. Our quantitative PCR data that showed significant underexpression of vigilin in 1 tumor sample and the same underexpression trend observed in 6 out of 9 samples (although not significant) are in some agreement with recent study by Woo *et al.* (2010) about tumor suppressor role of vigilin. To our knowledge, there has not been any literature linking vigilin to cancer until recent studies by Woo *et al.* (2010).

*BNIP2* was previously found to be underexpressed in 3 tumor biopsy samples via conventional PCR. However, quantitative PCR on *BNIP2* was not successfully carried out due to failure in obtaining the reaction efficiency that is close to 1. Thus, switching from comparative  $C_T$  method to relative standard curve method was one option that had been considered but the later method requires that each reaction plate contains standard curve and thus more reagents use. Unfortunately, due to insufficiency of reagents (as a result of previous contamination problem and the need of reagents sharing between a few postgraduates in the same laboratory), quantitative PCR analysis for this gene was not done. Furthermore, much of the reagents had been used up in troubleshooting and analysis of *TRAF6* and vigilin.

*TRAF6* and vigilin genes were further investigated for their protein expression level via Western blot approach and is described in Chapter 6.



## CHAPTER SIX

### PROTEIN EXPRESSION OF TRAF6 AND VIGILIN IN NASOPHARYNGEAL CELL LINES

#### 6.1 Introduction

TRAF6 protein was found to be a direct E3 ligase for Akt and was essential for Akt ubiquitination, membrane recruitment, and phosphorylation upon growth-factor stimulation (Yang *et al.*, 2009). Akt signaling plays a central role in many biological functions, such as cell proliferation and apoptosis (Yang *et al.*, 2009). The human cancer-associated Akt mutant displayed an increase in Akt ubiquitination, in turn contributing to the enhancement of Akt membrane localization and phosphorylation (Yang *et al.*, 2009). Thus, Akt ubiquitination through TRAF6 is an important step for oncogenic Akt activation. The team found depleting TRAF6 in prostate cancer cells reduce Akt activation. Mice with *TRAF6* knocked down developed smaller prostate cancer tumors than those with active *TRAF6*. They suggested *TRAF6* as a previously unrecognized oncogene and is a new potential target for treating human cancers.

Vigilin contains 15 tandemly arranged KH domains for RNA binding (Gherzi *et al.*, 2004) and was shown to bind to the non-ARE-containing *Xenopus* vitellogenin mRNA 3'UTR and stabilized its mRNA (Cunningham *et al.*, 2000). RNA binding proteins together with non-coding regulatory RNAs are recognized to coordinate both mRNA stability and translation (Audic and Hartley, 2004). Aberrant expression of RNA binding protein was reported to modify the regulation of a given mRNA (Audic and Hartley, 2004). These alterations occur in

diverse cancer types (Audic and Hartley, 2004). Woo *et al.* (2010) showed that vigilin bound to the 69nt *c-fms* oncogenic mRNA 3'UTR sequence and inhibited its mRNA and protein expression. It was observed that vigilin protein suppressed cellular motility and invasion of breast cancer cells (Woo *et al.*, 2010).



## 6.2 General methodology

Total protein was isolated according to the protocol given in section 3.6.1. Protein extracts were prepared for loading in equal amounts and equal volumes (10 µg in 15 µl) for SDS-PAGE. The blotting was performed at 100V for 1-1.5 hrs. Cassettes were disassembled and the membrane was washed in dH<sub>2</sub>O for 2-3 minutes. Gels were stained subsequently to check for transfer efficiency.

To minimize background staining due to non-specific membrane-binding of the antibody tested, the membrane was saturated (“blocked”) with proteins which are not reacting with the antibody. 3% w/v BSA was used. The shortest possible blocking-time was determined experimentally.

In this study, blocking was performed for 1 hour at room temperature with 3% w/v BSA in PBST followed by incubation with the primary antibodies diluted in 1% w/v BSA in PBST for 1 hour at room temperature. Accessibility of a target protein for primary antibody was increased by a short wash using a wash buffer without blocking protein, performed before incubation with primary antibody.

The primary antibody (Santa Cruz, USA) was used at dilutions of 1:200 (Table 3.10). The secondary antibody used was reactive against the primary antibody and was coupled to an enzyme that allows subsequent visualization. The secondary antibodies (Santa Cruz, USA) were used at dilutions of 1:2000. Excess of blocking-protein, primary or secondary antibody was diminished by washing. For reasons of reproducibility washing volumes and times were kept constant. The blot was then incubated with SuperSignal® West Pico Chemiluminescent

Substrate (Pierce, Belgium) for 5 minutes. Excess substrate was drained off. Detection was performed using ImageQuant 400 Imager (GE Healthcare) and quantitation of the band was analysed with ImageQuant TL software.



6.3 Results

6.3.1 Protein sample concentration determination

The Bradford assay was used for determining protein concentration extracted from cell lines (HK1, HONE1, SUNE1 and NP69) before performing SDS electrophoresis. The absorbance reading at 595nm was recorded (Table 6.1) from protein standards prepared ranging from 0 to 2 mg protein BSA. A standard curve of absorbance versus miligrams protein was prepared as shown in Figure 6.1. Concentration of protein samples was determined (Table 6.2) from the standard curve prepared.

**Table 6.1:** Standard curve preparation. The concentration of protein in the stock solution was 5mg/ml.

Amount of BSA (mg)	Volume of stock solution (ul)	Volume of water (ul)	Absorbance at 595nm
0 (reference)	0	500	0
0.5	100	400	0.823
1	200	300	1.211
1.5	300	200	1.482
2	400	100	1.578

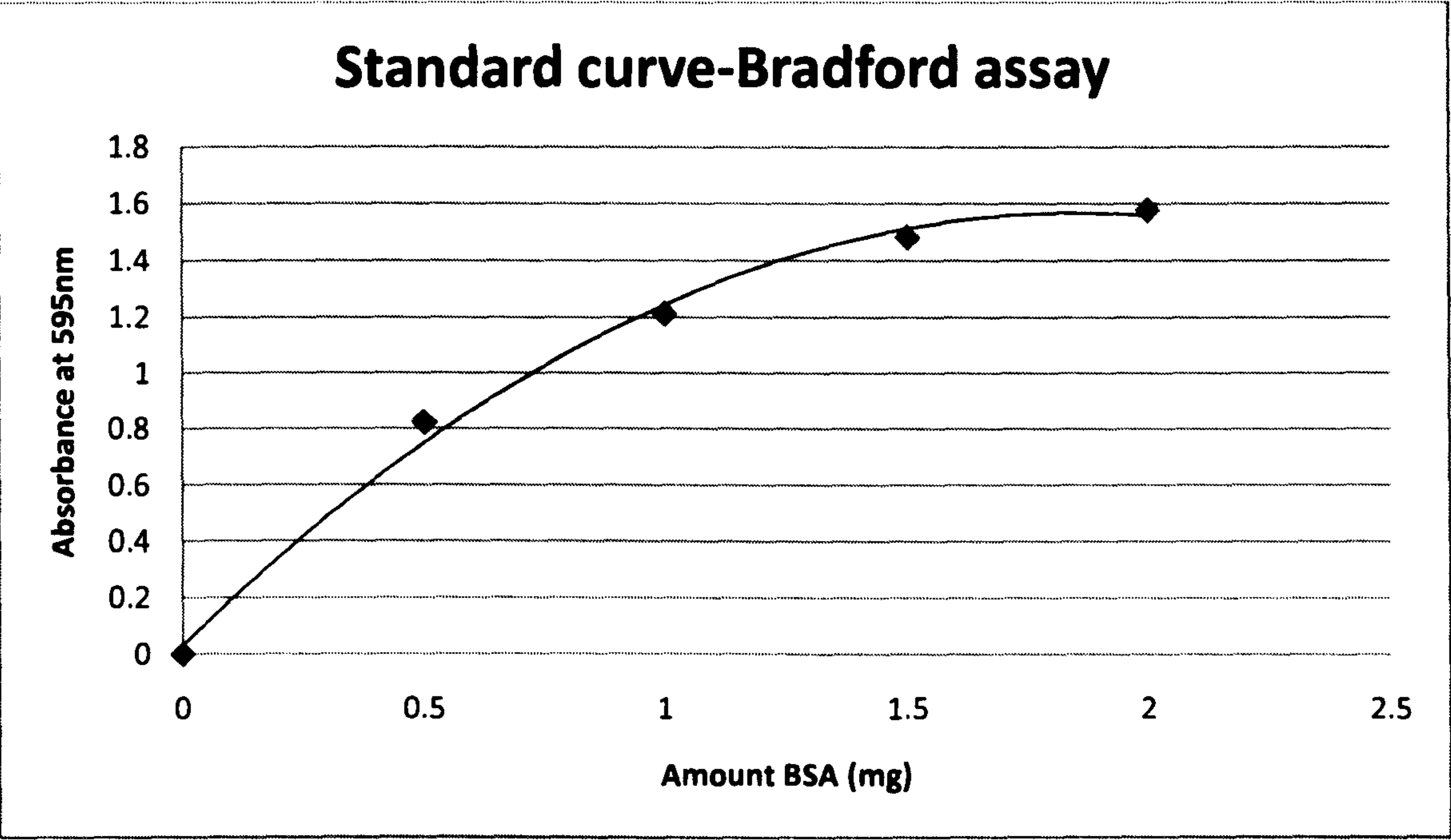


**Figure 6.1:** Protein quantification using Bradford assay. The intensity of the coloured reaction product is a direct function of protein amount. Protein amount was determined by comparing its absorbance value to a standard curve.



**Table 6.2:** Quantification of protein extract from cell lines.

Sample	Volume of Unknown protein	Absorbance at 595nm	Protein concentration (mg/ml)
HK1	500ul	1.162	1.91
SUNE1	500ul	1.194	2.03
HONE1	500ul	1.2	2.052
NP69	500ul	1.046	1.508

### **6.3.2 Vigilin and TRAF6 protein expression**

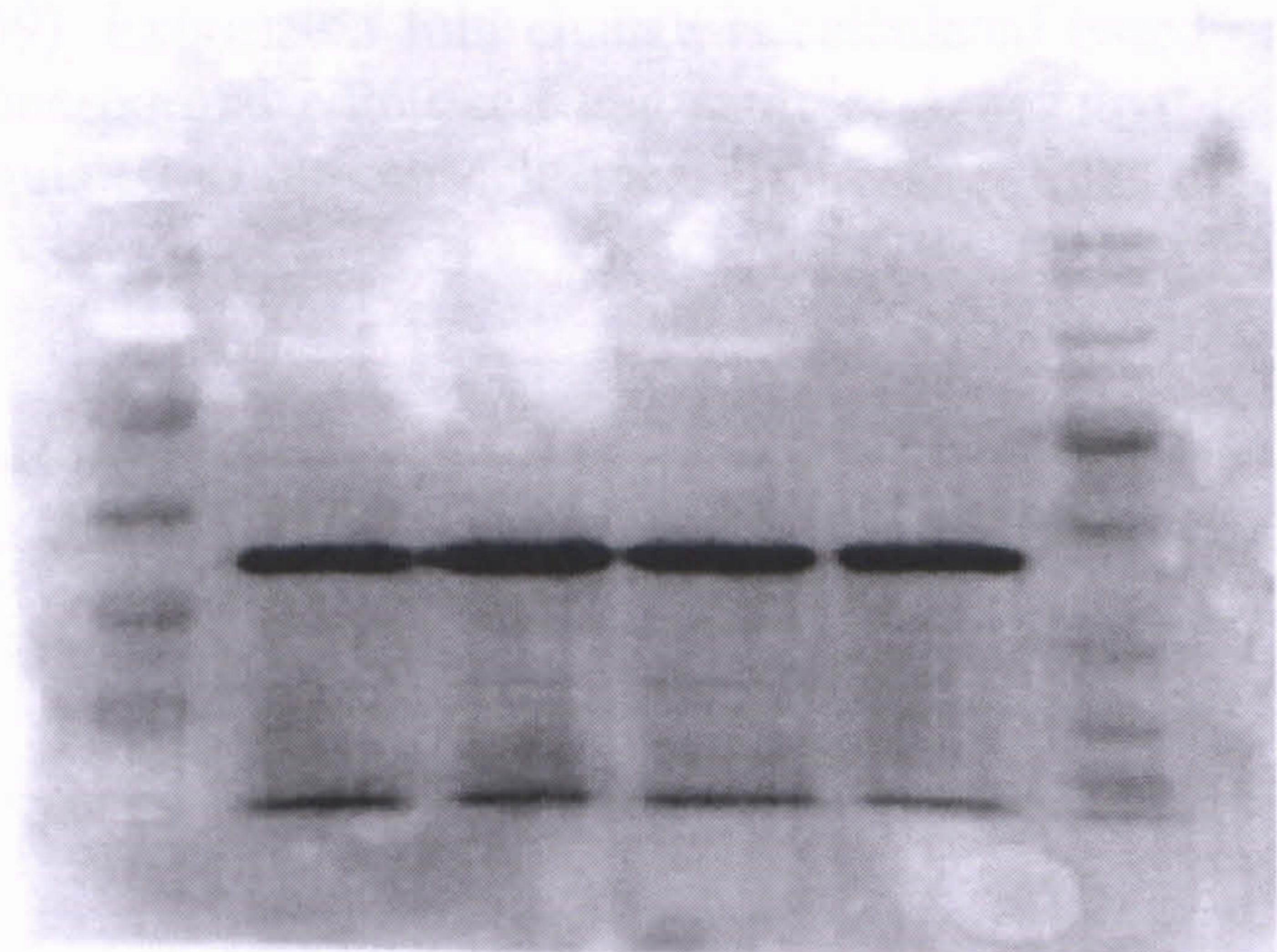
The western blot product for vigilin protein was a band of about 155kDa and 37kDa for GAPDH protein and is shown in Figure 6.2. Vigilin and GAPDH protein was detected in three NPC cell lines (HONE1, HK1 and SUNE1) and 1 normal NP cell line (NP69) used in this study. Table 6.3 is an average of vigilin protein expression (obtained from two replicates) calculated in fold change. Quantitation of the protein was done through analysis of the band intensity with ImageQuant TL software. Vigilin protein was found to be expressed lower in all three NPC cell lines in comparison to one normal NP cell line but the underexpression is not significant (Table 6.3). Statistical analysis revealed that the overall lower vigilin protein expression in NPC cell lines was not significant at  $P=0.05$ .

TRAF6 protein however is not detected in all three NPC cell lines (HONE1, HK1, SUNE1) and one normal NP69 cell lines. Many optimization steps have been done including changing from polyclonal to monoclonal antibodies and increased the amount of protein loaded, but TRAF6 protein remained undetected.



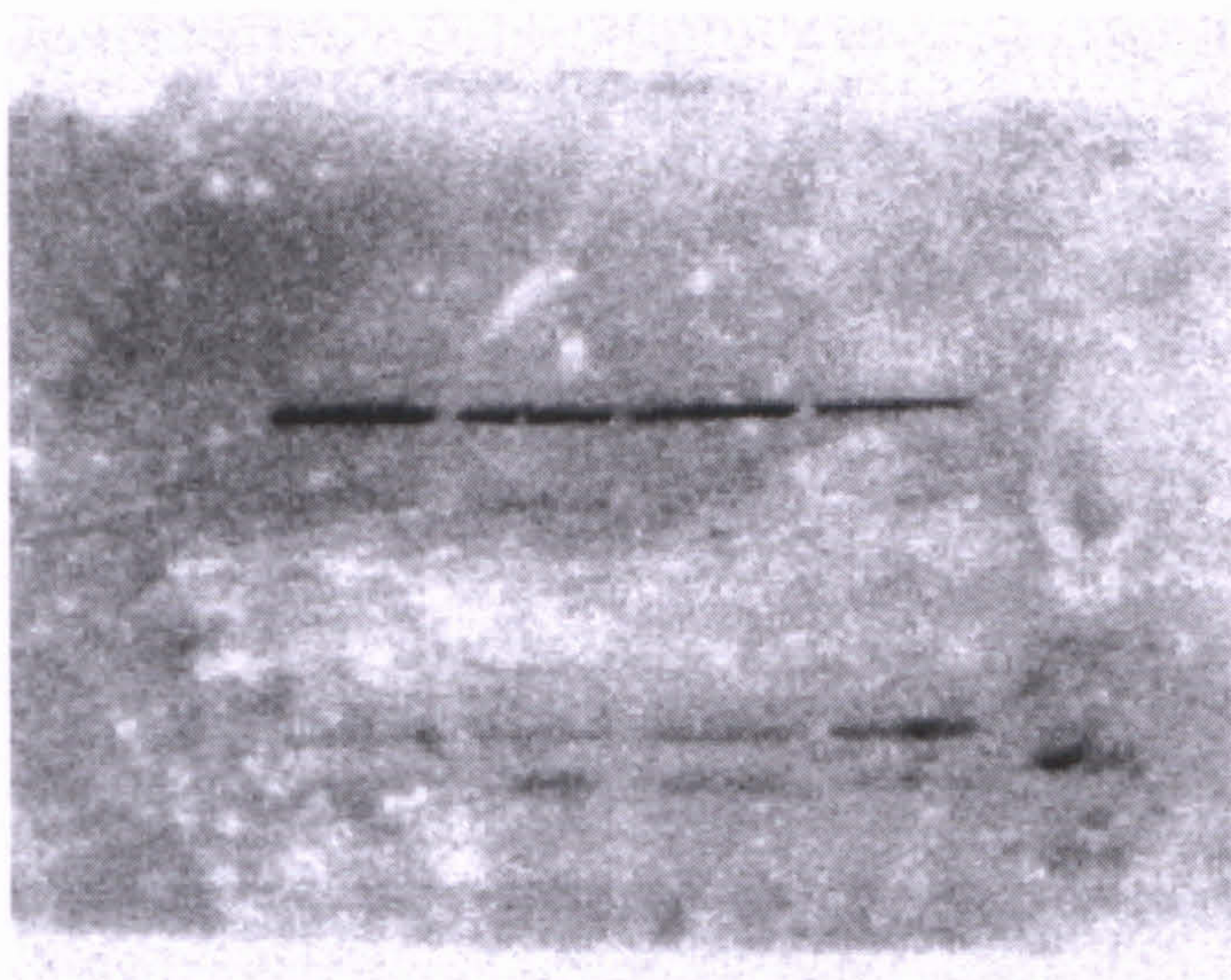
GAPDH

37 kDa



VIGILIN

155 kDa



	NP69	HONE1	HK1	SUNE1
VIG/GAP	0.045	0.035	0.028	0.029

**Figure 6.2:** Vigilin and GAPDH protein expression from 10μg total protein extracted from nasopharyngeal cell lines. Membranes were incubated with 1: 200 primary antibodies followed by incubation with 1: 2000 secondary anti-goat Ig-HRP (Santa Cruz) and visualized with ImageQuant 400 Imager (GE Healthcare). The ratio indicates vigilin protein expression level after normalized to GAPDH protein.



**Table 6.3:** Expression (fold change) of vigilin protein in 3 NPC cell lines relative to one normal cell line (NP69). Expression fold change is calculated based on expression of NPC cell lines relative to one normal NP69 cell line sample. A negative fold number means the expression is downregulated in tumour cell lines. Expression folds that are >2 is considered significant.

	sample name	Expression fold change	significance
vig/GAPDH	HONE1	-1.11	-
	HK1	-1.573	-
	SUNE1	-1.395	-



## 6.4 Discussions

Previously TRAF6 has been linked with NF- $\kappa$ B activation (Darnay *et al.*, 1999). Later study by Maeda *et al.* (2000) showed that *H. pylori* activates NF- $\kappa$ B through a signaling pathway involving TRAF6 in gastric cancer cells. Recent findings by Yang *et al.* (2009) showed that overexpression of TRAF6 protein activate Akt through Akt ubiquitination. It was found that increased Akt ubiquitination contributes to the hyperactivation of Akt in the mutant cells in breast cancer. They also found that depleting TRAF6 protein in prostate cancer cells reduced Akt activation. Moreover mice with *TRAF6* knocked down developed smaller prostate cancer tumors than those with active *TRAF6* (Yang *et al.*, 2009). Thus, findings by Maeda *et al.* (2000) and recent study with the more direct evidence by Yang *et al.* (2009) show its oncogenic character in tumorigenesis.

Our western blot study failed to detect TRAF6 protein in three NPC cell lines (HONE1, HK1 and SUNE1) and 1 normal NP69 cell line. It is suspected that TRAF6 protein might be present in the cell lines but nonetheless too minute to be detected via western blot. This is because *TRAF6* transcript was checked and PCR band was detected (refer section 4.33) and was confirmed via sequencing in those cell lines. *TRAF6* transcript expression could have been detected via PCR because the DNA went through many cycles of amplification process whereas this is not the case with western blot. However we did not have protein samples that could serve as positive control for TRAF6 protein at that time of study.

TRAF6 has been reported to suppress *oriP* activity when overexpressed (Shirakata, 2001). Thus by having *TRAF6* underexpressed in NPC, it will block suppression of *oriP*, which is important to maintain EBV genome and later expression of EBV viral oncoprotein. Though

our result is preliminary to suggest tumor suppressor role of *TRAF6* in cancer (in contrast to reported oncogenic character of *TRAF6*), this observation is however relevant and sensible in the context of NPC as EBV is a well established etiological factor for this cancer. This is further strengthened by the observation by Shirakata *et al.* (2001) that TRAF6 signal cascade activation has resulted in loss of EBV from Burkitt lymphoma cell line. It was suggested that EBV infection that occurred before clonal expansion of tumor cells (Raab-Traub, 2002) could imply that *TRAF6* may be one of the early genes that was altered in NPC tumorigenesis where its absence would help EBV genome to persist in human epithelium DNA during NPC latent infection.

Vigilin protein expression was found to be lower in NPC cell lines but the underexpression was not significant (Table 6.3). PCR study (both conventional and quantitative) found vigilin transcript to be significantly lower in only 1 sample but overall, more samples exhibited underexpression. As the transcript expression of vigilin was determined in biopsy samples whereas the protein expression was studied in cell lines, a direct comparison of the data (at transcript and protein level) could not be made. Lack of financial resources and facilities present the limitations to this study as to why a more direct method to evaluate protein expression in fixed tissue for example by immunohistochemistry was not carried out. Besides, due to sample limitations, we could not perform western blot study on biopsy specimens and thus have used cell lines instead. Although the data (at transcript and protein level) could not be directly compared, the results further confirmed the finding in which vigilin was expressed at relatively lower level in tumor than normal samples, an observation which supported recent findings by Woo *et al.* (2010). However, since the underexpression was not significant, we hypothesized that vigilin may not be directly involved in the pathogenesis of NPC.



## CHAPTER SEVEN

### GENERAL DISCUSSIONS

#### 7.1 *TRAF6*, *vigilin*, *BNIP2*, *MIF* and *GFER*

The expression analysis study demonstrated that *TRAF6* mRNA was underexpressed in tumor in 3 out of 8 samples screened (Table 4.1) via conventional PCR approach. This trend of underexpression was further confirmed via real time PCR as shown in 5 out of 9 samples (Table 5.7). Mutational analysis found no mutation in coding sequence of *TRAF6* (appendix). *TRAF6* protein however failed to be detected via Western blot. Our results also revealed significant underexpression of *vigilin* in 1 sample via conventional PCR (Table 4.3) and real time PCR (Table 5.8) respectively. Though the significance was only seen in one sample, there were more samples which exhibited the underexpression pattern (5 out of 8 samples with conventional PCR and 6 out of 9 samples with quantitative PCR). *Vigilin* protein expression was observed to be lower in NPC cell lines via Western blot but the underexpression was not significant (Table 6.3). Mutational analysis revealed no mutation in *vigilin* coding region (appendix). *BNIP2* was found to be significantly underexpressed in 3 out of 8 samples. Further studies are needed to confirm the expression. Our expression study did not find significant deregulation of *MIF* expression in tumor and normal samples via conventional PCR. *GFER* was observed to be significantly underexpressed in 1 out of 8 samples via conventional PCR. Of these, 4 samples exhibited underexpression pattern while other 4 samples exhibited overexpression pattern (though not significant). It is suspected that *MIF* and *GFER* may not be directly involved in the development of NPC.

Our *TRAF6* underexpression data (transcript level) supported the role of *TRAF6* in suppressing *oriP* activity of EBV (Shirakata, 2001). As EBV is a well established etiological factor NPC, this observation is relevant and coherent. This is further strengthened by the observation by Shirakata *et al.* (2001) in loss of EBV from Burkitt lymphoma cell line with activation of TRAF6 signal cascade . *OriP* activity is important for EBV latent infection in NPC (Shirakata *et al.*, 2001) as it enables proper segregation of replicated EBV episomes to daughter cells, upon cell division (Sugden *et al.*, 1994; Yates, 1996). Hence our data suggest that by having *TRAF6* underexpressed, *oriP* activity is activated to maintain EBV genome during latent infection in NPC. These suggest tumor suppressive role for *TRAF6* in NPC.

Vigilin has not been associated with cancer until a recent report by Woo *et al.* (2010) that revealed post-transcriptional suppression of oncogenic *c-fms* expression by vigilin in breast cancer. They suggested vigilin may function as tumor repressor, inhibiting breast cancer invasion and metastasis through its ability to bind and downregulate *c-fms* mRNA. Though in our study vigilin mRNA was only observed to be significantly underexpressed in 1 biopsy sample, majority of the samples however revealed underexpression pattern. These observations are in some agreement with tumor suppressor role of vigilin as reported by Woo *et al.* (2010). Nevertheless, because the underexpression was not significantly lower in both transcript and protein level, we hypothesized that vigilin may not be directly involved in the pathogenesis of NPC.



## 7.2 Limitations

DNA contamination from our isolated RNAs presented a great challenge to the PCR assays. Though our primers have been designed in such a way that either the 5' or the 3' primers span the junction of two exons, so that the amplification product obtained from the cDNA would be of different length from that obtained from any DNA contaminant, however, the presence of *GAPDH* and *ACTB* pseudogenes sequences has also been reported (Raff *et al.*, 1997). DNase treatment of our RNA samples followed by purification which has caused significant loss of RNA was another challenge faced in this study. A lot of time has also been spent on real time PCR in optimizing the reaction efficiencies between the different genes. Target and normalizer genes have to be relatively similar before  $\Delta\Delta C_T$  method can be used for data analysis. Contamination shown by amplification in NTC also posed some problems as real time PCR is a very sensitive detection assay.

## 7.3 Conclusions and future direction

Our expression analysis study demonstrated that *TRAF6* mRNA was underexpressed in tumor in 3 out of 8 samples screened via conventional PCR approach. This observation was further confirmed via real time PCR in 5 out of 9 samples. Mutational analysis did not reveal any mutation in the coding sequence of *TRAF6*. TRAF6 protein expression failed to be detected via Western blot. Our data suggest that by having *TRAF6* underexpressed, *oriP* activity is activated to maintain EBV in NPC cells. These suggest tumor suppressive role for *TRAF6* in NPC.

Our results also revealed significant underexpression of vigilin in 1 sample via conventional and real time PCR. Western blot analysis of vigilin expression found no significant difference in the protein level and mutational analysis showed no mutation in the coding region (appendix). We postulated that vigilin may not be directly associated in the pathogenesis of NPC.

*BNIP2* was found to be significantly underexpressed in 3 out of 8 samples. This however needs further confirmation studies. Our conventional PCR study found no significant deregulation of *MIF* expression. *GFER* was observed to be significantly underexpressed in 1 out of 8 samples. Overall, half of the samples showed underexpression and overexpression respectively (though not significant). It is suspected that *MIF* and *GFER* may not be directly involved with development of NPC.

Future research works should concentrate on the expression study of TRAF6 protein via Western blot and more tumor biopsy samples should be included and tested. Besides, underexpression pattern of *GFER* should also be confirmed with quantitative PCR. This would help us to better delineate the roles of *TRAF6* and *GFER* genes in NPC tumorigenesis.



## REFERENCES

- Anantharaman, V., Koonin, E.V. & Aravind, L. (2002). Comparative genomics and evolution of proteins involved in RNA metabolism. *Nucleic Acids Res*, 30: 1427–1464.
- Audic, Y. & Hartley, R.S. (2004). Post-transcriptional regulation in cancer. *Biology of the cell*, 96(7):479-498.
- Bando, H., Matsumoto, G. & Bando, M. (2002). Expression of macrophage migration inhibitory factor in human breast cancer: association with nodal spread. *Jpn J Cancer Res* 93(4):389– 396.
- Bloom, B. & Bennett, B. (1966). Mechanism of a reaction in vitro associated with delayed-type hypersensitivity, *Science*, 153: 80–82.
- Brock, M. L. & D. J. Shapiro. (1983). Estrogen stabilizes vitellogenin mRNA against cytoplasmic degradation. *Cell*, 34:207–214
- Budarf, M., McDonald, T., Sellinger, B., Kozak, C., Graham, C. & Wistow, G.(1997). Localization of the human gene for macrophage migration inhibitory factor (MIF) to chromosome 22q11.2. *Genomics*. 39(2):235-236.
- Cao, Y., Fu, Y.L., Yu, M., Yue, P.B., Ge, C.H., Xu, W.X., Zhan, Y.Q., Li, C.Y., Li, W., Wang, X.H., Wang, Z.D., Li, Y.H. & Yang, X.M. (2009) .Human augments liver regeneration is important for hepatoma cell viability and resistance to radiation-induced oxidative stress. *Free Radic Biol Med*, 47(7):1057-1066.
- Cao, Z., Xiong, J., Takeuchi, M., Kurama, K. & Goeddel, D. V. (1996). TRAF6 is a signal transducer for interleukin-1. *Nature*, 383:443-446
- Chambers, S. K., Kacinski, B. M., Ivins, C. M. & Carcangiu, M. L. (1997). Overexpression of epithelial macrophage colony-stimulating factor (CSF-1) and CSF-1 receptor: a poor prognostic factor in epithelial ovarian cancer, contrasted with a protective effect of stromal CSF-1. *Clin. Cancer Res*, 3: 999-1007.

- Chambers, S. K. (2009). Role of CSF-1 in progression of epithelial ovarian cancer. *Future Oncol*, 5:1429-1440.
- Chan, A.S., To, K.F., Lo, K.W., Mak, K.F., Pak, W., Chiu, B., Tse, G.M., Ding, M., Li, X.H., Lee, J.C. & Huang, D.P. (2000). High frequency of chromosome 3p deletion in histologically normal nasopharyngeal epithelia from southern Chinese. *Cancer Res*, 60: 5365–5370.
- Chan, A.S., To, K.F., Lo, K.W., Ding, M., Li, X., Johnson, P., and Huang, D.P. (2002). Frequent chromosome 9p losses in histologically normal nasopharyngeal epithelia from southern Chinese. *Int. J. Cancer* 102: 300–303.
- Chesney, J., Metz, C., Bacher, M., Peng, T., Meinhardt, A. & Bucala, R.(1999). An essential role for macrophage migration inhibitory factor (MIF) in angiogenesis and the growth of a murine lymphoma. *Mol Med* 5(3):181– 191.
- Cho, E.Y., Hildesheim, A., Chen, C.J., Hsu, M.M., Chen, I.H., Mittl, B.F., Levine, P.H., Liu, M.Y., Chen, J.Y. & Brinton, L.A. (2003). Nasopharyngeal carcinoma and genetic polymorphisms of DNA repair enzymes XRCC1 and hOGG1. *Cancer Epidemiol. Biomarkers Prev.* 12: 1100–1104.
- Chow, L.S., Lo, K.W., Kwong, J., To, K.F., Tsang, K.S., Lam, C.W., Dammann, R., and Huang, D.P. (2004).RASSF1A is a target tumor suppressor from 3p21.3 in nasopharyngeal carcinoma. *Int. J. Cancer* 109: 839–847.
- Colegrove-Otero, L. J., Minshall, N. & Standart, N. (2005). RNA-binidng proteins in early development. *Cri. Rev. Biochem. Mol. Biol*, 40: 21-73.
- Crook, T., Nicholls, J.M., Brooks, L., O’Nions, J. & Allday, M.J. (2000). High level expression of N-p63: a mechanism for the inactivation of p53 in undifferentiated nasopharyngeal carcinoma (NPC). *Oncogene*, 19:3439–3444.
- Cunningham, K. S., Dodson, R.E., Nagel, M. A., Shapiro, D. J. & Schoenberg. D. R. (2000). Vigilin binding selectively inhibits cleavage of the vitellogenin mRNA 3’-untranslated region by the mRNA endonucleases polysomal ribonuclease 1. *Proc. Natl. Acad. Sci. USA* 97: 12498-12502.



- Dai, X.M., Ryan, G.R., Hapel, A.J., Dominguez, M.G., Russell, R.G., Kapp, S., Sylvestre, V., & Stanley, E.R. (2009). Targeted disruption of the mouse colony-stimulating factor 1 receptor gene results in osteopetrosis, mononuclear phagocyte deficiency, increased primitive progenitor cell frequencies, and reproductive defects. *Blood*, 99: 111-120.
- Darnay, B.G., Ni, J., Moore, P.A. & Aggarwal, B.B. (1999). Activation of NF-kappaB by RANK requires tumor necrosis factor receptor-associated factor (TRAF) 6 and NF-kappaB-inducing kinase. Identification of a novel TRAF6 interaction motif. *J Biol Chem*. 274(12):7724-7731.
- David, J. R. (1966). Delayed hypersensitivity in vitro: its mediation by cell-free substances formed by lymphoid cell-antigen interaction. *Proc. Natl. Acad. Sci. USA*, 56: 72-77.
- Del Vecchio, M.T., Tripodi, S.A., Arcuri, F., Pergola, L., Hako, L., Vatti, R. & Cintorino, M. (2000). Macrophage migration inhibitory factor in prostatic adenocarcinoma: correlation with tumor grading and combination endocrine treatment-related changes. *Prostate*, 45: 51-57
- Devi, B.C., Pisani, P., Tang, T.S. & Parkin, D.M. (2004). High incidence of nasopharyngeal carcinoma in native people of Sarawak, Borneo Island. *Cancer Epidemiol Biomarkers Prev* 13:482-486
- Dodson, R. E., & Shapiro, D.J. (1997). Vigilin, a ubiquitous protein with 14 K homology domains, is the estrogen-inducible vitellogenin mRNA 3'-untranslated region-binding protein. *J.B.C*, 272: 12249-12252.
- Dolcet, X., Llobet, D., Pallares, J. & Matias-Guiu, X. (2005). NF-kB in development and progression of human cancer, *Virchows Arch*, 446(5):475-482.
- Fan, X. C. & Steitz, J. (1998). Overexpression of HuR, a nuclear-cytoplasmic shuttling protein, increases the in vivo stability of ARE-containing mRNAs. *The EMBO J*, 17: 3448-3460.
- Fang, W., Li, X., Jiang, Q., Liu, Z., Yang, H., Wang, S., Xie, S., Liu, Q., Liu, T., Huang, J., Xie, W., Li, Z., Zhao, Y., Wang, E., Marincola, F.M. & Yao, K. (2008). Transcriptional patterns, biomarkers and pathways characterizing nasopharyngeal carcinoma of Southern China. *J Transl Med*, 6:32.

- Feng, B.J., Huang, W., Shugart, Y.Y., Lee, M.K., Zhang, F., Xia, J.C., Wang, H.Y., Huang, T.B., Jian, S.W. & Huang, P. (2002). Genome-wide scan for familial nasopharyngeal carcinoma reveals evidence of linkage to chromosome 4. *Nat. Genet.* 31: 395–399.
- Fidge, N.H. (1999). High density lipoprotein receptors, binding proteins, 1 and ligands. *J. Lipid Res.* 40: 187-201.
- Forman, D., Newell, D.G., Fullerton, F., Yarnell, J.W., Stacey, A.R., Wald, N. & Sitas, F. (1991). Association between infection with *Helicobacter pylori* and risk of gastric cancer: evidence from a prospective investigation. *Br Med J*, 302:1302–1305.
- Gherzi, R., Lee, K. Y., Briata, P., Wegmüller, D., Moroni, C., Karin, M. & Chen, C. Y. (2004). A KH domain RNA binding protein, KSRP, promotes ARE-directed mRNA turnover by recruiting the degradation machinery. *Mol. Cell*, 14: 571-583.
- Goolsby, K.M. & Shapiro, D.J. (2003). RNAi-mediated depletion of the 15 KH domain protein, vigilin, induces death of dividing and non-dividing human cells but does not initially inhibit protein synthesis. *Nucleic Acids Res.*, 31:5644–5653.
- Gouble, A., Grazide, S., Meggetto, F., Mercier, P., Delsol, G. & Morello, D. (2002). A new player in oncogenesis: AUF1/hnRNPD overexpression leads to tumorigenesis in transgenic mice. *Cancer Res*, 62:1489–1495.
- Graham, D.Y., Lew, G.M., Klein, P.D., Evans, D.G., Evans, D.J., Saeed, Z.A. & Malaty, H.M. (1992). Effect of treatment of *Helicobacter pylori* infection on the long-term recurrence of gastric or duodenal ulcer: a randomized, controlled study. *Ann Intern Med*, 116:705–708.
- Hasselt, C, A, V, & Gibb A, G 1999, *Nasopharyngeal carcinoma*, The Chinese University Press, Hong Kong.
- Hau, H. H., Walsh, R.J., Ogilvie, R.L., Williams, D.A., Reilly, C.S. & Bohjanen, P.R. (2007). Tristetraproline recruits functional mRNA decay complexes to ARE sequences. *J. Cell. Biochem*, 100: 1477-1492.



- Hildesheim, A., Anderson, L.M., Chen, C.J., Cheng, Y.J., Brinton, L.A., Daly, A.K., Reed, C.D., Chen, I.H., Caporaso, N.E. & Hsu, M.M. (1997). CYP2E1 genetic polymorphisms and risk of nasopharyngeal carcinoma in Taiwan. *J. Natl. Cancer Inst.* 89: 1207–1212.
- Hildesheim, A., Apple, R.J., Chen, C.J., Wang, S.S., Cheng, Y.J., Klitz, W., Mack, S.J., Chen, I.H., Hsu, M.M. & Yang, C.S. (2002). Association of HLA class I and II alleles and extended haplotypes with nasopharyngeal carcinoma in Taiwan. *J. Natl. Cancer Inst.* 94: 1780–1789.
- Hirai, K., & Shirakata, M. (2001). Replication licensing of the EBV *oriP* minichromosome. *Curr. Top. Microbiol. Immunol.* 258:13–33
- Honda, A., Abe, R., Yoshihisa, Y., Makino, T., Matsunaga, K., Nishihira, J., Shimizu, H. & Shimizu, T. (2009). Deficient deletion of apoptotic cells by macrophage migration inhibitory factor (MIF) overexpression accelerates photocarcinogenesis. *Carcinogenesis*, 30: 1597–1605.
- Huang, D.P., Ho, J.H., Saw, D. & Teoh, T.B. (1978). Carcinoma of the nasal and paranasal regions in rats fed Cantonese salted marine fish. *IARC Sci Publ* 20(3):315–328.
- Hui, A.B., Lo, K.W., Leung, S.F., Teo, P., Mak, K.F., To, K.F., Wong, N., Choi, P.H., Lee, J.C. & Huang, D.P. (1999). Detection of recurrent chromosomal gains and losses in primary nasopharyngeal carcinoma by comparative genomic hybridization. *Int. J. Cancer* 48: 498–503
- Hui, A.B., Lo, K.W., Kwong, J., Lam, E.C., Chan, S.Y., Chow, L.S., Chan, A.S., Teo, P.M. & Huang, D.P. (2003). Epigenetic inactivation of TSLC1 gene in nasopharyngeal carcinoma. *Mol. Carcinog.* 38: 170–178.
- Hui, E.P., Chan, A.T., Pezzella, F., Turley, H., To, K.F., Poon, T.C., Zee, B., Mo, F., Teo, P.M. & Huang, D.P. (2002). Coexpression of hypoxia-inducible factors 1 alpha and 2 alpha, carbonic anhydrase IX, and vascular endothelial growth factor in nasopharyngeal carcinoma and relationship to survival. *Clin Cancer Res.* 8: 2595–2604.
- Izumi, K. M., McFarland, E.C., Ting, A. T., Riley, E. A., Seed, B. & Kieff, E. D. (1999). The Epstein-Barr virus oncoprotein latent membrane protein 1 engages the tumor necrosis factor receptor-associated proteins TRADD and receptor-interacting protein (RIP) but does not induce apoptosis or require RIP for NF-kB activation. *Mol. Cell. Biol.* 19:5759–5767.

- Jayasurya, A., Bay, B.H., Yap, W.M. & Tan, N.G. (2000). Correlation of metallothionein expression with apoptosis in nasopharyngeal carcinoma. *Br. J. Cancer* 82: 1198–1203.
- Kacinski, B. M., Scata, K. A., Carter, D., Yee, L. D., Sapi, E., King, B. L., Chambers, S. K., Jones, M. A., Pirro, M. H. & Stanley, E. R. (1991). FMS (CSF-1 receptor) and CSF-1 transcripts and protein are expressed by human breast carcinomas in vivo and in vitro. *Oncogene*, 6: 941-952.
- Kamimura, A., Kamachi, M. & Nishihira, J. (2000). Intracellular distribution of macrophage migration inhibitory factor predicts the prognosis of patients with adenocarcinoma of the lung. *Cancer* 89(2):334–341.
- Kanamori, H., Dodson, R.E., & Shapiro, D.J. (1998). In vitro genetic analysis of the RNA binding site of vigilin, a multi-KH-domain protein. *Mol. Cell. Biol.* 18: 3991-4003.
- Kitaichi, N., Shimizu, T., Yoshida, K., Honda, A., Yoshihisa, Y., Kase, S., Ohgami, K., Norisugi, O., Makino, T., Nishihira, J., Yamagishi, S. & Ohno, S. (2008). Macrophage migration inhibitory factor ameliorates UV-induced photokeratitis in mice. *Exp. Eye Res*, 86: 929–935
- Kwong, J., Lo, K.W., To, K.F., Teo, P.M., Johnson, P.J. & Huang, D.P. (2002). Promoter hypermethylation of multiple genes in nasopharyngeal carcinoma. *Clin. Cancer Res.* 8: 131–137.
- Lai, A., Mazan-Mamczarz, K., Kawai, T., Yang, X., Martindale, J.L., & Gorospe, M. (2004). Concurrent versus individual binding of HuR and AUF1 to common labile target mRNAs. *The EMBO J*, 23: 3092–3102.
- Lang, B. D., & Fridovich-Keil, J.L. (2000). Scp160p, a multiple KH-domain protein, is a component of mRNP complexes in yeast. *Nuc. Acids Res*, 28: 1576-1584.
- Li, Z., Lin, S.X. & Liang, Y.J. (2004). Increased cell migration of nasopharyngeal carcinoma cell lines in vitro by macrophage migration inhibitory factor, *Zhonghua Bing Li Xue Za Zhi*.33(1):57-61.
- Lim, G.C.C. & Halimah, Y. (2004). eds. Second Report of the National Cancer Registry. Cancer Incidence in Malaysia 2003. Kuala Lumpur: National Cancer Registry, 2004



- Lin, E. Y., Nguyen, A. V., Russell, R. G. & Pollard, J. W. (2001). Colony-stimulating factor 1 promotes progression of mammary tumors to malignancy. *J. Exp. Med*, 193: 727-740.
- Lo, A.K., Huang, D.P., Lo, K.W., Chui, Y.L., Li, H.M., Pang, J.C. & Tsao, S.W. (2004). Phenotypic alterations induced by the Hong Kong-prevalent Epstein-Barr virus-encoded LMP1 variant (2117-LMP1) in nasopharyngeal epithelial cells. *Int. J. Cancer* 109: 919–925.
- Lo, K.W., Cheung, S.T., Leung, S.F., van Hasselt, A., Tsang, Y.S., Mak, K.F., Chung, Y.F., Woo, J.K., Lee, J.C. & Huang, D.P. (1996). Hypermethylation of the p16 gene in nasopharyngeal carcinoma. *Cancer Res.* 56: 2721–2725.
- Lo, K.W., Teo, P.M., Hui, A.B., To, K.F., Tsang, Y.S., Chan, S.Y., Mak, K.F., Lee, J.C., and Huang, D.P. (2000). High resolution allelotype of microdissected primary nasopharyngeal carcinoma. *Cancer Res.* 60, 3348–3353.
- Lo, K.W., Kwong, J., Hui, A.B., Chan, S.Y., To, K.F., Chan, A.S., Chan, L.S., Teo, P.M., Johnson, P.J. & Huang, D.P. (2001). High frequency of promoter hypermethylation of RASSF1A in nasopharyngeal carcinoma. *Cancer Res.* 61: 3877–3881.
- Lo, K. W. & Huang, D. P. (2002) Genetic and epigenetic changes in nasopharyngeal carcinoma. *Semin. Cancer Biol*, 12: 451–462.
- Lo, K.W., To, K.F. & Huang, D.P. (2004) Focus on nasopharyngeal carcinoma. *Cancer Cell*, 5:423-428.
- Lu, J., Chua, H.H., Chen, S.Y., Chen, J.Y. & Tsai, C.H. (2003). Regulation of matrix metalloproteinase-1 by Epstein-Barr virus proteins. *Cancer Res*, 63:256–262.
- Lu, S.J., Day, N.E., Degos, L., Lepage, V., Wang, P.C., Chan, S.H., Simons, M., Mcknight, B., Easton, D., Yi, Z. & de The, G. (1990). Linkage of a nasopharyngeal carcinoma susceptibility locus to the HLA region. *Nature* 346: 470–471.
- Lu, Q.L., Elia, G., Lucas, S. & Thomas, J.A. (1993). Bcl-2 proto-oncogene expression in Epstein-Barr-virus-associated nasopharyngeal carcinoma. *Int. J. Cancer* 53:29–35.
- Maeda, S., Yoshida, H., Ogura, K., Mitsuno, Y., Hirata, Y., Yamaji, Y., Akanuma, M., Shiratori, Y., & Omata, M. (2000). H. pylori activates NF-kappaB through a signaling pathway involving

- IkappaB kinases, NF-kappaB-inducing kinase, TRAF2, and TRAF6 in gastric cancer cells. *Gastroenterology* 119: 97–108
- Marker, D. & Craig Woodworth, C. (2005). Activation of NF-κB in Epithelial Cells Expressing HPV Oncogenes, *6th Annual Symposium on Undergraduate Research Experiences (SURE)* Clarkson University
- Markert, J.M., Fuller, C.M., Gillespie, G.Y., Bubien, J.K., McLean, L.A., Hong, R.L., Lee, K., Gullans, S.R., Mapstone, T.B.& Benos, D.J. (2001). Differential gene expression profiling in human brain tumors. *Physiol Genomics*.5:21–33.
- Marks, J.E., Philips, J.L. & Menck, H.R. (1998). The National Cancer Data Base report on the relationship of race and national origin to the histology of nasopharyngeal caecinoma. *Cancer* 83: 582-588.
- Martin, J., Duncan, F.J., Keiser, T., Shin, S., Kusewitt, D.F., Oberyszyn, T., Satoskar A.R. & VanBuskirk, A.M. (2009). Macrophage migration inhibitory factor (MIF) plays a critical role in pathogenesis of ultraviolet-B (UVB) -induced nonmelanoma skin cancer (NMSC). *FASEB J.*, 23: 720–730.
- McDermott, A. L., Dutt, S. N. & Watkinson, J. C. (2001) The aetiology of nasopharyngeal carcinoma. *Clin. Otolaryngol. Allied Sci.* 26: 82 –92.
- McKnight, G.L., Redasoner, J., Sundquist, K.O., Hokland, B., McKernan, P.A., Champagne, J., Johnson, C.J., Bailey, M.C., Holly, R., O'Hara, P.J. & Oram, J. F (1992).Cloning and expression of a cellular high density lipoprotein-binding protein that is upregulated by cholesterol loading of cells. *J. Biol. Chem*, 267: 12131-12141
- Meyer-Siegler K, Fattor, R.A. & Hudson, P.B. (1998) Expression of macrophage migration inhibitory factor in the human prostate. *Diagn Mol Pathol* :7(1):44– 50.
- Mitchell, R.A. (2003). Mechanisms and effectors of MIF-dependent promotion of tumorigenesis. *Cell. Signal.*, 16(1):13-19



- Morgan, E.T. (2001) Regulation of cytochrome p450 by inflammatory mediators: why and how. *Drug Metab Dispos*, 29:207–212.
- Morris, A.K., Mukherjee, N. & Keene, J.D. (2010). Systematic analysis of posttranscriptional gene expression. *WIREs Syst. Biol. Med*, 2:162-180.
- Nakshatri, H., Bhat-Nakshatri, P., Martin, D.A., Goulet, R.J. & Sledge, G.W. (1997). Constitutive activation of NF-kappaB during progression of breast cancer to hormone-independent growth. *Mol. Cell. Biol.* 17(7): 3629-3639.
- Nazar-Stewart, V., Vaughan, T.L., Burt, R.D., Chen, C., Berwick, M. & Swanson, G.M. (1999). Glutathione S-transferase M1 and susceptibility to nasopharyngeal carcinoma. *Cancer Epidemiol. Biomarkers Prev.* 8: 547–551
- Niedobitek, G., Young, L.S., Sam, C.K., Brooks, L., Prasad, U. & Rickinson, A.B. (1992). Expression of Epstein-Barr virus genes and of lymphocyte activation molecules in undifferentiated nasopharyngeal carcinomas. *Am J Pathol.* 140(4):879-887.
- Nomura, A., Stemmermann, G.N., Chyou, .PH., Kato, I., Perez-Perez, G.I. & Blaser, M.J. (1991). Helicobacter pylori infection and gastric carcinoma among Japanese Americans in Hawaii. *N Engl J Med*, 325: 1132–1136.
- Ogawa, H., Nishihira, J. & Sato, Y. (2000). An antibody for macrophage migration inhibitory factor suppresses tumour growth and inhibits tumour-associated angiogenesis. *Cytokine* 12(4):309 – 314
- Paralkar, V. & Wistow, G.(1994). Cloning the human gene for macrophage migration inhibitory factor (MIF). *Genomics*.9(1):48-51.
- Parkin, D. M., Bray, F., Ferlay, J. & Pisani, P. (2005) Global cancer statistics, 2002. *CA Cancer J. Clin.* 55: 74 –108.
- Parsonnet, J., Friedman, G.D., Vandersteen, D.P., Chang, Y., Vogelman, J.H. & Orentreich, N. (1991). Helicobacter pylori infection and the risk of gastric carcinoma. *N Engl J Med*, 325:1127–1131.
- Pattle, S.B. & Farrell, P.J. (2006). The role of Epstein-Barr virus in cancer. *Expert Opin Biol Ther.* 6(11):1193-205.

- Pawlowski, R. & Jura, J. (2006). ALR and liver regeneration. *Mol Cell Biochem*, 288(1-2):159-169.
- Plenz, G., Kugler, S., Schnittger, S., Rieder, H., Fonatsch, C. & Muller, P. K. (1994). The human vigilin gene: identification, chromosomal localization and expression pattern. *Hum. Genet.* 93: 575-582
- Prasad, U. (2000). *Nasopharyngeal carcinoma*, Univesity of Malaya Press, Kuala Lumpur.
- Qian, C.N., Guo, X., Cao, B., Kort, E.J., Lee, C.C., Chen, J., Wang, L.M., Mai, W.Y., Min, H.Q. & Hong, M.H. (2002). Met protein expression level correlates with survival in patients with late-stage nasopharyngeal carcinoma. *Cancer Res*, 62:589–596.
- Qin, W., Hu, J. & Guo, M. (2003). BNIP-2, a novel homologue of BNIP-2, interacts with Bcl-2 and Cdc42GAP in apoptosis. *Biochem. Biophys. Res. Commun.*, 308 (2): 379–85.
- Raab-Traub, N. & Flynn, K. (1986). The structure of the termini of the Epstein-Barr virus as a marker of clonal cellular proliferation. *Cell* 47: 883–889.
- Raab-Traub, N. (2002). Epsrein-Barr virus in the pathogenesis of NPC. *Semin Cancer Biol* 12, 431-441.
- Ren, Y., Law, S., Huang, X., Lee, P. Y., Bacher, M., Srivastava, G. & Wong, J. (2005). Macrophage migration inhibitory factor stimulates angiogenic factor expression and correlates with differentiation and lymph node status in patients with esophageal squamous cell carcinoma. *Ann. Surg.*, 242: 55-63.
- Sarkar, B., Xi, Q., He, C. & Schneider, R.J. (2003). Selective degradation of AU-rich mRNAs promoted by the p37 AUF1 protein isoform. *Mol. Cell Biol*, 23: 6685-6693.
- Shang, X., Zhou, Y.T. & Low, B.C. (2003). Concerted regulation of cell dynamics by BNIP-2 and Cdc42GAP homology/Sec14p-like, proline-rich, and GTPase-activating protein domains of a novel Rho GTPase-activating protein, BPGAP1. *J Biol Chem* 278: 45903-45914.
- Shanmugaratnam, K. & Sobin, L.H. (1991). Histology Typing of Tumours of the Upper Respiratory Tract and Ear, 2nd ed. (Berlin: Springer-Verlag).



- Shen, L., Hu, J. & Lu, H. (2003). The apoptosis-associated protein BNIP1 interacts with two cell proliferation-related proteins, MIF and GFER. *FEBS Lett*, 540 (1-3): 86–90.
- Shimizu, T., Abe, R., Nakamura, H., Ohkawara, A., Suzuki, M. & Nishihira, J. (1999). High expression of macrophage migration inhibitory factor in human melanoma cells and its role in tumor cell growth and angiogenesis. *Biochem Biophys Res Commun*, 264(3):751–758.
- Shirakata, M., Imadome, K. & Hirai, K. (1999). Requirement of replication licensing for the dyad symmetry element-dependent replication of the Epstein-Barr virus *oriP* minichromosome. *Virology*, 263:42–54.
- Shirakata, M., Imadome, K.I., Okazaki, K. & Hirai, K. (2001). Activation of TRAF5 and TRAF6 Signal Cascades Negatively Regulates the Latent Replication Origin of Epstein-Barr Virus through p38 Mitogen-Activated Protein Kinase. *Journal of Virology*, 75 (11): 5059-5068
- Sim, E. U. H., Toh, A. K.L., & Tiong, T. S. (2008). Preliminary findings of down-regulated genes in nasopharyngeal carcinoma. *Asia Pacific Journal of Molecular Biology and Biotechnology* 16 (3) : 79-84
- Siomi, H., Matunis, M. J., Michael, W. M. & Dreyfuss, G. (1993). The pre-mRNA binding K protein contains a novel evolutionarily conserved motif. *Nucleic Acids Res.* 21:1193–1198
- Sugden, Sem (1994). DNA Viruses - Herpesviruses II (EBV). *Virol.* 5:197-205,
- Takahashi, N., Nishihira, J., Sato, Y., Kondo, M., Ogawa, H., Ohshima, T., Une, Y. & Todo, S. (1998). Involvement of macrophage migration inhibitory factor (MIF) in the mechanism of tumor cell growth, *Mol. Med*, 4: 707–714.
- Takahashi, N., Nishihira, J. & Sato, Y. (1998). Involvement of macrophage migration inhibitory factor (MIF) in the mechanism of tumor cell growth. *Mol Med*. 4 (11): 707–714.
- Tanigawa, K., Sakaida, I., Masuhara, M., Hagiya, M., and Okita, K. (2000). Augmenter of liver regeneration (ALR) may promote liver regeneration by reducing natural killer (NK) cell activity in human liver diseases. *J Gastroenterol*, 35:112–119.
- Tao, Q. & Chan, A.T.C. (2007). Nasopharyngeal carcinoma - Molecular pathogenesis and therapeutic developments. (Invited review) *Expert Rev Mol Med*. 9:1-24.

- Thasler, W.E., Dayoub, R., Mühlbauer, M., Hellerbrand, C., Singer, T., Gräbe, A., Jauch, K.W., Schlitt, H.J. & Weiss, T.S. (2006). Repression of cytochrome P450 activity in human hepatocytes in vitro by a novel hepatotrophic factor, augmenter of liver regeneration. *J. Pharmacol. Exp. Ther.* 316(2):822-829.
- Thirunavukkarasu, C., Wang, L.F., Harvey, S.A., Watkins, S.C., Chaillet, J.R., Prelich, J., Starzl, T.E. & Gandhi, C.R. (2008). Augmenter of liver regeneration: an important intracellular survival factor for hepatocytes. *J Hepatol.* 48(4):578-88.
- Thornburg, N.J., Pathmanathan, R. & Raab-Traub, N. (2003). Activation of nuclear factor-B p50 homodimer/Bcl-3 complexes in nasopharyngeal carcinoma. *Cancer Res.* 63: 8293–8301.
- Tomiyasu, M., Yoshino, I., Suemitsu, R., Okamoto, T. & Sugimachi, K. (2002). Quantification of macrophage migration inhibitory factor mRNA expression in non-small cell lung cancer tissues and its clinical significance. *Clin Cancer Res*, 8(12):3755– 3760.
- Toy, E.P., Bonafé, N., Savlu, A., Zeiss, C., Zheng, W., Flick, M. & Chambers, S. K. (2005). Correlation of tumor phenotype with c-fms proto-oncogene expression in an in vivo intraperitoneal model for experimental human breast cancer metastasis. *Clin. Exp. Metastasis* 22: 1-9.
- Villeneuve, J.P. & Pichette, V. (2004). Cytochrome p450 and liver diseases. *Curr Drug Metab*, 5:273–282.
- Wang, G.L., Lo, K.W., Tsang, K.S., Chung, N.Y., Tsang, Y.S., Cheung, S.T., Lee, J.C., and Huang, D.P. (1999). Inhibiting tumorigenic potential by restoration of p16 in nasopharyngeal carcinoma. *Br. J. Cancer* 81: 1122–1126.
- Wang, W., Caldwell, M.C., Lin, S., Furneaux, H. & Gorospe, M. (2000). HuR regulates cyclin A and cyclin B1 mRNA stability during cell proliferation. *Embo J.* 19: 2340–2350.
- Wang, X., Xu, K., Ling, M.T., Wong, Y.C., Feng, H.C., Nicholls, J. & Tsao, S.W. (2002). Evidence of increased Id-1 expression and its role in cell proliferation in nasopharyngeal carcinoma cells. *Mol. Carcinog.* 35: 42–49.



- Warren, J.R. & Marshall, B.J. (1983). Unidentified curved bacilli on gastric epithelium in active chronic gastritis. *Lancet*. 1:1273–1275.
- Wei, M.X., de Turenne-Tessier, M., Decaussin, G., Benet, G. & Ooka, T. (1997). Establishment of a monkey kidney epithelial cell line with the BARP1 open reading frame from Epstein-Barr virus. *Oncogene* 14: 3073–3081
- Wei, W. I. & Sham, J. S. (2005). Nasopharyngeal carcinoma. *Lancet* 365: 2041–2054.
- Weiser, W.Y., Temple, D.M., Witek-Gianotti, J.S., Remold, H.G., Clark, S.C. & David, J.R. 1989). Molecular cloning of cDNA encoding a human macrophage migration inhibition factor. *Proc. Natl. Acad. Sci. USA*. 86 :7522–7526.
- Woo, H.H., Yi, X., Lamb, T., Menzl, I., Baker, T., Shapiro, D.J. & Chambers, S.K. (2010). Post-Transcriptional Suppression of Proto-Oncogene c-fms Expression by Vigilin in Breast Cancer. *Mol Cell Biol*. 31(1):215-225.
- Xie, L., Qin, W.X. & He, X.H. (2004). Differential gene expression in human hepatocellular carcinoma Hep3B cells induced by apoptosis-related gene BNIPL-2. *World J. Gastroenterol*. 10(9): 1286–1291.
- Xie, L., Qin, W, Li, J., He, X., Zhang, H., Yao, G., Shu, H., Yao, M., Wan, D. & Gu, J. (2007). BNIPL-2 promotes the invasion and metastasis of human hepatocellular carcinoma cells. *Oncol Rep*. 17(3):605-10.
- Xiong, W., Zeng, Z.Y., Xia, J.H., Xia, K., Shen, S.R., Li, X.L., Hu, D.X., Tan, C., Xiang, J.J. & Zhou, J. (2004). A susceptibility locus at chromosome 3p21 linked to familial nasopharyngeal carcinoma. *Cancer Res*. 64: 1972–1974.
- Yang, W.L., Wang, J., Chan, C.H., Lee, S.W., Campos, A.D., Lamothe, B., Hur, L., Grabiner, B.C., Lin, X., Darnay, B.G. & Lin, H.K. (2009). The E3 Ligase TRAF6 Regulates Akt Ubiquitination and Activation, *Science*, 325(5944):1134-1138.
- Yang, Y., Degranpre, P., Kharfi, A. & Akoum, A. (2000). Identification of macrophage migration inhibitory factor as a potent endothelial cell growth-promoting agent released by ectopic human endometrial cells. *J Clin Endocrinol Metab*, 85:4721–4727.

- Yates, J. L., N. Wallen, and B. Sugden. (1985). Stable replication of plasmids derived from Epstein-Barr virus in various mammalian cells. *Nature* 313: 812–815.
- Yates, J. L. (1996). Epstein-Barr virus DNA replication. DNA Replication in Eukaryotic Cells, *Cold Spring Harbor Laboratory Press, Cold Spring Harbor* 751–773.
- Yu, M.C. & Yuan, J.M. (2002). Epidemiology of nasopharyngeal carcinoma. *Semin. Cancer Res.* 12: 421–430.
- Zheng, M., Simon, R., Kononen, J., Sauter, G., Mihatsch, M. J. & Moch, H. (2004). ,*International Journal of Gynecological Cancer*, 14: 31-32



APPENDIX

Mutational analysis of *TRAF6*

>☐ref|NM\_004620.2| **UEGM** Homo sapiens TNF receptor-associated factor 6 (TRAF6), transcript variant 2, mRNA  
Length=2515

GENE ID: 7189 TRAF6 | TNF receptor-associated factor 6 [Homo sapiens]  
(Over 100 PubMed links)

Score = 1773 bits (960), Expect = 0.0  
Identities = 960/960 (100%), Gaps = 0/960 (0%)  
Strand=Plus/Plus

Query	1	GGGGAGCCCTGCCCTCCTGGTTCGGCCTCCCCGGCGCACTAGAACGAGCAAGTGATAATCA	60
Sbjct	181	GGGGAGCCCTGCCCTCCTGGTTCGGCCTCCCCGGCGCACTAGAACGAGCAAGTGATAATCA	240
Query	61	AGTTACTATGAGTCTGCTAAACTGTGAAAACAGCTGTGGATCCAGCCAGTCTGAAAGTGA	120
Sbjct	241	AGTTACTATGAGTCTGCTAAACTGTGAAAACAGCTGTGGATCCAGCCAGTCTGAAAGTGA	300
Query	121	CTGCTGTGTGGCCATGGCCAGCTCCTGTAGCGCTGTAACAAAAGATGATAGTGTGGGTGG	180
Sbjct	301	CTGCTGTGTGGCCATGGCCAGCTCCTGTAGCGCTGTAACAAAAGATGATAGTGTGGGTGG	360
Query	181	AACTGCCAGCACGGGGAACCTCTCCAGCTCATTTATGGAGGAGATCCAGGGATATGATGT	240
Sbjct	361	AACTGCCAGCACGGGGAACCTCTCCAGCTCATTTATGGAGGAGATCCAGGGATATGATGT	420
Query	241	AGAGTTTGACCCACCCCTGGAAAGCAAGTATGAATGCCCCATCTGCTTGATGGCATTACG	300
Sbjct	421	AGAGTTTGACCCACCCCTGGAAAGCAAGTATGAATGCCCCATCTGCTTGATGGCATTACG	480
Query	301	AGAAGCAGTGCAAACGCCATGCGGCCATAGGTTCTGCAAAGCCTGCATCATAAAATCAAT	360
Sbjct	481	AGAAGCAGTGCAAACGCCATGCGGCCATAGGTTCTGCAAAGCCTGCATCATAAAATCAAT	540
Query	361	AAGGGATGCAGGTCACAAATGTCCAGTTGACAATGAAATACTGCTGGAAAATCAACTATT	420
Sbjct	541	AAGGGATGCAGGTCACAAATGTCCAGTTGACAATGAAATACTGCTGGAAAATCAACTATT	600

Query	421	TCCAGACAATTTTGCAAAACGTGAGATTCTTTCTCTGATGGTGAAATGTCCAAATGAAGG	480
Sbjct	601	TCCAGACAATTTTGCAAAACGTGAGATTCTTTCTCTGATGGTGAAATGTCCAAATGAAGG	660
Query	481	TTGTTTGCACAAGATGGAACGTGAGACATCTTGAGGATCATCAAGCACATTGTGAGTTTGC	540
Sbjct	661	TTGTTTGCACAAGATGGAACGTGAGACATCTTGAGGATCATCAAGCACATTGTGAGTTTGC	720
Query	541	TCTTATGGATTGTCCCCAATGCCAGCGTCCCTTCCAAAAATTCCATATTAATATTCACAT	600
Sbjct	721	TCTTATGGATTGTCCCCAATGCCAGCGTCCCTTCCAAAAATTCCATATTAATATTCACAT	780
Query	601	TCTGAAGGATTGTCCAAGGAGACAGGTTTCTTGAGCAACTGTGCTGCATCAATGGCATT	660
Sbjct	781	TCTGAAGGATTGTCCAAGGAGACAGGTTTCTTGAGCAACTGTGCTGCATCAATGGCATT	840
Query	661	TGAAGATAAAGAGATCCATGACCAGAACTGTCCTTTGGCAAATGTCATCTGTGAATACTG	720
Sbjct	841	TGAAGATAAAGAGATCCATGACCAGAACTGTCCTTTGGCAAATGTCATCTGTGAATACTG	900
Query	721	CAATACTATACTCATCAGAGAACAGATGCCTAATCATTATGATCTAGACTGCCCTACAGC	780
Sbjct	901	CAATACTATACTCATCAGAGAACAGATGCCTAATCATTATGATCTAGACTGCCCTACAGC	960
Query	781	CCCAATTCCATGCACATTCAGTACTTTTGGTTGCCATGAAAAGATGCAGAGGAATCACTT	840
Sbjct	961	CCCAATTCCATGCACATTCAGTACTTTTGGTTGCCATGAAAAGATGCAGAGGAATCACTT	1020
Query	841	GGCACGCCACCTACAAGAGAACACCCAGTCACACATGAGAATGTTGGCCCAGGCTGTTCA	900
Sbjct	1021	GGCACGCCACCTACAAGAGAACACCCAGTCACACATGAGAATGTTGGCCCAGGCTGTTCA	1080
Query	901	TAGTTTGAGCGTTATACCCGACTCTGGGTATATCTCAGAGGTCCGGAATTTCCAGGAAAC	960
Sbjct	1081	TAGTTTGAGCGTTATACCCGACTCTGGGTATATCTCAGAGGTCCGGAATTTCCAGGAAAC	1140

>☐ref|NM\_004620.2| **UEGM** Homo sapiens TNF receptor-associated factor 6 (TRAF6), transcript variant 2, mRNA  
Length=2515

GENE ID: 7189 TRAF6 | TNF receptor-associated factor 6 [Homo sapiens]  
(Over 100 PubMed links)

Score = 1441 bits (780), Expect = 0.0  
Identities = 780/780 (100%), Gaps = 0/780 (0%)  
Strand=Plus/Plus

Query	1	TATTCACCAGTTAGAGGGTCGCCCTTGTAAGACAAGACCATCAAATCCGGGAGCTGACTGC	60
Sbjct	1141	TATTCACCAGTTAGAGGGTCGCCCTTGTAAGACAAGACCATCAAATCCGGGAGCTGACTGC	1200
Query	61	TAAAATGGAAACTCAGAGTATGTATGTAAGTGAGCTCAAACGAACCATTCGAACCCCTTGA	120
Sbjct	1201	TAAAATGGAAACTCAGAGTATGTATGTAAGTGAGCTCAAACGAACCATTCGAACCCCTTGA	1260
Query	121	GGACAAAGTTGCTGAAATCGAAGCACAGCAGTGCAATGGAATTTATATTTGGAAGATTGG	180
Sbjct	1261	GGACAAAGTTGCTGAAATCGAAGCACAGCAGTGCAATGGAATTTATATTTGGAAGATTGG	1320
Query	181	CAACTTTGGAATGCATTTGAAATGTCAAGAAGAGGAGAAACCTGTTGTGATTCATAGCCC	240
Sbjct	1321	CAACTTTGGAATGCATTTGAAATGTCAAGAAGAGGAGAAACCTGTTGTGATTCATAGCCC	1380
Query	241	TGGATTCTACACTGGCAAACCCGGGTACAAACTGTGCATGCGCTTGCACCTTCAGTTACC	300
Sbjct	1381	TGGATTCTACACTGGCAAACCCGGGTACAAACTGTGCATGCGCTTGCACCTTCAGTTACC	1440
Query	301	GACTGCTCAGCGCTGTGCAAACCTATATATCCCTTTTTGTCCACACAATGCAAGGAGAATA	360
Sbjct	1441	GACTGCTCAGCGCTGTGCAAACCTATATATCCCTTTTTGTCCACACAATGCAAGGAGAATA	1500



Query	361	TGACAGCCACCTCCCTTGGCCCTTCCAGGGTACAATACGCCTTACAATTCTTGATCAGTC	420
Sbjct	1501	TGACAGCCACCTCCCTTGGCCCTTCCAGGGTACAATACGCCTTACAATTCTTGATCAGTC	1560
Query	421	TGAAGCACCTGTAAGGCAAAACCACGAAGAGATAATGGATGCCAAACCAGAGCTGCTTGC	480
Sbjct	1561	TGAAGCACCTGTAAGGCAAAACCACGAAGAGATAATGGATGCCAAACCAGAGCTGCTTGC	1620
Query	481	TTTCCAGCGACCCACAATCCCACGGAACCCAAAAGGTTTTGGCTATGTAACTTTATGCA	540
Sbjct	1621	TTTCCAGCGACCCACAATCCCACGGAACCCAAAAGGTTTTGGCTATGTAACTTTATGCA	1680
Query	541	TCTGGAAGCCCTAAGACAAAGAACTTTCATTAAGGATGACACATTATTAGTGCGCTGTGA	600
Sbjct	1681	TCTGGAAGCCCTAAGACAAAGAACTTTCATTAAGGATGACACATTATTAGTGCGCTGTGA	1740
Query	601	GGTCTCCACCCGCTTTGACATGGGTAGCCTTCGGAGGGAGGGTTTTTCAGCCACGAAGTAC	660
Sbjct	1741	GGTCTCCACCCGCTTTGACATGGGTAGCCTTCGGAGGGAGGGTTTTTCAGCCACGAAGTAC	1800
Query	661	TGATGCAGGGGTATAGCTTGCCCTCACTTGCTCAAAAACAACCTACCTGGAGAAAACAGTG	720
Sbjct	1801	TGATGCAGGGGTATAGCTTGCCCTCACTTGCTCAAAAACAACCTACCTGGAGAAAACAGTG	1860
Query	721	CCTTTCCCTTGCCCTGTTCTCAATAACATGCAAACAAACAAGCCACGGGAAATATGTAATA	780
Sbjct	1861	CCTTTCCCTTGCCCTGTTCTCAATAACATGCAAACAAACAAGCCACGGGAAATATGTAATA	1920

Mutational analysis of vigilin

> ☐ ref|NM\_005336.3| **UEGM** Homo sapiens high density lipoprotein binding protein (HDLBP), transcript variant 1, mRNA  
Length=6516

GENE ID: 3069 HDLBP | high density lipoprotein binding protein [Homo sapiens]  
(Over 10 PubMed links)

Score = 1995 bits (1080), Expect = 0.0  
Identities = 1080/1080 (100%), Gaps = 0/1080 (0%)  
Strand=Plus/Plus

Query	1	CAGGACGGACCTTCTGGCTACTGACCGTTTTGCTGTGGTTTTCCCGGATTGTGTGTAGGT	60
Sbjct	301	CAGGACGGACCTTCTGGCTACTGACCGTTTTGCTGTGGTTTTCCCGGATTGTGTGTAGGT	360
Query	61	GTGAGATCAACCATGAGTTCCGTTGCAGTTTTGACCCAAGAGAGTTTTGCTGAACACCGA	120
Sbjct	361	GTGAGATCAACCATGAGTTCCGTTGCAGTTTTGACCCAAGAGAGTTTTGCTGAACACCGA	420
Query	121	AGTGGGCTGGTTCCGCAACAAATCAAAGTTGCCACTCTAAATTCAGAAGAGGAGAGCGAC	180
Sbjct	421	AGTGGGCTGGTTCCGCAACAAATCAAAGTTGCCACTCTAAATTCAGAAGAGGAGAGCGAC	480
Query	181	CCTCCAACCTACAAGGATGCCTTCCCTCCACTTCCTGAGAAAGCTGCTTGCTGGAAAGT	240
Sbjct	481	CCTCCAACCTACAAGGATGCCTTCCCTCCACTTCCTGAGAAAGCTGCTTGCTGGAAAGT	540
Query	241	GCCCAGGAACCCGCTGGAGCCTGGGGGAACAAGATCCGACCCATCAAGGCTTCTGTCATC	300
Sbjct	541	GCCCAGGAACCCGCTGGAGCCTGGGGGAACAAGATCCGACCCATCAAGGCTTCTGTCATC	600

Query	301	ACTCAGGTGTTCCATGTACCCCTGGAGGAGAGAAAATACAAGGATATGAACCAGTTTGGA	360
Sbjct	601	ACTCAGGTGTTCCATGTACCCCTGGAGGAGAGAAAATACAAGGATATGAACCAGTTTGGA	660
Query	361	GAAGGTGAACAAGCAAAAATCTGCCTTGAGATCATGCAGAGAACTGGTGCTCACTTGAG	420
Sbjct	661	GAAGGTGAACAAGCAAAAATCTGCCTTGAGATCATGCAGAGAACTGGTGCTCACTTGAG	720
Query	421	CTGTCTTTGGCCAAAGACCAAGGCCTCTCCATCATGGTGTGAGGAAAGCTGGATGCTGTC	480
Sbjct	721	CTGTCTTTGGCCAAAGACCAAGGCCTCTCCATCATGGTGTGAGGAAAGCTGGATGCTGTC	780
Query	481	ATGAAAGCTCGGAAGGACATTGTTGCTAGACTGCAGACTCAGGCCTCAGCAACTGTTGCC	540
Sbjct	781	ATGAAAGCTCGGAAGGACATTGTTGCTAGACTGCAGACTCAGGCCTCAGCAACTGTTGCC	840
Query	541	ATTCCCAAAGAACACCATCGCTTTGTTATTGGCAAAAATGGAGAGAACTGCAAGACTTG	600
Sbjct	841	ATTCCCAAAGAACACCATCGCTTTGTTATTGGCAAAAATGGAGAGAACTGCAAGACTTG	900
Query	601	GAGCTAAAAACTGCAACCAAAATCCAGATCCCACGCCCAGATGACCCAGCAATCAGATC	660
Sbjct	901	GAGCTAAAAACTGCAACCAAAATCCAGATCCCACGCCCAGATGACCCAGCAATCAGATC	960
Query	661	AAGATCACTGGCACCAAAGAGGGCATCGAGAAAGCTCGCCATGAAGTCTTACTCATCTCT	720
Sbjct	961	AAGATCACTGGCACCAAAGAGGGCATCGAGAAAGCTCGCCATGAAGTCTTACTCATCTCT	1020
Query	721	GCCGAGCAGGACAAACGTGCTGTGGAGAGGCTAGAAGTAGAAAAGGCATTCCACCCCTTC	780
Sbjct	1021	GCCGAGCAGGACAAACGTGCTGTGGAGAGGCTAGAAGTAGAAAAGGCATTCCACCCCTTC	1080
Query	781	ATCGCTGGGCCGTATAATAGACTGGTTGGCGAGATCATGCAGGAGACAGGCACGCGCATC	840
Sbjct	1081	ATCGCTGGGCCGTATAATAGACTGGTTGGCGAGATCATGCAGGAGACAGGCACGCGCATC	1140
Query	841	AACATCCCCCACCAGCGTGAACCGGACAGAGATTGTCTTCACTGGAGAGAAGGAACAG	900
Sbjct	1141	AACATCCCCCACCAGCGTGAACCGGACAGAGATTGTCTTCACTGGAGAGAAGGAACAG	1200
Query	901	TTGGCTCAGGCTGTGGCTCGCATCAAGAAGATTTATGAGGAGAAGAAAAAGAAGACTACA	960
Sbjct	1201	TTGGCTCAGGCTGTGGCTCGCATCAAGAAGATTTATGAGGAGAAGAAAAAGAAGACTACA	1260
Query	961	ACCATTGCAGTGGAAGTGAAGAAATCCCAACACAAGTATGTCATTGGGCCCAAGGGCAAT	1020
Sbjct	1261	ACCATTGCAGTGGAAGTGAAGAAATCCCAACACAAGTATGTCATTGGGCCCAAGGGCAAT	1320
Query	1021	TCATTGCAGGAGATCCTTGAGAGAACTGGAGTTTCCGTTGAGATCCCACCCTCAGACAGC	1080
Sbjct	1321	TCATTGCAGGAGATCCTTGAGAGAACTGGAGTTTCCGTTGAGATCCCACCCTCAGACAGC	1380



>[ref|NM\\_005336.3|](#) **UEGM** Homo sapiens high density lipoprotein binding protein (HDLBP), transcript variant 1, mRNA  
Length=6516

GENE ID: 3069 HDLBP | high density lipoprotein binding protein [Homo sapiens]  
(Over 10 PubMed links)

Score = 1884 bits (1020), Expect = 0.0  
Identities = 1020/1020 (100%), Gaps = 0/1020 (0%)  
Strand=Plus/Plus

Query	1	ATCTCTGAGACTGTAATACTTCGAGGCGAACCTGAAAAGTTAGGTCAGGCGTTGACTGAA	60
Sbjct	1381	ATCTCTGAGACTGTAATACTTCGAGGCGAACCTGAAAAGTTAGGTCAGGCGTTGACTGAA	1440
Query	61	GTCTATGCCAAGGCCAATAGCTTCACCGTCTCCTCTGTGCGCCGCCCTTCCTGGCTTCAC	120
Sbjct	1441	GTCTATGCCAAGGCCAATAGCTTCACCGTCTCCTCTGTGCGCCGCCCTTCCTGGCTTCAC	1500
Query	121	CGTTTCATCATTGGCAAGAAAGGGCAGAACCTGGCCAAAATCACTCAGCAGATGCCAAAG	180
Sbjct	1501	CGTTTCATCATTGGCAAGAAAGGGCAGAACCTGGCCAAAATCACTCAGCAGATGCCAAAG	1560
Query	181	GTTTCACATCGAGTTCACAGAGGGCGAAGACAAGATCACCCCTGGAGGGCCCTACAGAGGAT	240
Sbjct	1561	GTTTCACATCGAGTTCACAGAGGGCGAAGACAAGATCACCCCTGGAGGGCCCTACAGAGGAT	1620
Query	241	GTCAATGTGGCCCAGGAACAGATAGAAGGCATGGTCAAAGATTTGATTAAACCGGATGGAC	300
Sbjct	1621	GTCAATGTGGCCCAGGAACAGATAGAAGGCATGGTCAAAGATTTGATTAAACCGGATGGAC	1680
Query	301	TATGTGGAGATCAACATCGACCACAAGTTCCACAGGCACCTCATTGGGAAGAGCGGTGCC	360
Sbjct	1681	TATGTGGAGATCAACATCGACCACAAGTTCCACAGGCACCTCATTGGGAAGAGCGGTGCC	1740
Query	361	AACATAAACAGAATCAAAGACCAGTACAAGGTGTCCGTGCGCATCCCTCCTGACAGTGAG	420
Sbjct	1741	AACATAAACAGAATCAAAGACCAGTACAAGGTGTCCGTGCGCATCCCTCCTGACAGTGAG	1800
Query	421	AAGAGCAATTTGATCCGCATCGAGGGGGACCCACAGGGCGTGACGAGGCCAAGCGAGAG	480
Sbjct	1801	AAGAGCAATTTGATCCGCATCGAGGGGGACCCACAGGGCGTGACGAGGCCAAGCGAGAG	1860
Query	481	CTGCTGGAGCTTGCACTCTCGCATGGAAAATGAGCGTACCAAGGATCTAATCATTGAGCAA	540
Sbjct	1861	CTGCTGGAGCTTGCACTCTCGCATGGAAAATGAGCGTACCAAGGATCTAATCATTGAGCAA	1920
Query	541	AGATTTTCATCGCACAATCATTGGGCAGAAGGGTGAACGGATCCGTGAAATTTCGTGACAAA	600
Sbjct	1921	AGATTTTCATCGCACAATCATTGGGCAGAAGGGTGAACGGATCCGTGAAATTTCGTGACAAA	1980
Query	601	TTCCCAGAGGTCATCATTAACTTTCCAGACCCAGCACAAAAAAGTGACATTGTCCAGCTC	660
Sbjct	1981	TTCCCAGAGGTCATCATTAACTTTCCAGACCCAGCACAAAAAAGTGACATTGTCCAGCTC	2040
Query	661	AGAGGACCTAAGAATGAGGTGGAAAAATGCACAAAATACATGCAGAAGATGGTGGCAGAT	720
Sbjct	2041	AGAGGACCTAAGAATGAGGTGGAAAAATGCACAAAATACATGCAGAAGATGGTGGCAGAT	2100
Query	721	CTGGTGGAAAAATAGCTATTCAATTTCTGTTCGGATCTTCAAACAGTTTCACAAGAATATC	780
Sbjct	2101	CTGGTGGAAAAATAGCTATTCAATTTCTGTTCGGATCTTCAAACAGTTTCACAAGAATATC	2160
Query	781	ATTGGGAAAGGAGGCGCAACATTAAAAAGATTTCGTGAAGAAAGCAACACCAAAATCGAC	840
Sbjct	2161	ATTGGGAAAGGAGGCGCAACATTAAAAAGATTTCGTGAAGAAAGCAACACCAAAATCGAC	2220
Query	841	CTTCCAGCAGAGAATAGCAATTCAGAGACCATTATCATCACAGGCAAGCGAGCCAACTGC	900
Sbjct	2221	CTTCCAGCAGAGAATAGCAATTCAGAGACCATTATCATCACAGGCAAGCGAGCCAACTGC	2280
Query	901	GAAGCTGCCCCGGAGCAGGATTCTGTCTATTTCAGAAAGACCTGGCCAAACATAGCCGAGGTA	960
Sbjct	2281	GAAGCTGCCCCGGAGCAGGATTCTGTCTATTTCAGAAAGACCTGGCCAAACATAGCCGAGGTA	2340
Query	961	GAGGTCTCCATCCCTGCCAAGCTGCACAACTCCCTCATTGGCACCAAGGGCCGTCTGATC	1020
Sbjct	2341	GAGGTCTCCATCCCTGCCAAGCTGCACAACTCCCTCATTGGCACCAAGGGCCGTCTGATC	2400

>[ref|NM\\_005336.3|](#) **UEGM** Homo sapiens high density lipoprotein binding protein (HDLBP), transcript variant 1, mRNA  
Length=6516

GENE ID: 3069 HDLBP | high density lipoprotein binding protein [Homo sapiens]  
(Over 10 PubMed links)

Score = 1330 bits (720), Expect = 0.0  
Identities = 720/720 (100%), Gaps = 0/720 (0%)  
Strand=Plus/Plus

Query	1	CGCTCCATCATGGAGGAGTGC	60
Sbjct	2401	CGCTCCATCATGGAGGAGTGC	2460
Query	61	AGCGACACCGTTGTTATCAGGGGCCCTTCCTCGGATGTGGAGAAGGCCAAGAAGCAGCTC	120
Sbjct	2461	AGCGACACCGTTGTTATCAGGGGCCCTTCCTCGGATGTGGAGAAGGCCAAGAAGCAGCTC	2520
Query	121	CTGCATCTGGCGGAGGAGAAGCAAACCAAGAGTTTCACTGTTGACATCCGCGCCAAGCCA	180
Sbjct	2521	CTGCATCTGGCGGAGGAGAAGCAAACCAAGAGTTTCACTGTTGACATCCGCGCCAAGCCA	2580
Query	181	GAATACCACAAATTCCTCATCGGCAAGGGGGGCGGCAAAATTCGCAAGGTGCGCGACAGC	240
Sbjct	2581	GAATACCACAAATTCCTCATCGGCAAGGGGGGCGGCAAAATTCGCAAGGTGCGCGACAGC	2640
Query	241	ACTGGAGCACGTGTCATCTTCCCTGCGGCTGAGGACAAGGACCAGGACCTGATCACCATC	300
Sbjct	2641	ACTGGAGCACGTGTCATCTTCCCTGCGGCTGAGGACAAGGACCAGGACCTGATCACCATC	2700
Query	301	ATTGGAAGGAGGACGCCGTCCGAGAGGCACAGAAGGAGCTGGAGGCCTTGATCCAAAAC	360
Sbjct	2701	ATTGGAAGGAGGACGCCGTCCGAGAGGCACAGAAGGAGCTGGAGGCCTTGATCCAAAAC	2760
Query	361	CTGGATAATGTGGTGAAGACTCCATGCTGGTGGACCCCAAGCACCACCGCCACTTCGTC	420
Sbjct	2761	CTGGATAATGTGGTGAAGACTCCATGCTGGTGGACCCCAAGCACCACCGCCACTTCGTC	2820
Query	421	ATCCGCAGAGGCCAGGTCTTGCGGGAGATTGCTGAAGAGTATGGCGGGGTGATGGTCAGC	480
Sbjct	2821	ATCCGCAGAGGCCAGGTCTTGCGGGAGATTGCTGAAGAGTATGGCGGGGTGATGGTCAGC	2880
Query	481	TTCCCACGCTCTGGCACACAGAGCGACAAAGTCACCCTCAAGGGCGCCAAGGACTGTGTG	540
Sbjct	2881	TTCCCACGCTCTGGCACACAGAGCGACAAAGTCACCCTCAAGGGCGCCAAGGACTGTGTG	2940
Query	541	GAGGCAGCCAAGAAACGCATTTCAGGAGATCATTGAGGACCTGGAAGCTCAGGTGACATTA	600
Sbjct	2941	GAGGCAGCCAAGAAACGCATTTCAGGAGATCATTGAGGACCTGGAAGCTCAGGTGACATTA	3000
Query	601	GAATGTGCTATACCCAGAAATTCATCGATCTGTGATGGGCCCCAAAGGTTCCAGAATC	660
Sbjct	3001	GAATGTGCTATACCCAGAAATTCATCGATCTGTGATGGGCCCCAAAGGTTCCAGAATC	3060
Query	661	CAGCAGATTACTCGGGATTTCACTGTTCAAATTAATTTCCAGACAGAGAGGAGAACGCA	720
Sbjct	3061	CAGCAGATTACTCGGGATTTCACTGTTCAAATTAATTTCCAGACAGAGAGGAGAACGCA	3120



>[ref|NM\\_005336.3|](#) **UEGM** Homo sapiens high density lipoprotein binding protein (HDLBP), transcript variant 1, mRNA  
Length=6516

GENE ID: 3069 HDLBP | high density lipoprotein binding protein [Homo sapiens]  
(Over 10 PubMed links)

Score = 1995 bits (1080), Expect = 0.0  
Identities = 1080/1080 (100%), Gaps = 0/1080 (0%)  
Strand=Plus/Plus

Query	1	GTTACAGTACAGAGCCAGTTGTCCAGGAGAATGGGGACGAAGCTGGGGAGGGGAGAGAG	60
Sbjct	3121	GTTACAGTACAGAGCCAGTTGTCCAGGAGAATGGGGACGAAGCTGGGGAGGGGAGAGAG	3180
Query	61	GCTAAAGATTGTGACCCCGGCTCTCCAAGGAGGTGTGACATCATCATCTCTGGCCGG	120
Sbjct	3181	GCTAAAGATTGTGACCCCGGCTCTCCAAGGAGGTGTGACATCATCATCTCTGGCCGG	3240
Query	121	AAAGAAAAGTGTGAGGCTGCCAAGGAAGCTCTGGAGGCATTGGTTCTGTCAACATTGAA	180
Sbjct	3241	AAAGAAAAGTGTGAGGCTGCCAAGGAAGCTCTGGAGGCATTGGTTCTGTCAACATTGAA	3300
Query	181	GTAGAGGTGCCCTTTGACCTTCACCGTTACGTTATTGGGCAGAAAGGAAGTGGGATCCGC	240
Sbjct	3301	GTAGAGGTGCCCTTTGACCTTCACCGTTACGTTATTGGGCAGAAAGGAAGTGGGATCCGC	3360
Query	241	AAGATGATGGATGAGTTTGAGGTGAACATACATGTCCCGGCACCTGAGCTGCAGTCTGAC	300
Sbjct	3361	AAGATGATGGATGAGTTTGAGGTGAACATACATGTCCCGGCACCTGAGCTGCAGTCTGAC	3420
Query	301	ATCATCGCCATCACGGGCTCGCTGCAAATTTGGACCGGGCCAAGGCTGGACTGCTGGAG	360
Sbjct	3421	ATCATCGCCATCACGGGCTCGCTGCAAATTTGGACCGGGCCAAGGCTGGACTGCTGGAG	3480
Query	361	CGTGTGAAGGAGCTACAGGCCGAGCAGGAGGACCGGGCTTTAAGGAGTTTAAAGCTGAGT	420
Sbjct	3481	CGTGTGAAGGAGCTACAGGCCGAGCAGGAGGACCGGGCTTTAAGGAGTTTAAAGCTGAGT	3540
Query	421	GTCAGTGTAGACCCCAAATACCATCCCAAGATTATCGGGAGAAAGGGGGCAGTAATTACC	480
Sbjct	3541	GTCAGTGTAGACCCCAAATACCATCCCAAGATTATCGGGAGAAAGGGGGCAGTAATTACC	3600
Query	481	CAAATCCGGTTGGAGCATGACGTGAACATCCAGTTTCTGATAAGGACGATGGGAACCAG	540
Sbjct	3601	CAAATCCGGTTGGAGCATGACGTGAACATCCAGTTTCTGATAAGGACGATGGGAACCAG	3660
Query	541	CCCCAGGACCAAATTACCATCACAGGGTACGAAAAGAACACAGAAGCTGCCAGGGATGCT	600
Sbjct	3661	CCCCAGGACCAAATTACCATCACAGGGTACGAAAAGAACACAGAAGCTGCCAGGGATGCT	3720
Query	601	ATACTGAGAATTGTGGGTGAACTTGAGCAGATGGTTTCTGAGGACGTCCCGCTGGACCAC	660
Sbjct	3721	ATACTGAGAATTGTGGGTGAACTTGAGCAGATGGTTTCTGAGGACGTCCCGCTGGACCAC	3780
Query	661	CGCGTTCACGCCCGCATCATTGGTGGCCCGCGGCAAAGCCATTTCGCAAAATCATGGACGAA	720
Sbjct	3781	CGCGTTCACGCCCGCATCATTGGTGGCCCGCGGCAAAGCCATTTCGCAAAATCATGGACGAA	3840
Query	721	TTCAAGGTGGACATTTCGCTTCCACAGAGCGGAGCCCCAGACCCCAACTGCGTCACTGTG	780
Sbjct	3841	TTCAAGGTGGACATTTCGCTTCCACAGAGCGGAGCCCCAGACCCCAACTGCGTCACTGTG	3900

Query	781	ACGGGGCTCCCAGAGAATGTGGAGGAAGCCATCGACCACATCCTCAATCTGGAGGAGGAA	840
Sbjct	3901	ACGGGGCTCCCAGAGAATGTGGAGGAAGCCATCGACCACATCCTCAATCTGGAGGAGGAA	3960
Query	841	TACCTAGCTGACGTGGTGGACAGTGAGGCGCTGCAGGTATACATGAAACCCCCAGCACAC	900
Sbjct	3961	TACCTAGCTGACGTGGTGGACAGTGAGGCGCTGCAGGTATACATGAAACCCCCAGCACAC	4020
Query	901	GAAGAGGCCAAGGCACCTTCCAGAGGCTTTGTGGTGCGGGACGCACCCTGGACCGCCAGC	960
Sbjct	4021	GAAGAGGCCAAGGCACCTTCCAGAGGCTTTGTGGTGCGGGACGCACCCTGGACCGCCAGC	4080
Query	961	AGCAGTGAGAAGGCTCCTGACATGAGCAGCTCTGAGGAATTTCCCAGCTTTGGGGCTCAG	1020
Sbjct	4081	AGCAGTGAGAAGGCTCCTGACATGAGCAGCTCTGAGGAATTTCCCAGCTTTGGGGCTCAG	4140
Query	1021	GTGGCTCCCAAGACCCTCCCTTGGGGCCCCAAACGATAATGATCAAAAAGAACAGAACCC	1080
Sbjct	4141	GTGGCTCCCAAGACCCTCCCTTGGGGCCCCAAACGATAATGATCAAAAAGAACAGAACCC	4200